PLANNING VIRTUAL POWER PLANTS FOR SMART FACTORIES AND INDUSTRY 4.0 WITH RENEWABLE AND THERMAL COGENERATION

by

Honglin Li, B.A., M.E.

A thesis submitted to the Graduate Council of
Texas State University in partial fulfillment
of the requirements for the degree of
Master of Science
with a Major in Engineering
August 2021

Committee Members:

Tongdan Jin, Chair

Francis Mendez

Keisuke Ikehata

COPYRIGHT

by

Honglin Li

2021

FAIR USE AND AUTHOR'S PERMISSION STATEMENT

Fair Use

This work is protected by the Copyright Laws of the United States (Public Law 94-553, section 107). Consistent with fair use as defined in the Copyright Laws, brief quotations from this material are allowed with proper acknowledgement. Use of this material for financial gain without the author's express written permission is not allowed.

Duplication Permission

As the copyright holder of this work I, Honglin Li, authorize duplication of this work, in whole or in part, for educational or scholarly purposes only.

DEDICATION

I would like to dedicate this thesis to my beloved late mother.

ACKNOWLEDGEMENTS

First of all, I would like to express my deep gratitude to my thesis advisor Dr. Tongdan Jin. Without his help, it would have been impossible for me to complete this thesis work and gain so much knowledge during the study at Texas State University. Additionally, he is a humorous person with positive attitude towards both work and life.

I want to appreciate my thesis committee, Dr. Francis Mendez and Dr. Keisuke Ikehata, for their time in serving on my thesis committee. Their constructive insights and suggestion on the arrangement of the thesis work, and the research relevance to industries are very helpful for me to improve the thesis.

Besides, I am also very grateful to Dr. Clara Novoa, whose expertise in the field of operations research has been of great help in the accomplishment of my thesis.

Additionally, my thanks also go to Dr. Vishu Viswanathan, for all the great advice he provided for me during my study at Texas State University. My appreciations are extended to the Ingram School of Engineering faculty and staff who taught me or provided necessary supports.

I am also grateful for the financial support from the National Science Foundation for funding this thesis research under ME-GREEN CBET project (grant # 1704933).

Last but not least, I want to thank my family far in my homeland in China. They are the strongest shield behind me. Whatever I meet, my family are always staying with me with their wise, inclusion, and deep love.

TABLE OF CONTENTS

Page

ACKNOWLEDGEMENTS v

LIST OF TABLES viii

LIST OF FIGURES xi

LIST OF ABBREVIATIONS xiv

ABSTRACT xvii

CHAPTER

1. INTRODUCTION AND LITERATURE REVIEW 1

    1.1 Research Motivation and Background 1
    1.2 Literature Review 6
    1.3 Research Contributions 13
    1.4 Thesis Outline 14

2. NEURAL NETWORK ALGORITHMS FOR LOAD FORECASTING 16

    2.1 Long Short-Term Memory (LSTM) 16
    2.2 Numerical Experiment 22
    2.3 Sensitivity Analysis 25

3. VIRTUAL POWER PLANTS PARTICIPATION IN ELECTRICITY MARKET 27

    3.1 Background and Decision-making Algorithm 27
    3.2 Model Formulation 29
    3.3 System Setting 34
    3.4 Results and Discussion 37

4. FACILITY-MICROGRID LOCATION-ALLOCATION MODEL 42

    4.1 Location-Allocation Model 42
    4.2 Two-Echelon Location-Allocation Model with Microgrid Integration 47
    4.3 Three-Echelon Location-Allocation Model with Microgrid

Integration 55
4.4 Numerical Experiments 67
4.5 Sensitivity Analysis 76

5. FACILITY-MICROGRID LOCATION ALLOCATION FOR RISK AVERSE DESIGN 84

5.1 Introduction 84
5.2 Model Formulation 86
5.3 Value at Risk (VaR) 92
5.4 Conditional Value at Risk (CVaR) 95
5.5 Minimax 98
5.6 Numerical Experiment 100

6 CONCLUSION 110

6.1 Research Summary 110
6.2 Future Research 113

APPENDIX SECTION 115

REFERENCES 128

LIST OF TABLES

Table **Page**

2.1 Part of the Dataset 24

2.2 Sensitivity Analysis Results 26

3.1 Notation for Model Parameters 30

3.2 Decision Variables of VPP Model 30

3.3 Data of the VPP Intra-Day Planning 34

3.4 Hourly Electricity Price (unit: $/MWh) 35

3.5 Forecastion of Renewable Generation, Thermal and Power Load (unit: MW) 36

3.6 Day-ahead Energy Planning (unit: MWh) 38

3.7 Intra-day Energy Planning (Unit: MWh) 39

3.8 Sensitivity Analysis 41

4.1 Parameters and Variables for Model 4.1 or Fixed Charge Model 43

4.2 Fixed Setup Cost and Capacity of the Candidate Sites 45

4.3 Unit Shipment Cost ($/item/km) 46

4.4 Distance Between Store *s* and DC Site *n* (unit: km) 46

4.5 Customer Demands of Stores 46

4.6 Transportation Plan 47

4.7 Parameters for Model 4.2 47

4.8 Decision Variables for Model 4.2 48

4.9 Parameters for Three-Echelon FMLA Model 56
4.10 Decision Variables of Three-Echelon FMLA Model 57
4.11 Weekly Product Demand of the 4F-2W-4S Network 68
4.12 Parameters for Production Planning in FMLA Problem 69
4.13 Parameters for Microgrid System in FMLA Problem 69
4.14 Setup Cost, Energy Demand and Capacity of Facilities 70
4.15 The Size of Three Optimization Models 70
4.16 Optimal Cost and Computation Time of Three Models 71
4.17 Decisions on Facility Location and Allocation 71
4.18 Microgrid Allocation of Three Method Models 72
4.19 Sensitivity Analysis on Production Planning 76
4.20 Sensitivity Analysis on Microgrid Sizing 78
4.21 Distance between the Facilities (km) 79
4.22 Weekly Product Demand of the 8F-4W-8S Network 79
4.23 Setup Cost, Energy Demand, and Capacity of New Candidate Locations 80
4.24 Microgrid Allocation of the 8F-4W-8S Network 83
5.1 Parameters for Stochastic Model 86
5.2 Decision Variables of Stochastic Model 87
5.3 Summary of the Three Scenarios 100
5.4 Decisions on Location of Factories and Warehouse 101
5.5 Microgrid Sizing for the 4F-2W-4S Network Design 101

5.6 Optimal Costs..... 101

5.7 Results of Four Cases..... 107

LIST OF FIGURES

Figure **Page**

1.1 Virtual Power Plant 3

1.2 Industry 4.0 5

2.1 RNN Structure Diagram 16

2.2 RNN Internal Structure Diagram 17

2.3 LSTM Internal Structure Diagram 19

2.4 The Four Gates of the Model 19

2.5 Tanh and Sigmoid Function 21

2.6 The Model Structure 22

2.7 Forecasting Model Flowchart 22

2.8 The Four Gates of the Model 24

2.9 One Hour Ahead Prediction Result 25

3.1 Rolling Horizon 29

3.2 Flowchart of the Model 31

3.3 Input Data 37

3.4 Results of Models 40

4.1 Location-Allocation in a DC-to-Retailor Network 42

4.2 A Network with 3 Candidate DC Sites and 6 Demand Nodes 45

4.3 Candidate Locations for Supply Chain Facilities and Microgrid 68

4.4 Production, Inventory, and Backorder of Product A 72

4.5 Production, Inventory, and Backorder of Product B..... 73

4.6 Prosumer Hourly Energy Trading of Factory 4 in Week 10..... 74

4.7 Prosumer Hourly Energy Trading of Factory 4 in Weeks 5 to 20 74

4.8 Prosumer Hourly Energy Trading of Factory 3 75

4.9 Prosumer Hourly Energy Trading of Warehouse 1 75

4.10 Production and Inventory Planning Product A in Warehouse 1 81

4.11 Production and Inventory Planning Product B in Warehouse 1 81

4.12 Production and Inventory Planning Product A in Warehouse 2 82

4.13 Production and Inventory Planning Product B in Warehouse 2 82

5.1 Graphical Illustration of VaR..... 94

5.2 Flowchart of VaR Algorithm 94

5.3 Graphical Illustration of CVaR..... 96

5.4 Flowchart of CVaR Algorithm 97

5.5 Flowchart of Minimax algorithm..... 99

5.6 System Optimal Cost 102

5.7 Product A Production and Inventory Decision of Model SFMLA 103

5.8 Product B Production and Inventory Decision of Model SFMLA 104

5.9 Difference in Production Quantity of Two Models 105

5.10 Difference in Inventory and Backorder of the Network 105

5.11 Difference in Energy Trading 106

5.12 The Results of VaR, CVaR and Minimax 108

LIST OF ABBREVIATIONS

Abbreviation	Description
AMPL	Advanced Mathematical Programming Language
ANFIS	Adaptive Neural Network Based Fuzzy Inference System
ANN	Artificial Neural Network
ARIMA	Auto Regressive Integrated Moving Average
BBV	Basic Big Value
CF	Capacity Factor
CHP	Combined Heat and Power
CNN	Convolutional Neural Network
CVaR	Conditional Value at Risk
DA	Day-Ahead
DC	Distribution Center
DER	Distributed Energy Resource
DG	Distributed Generation
DNN	Deep Neural Network
EEMD	Ensemble Empirical Mode Decomposition
ELM	Extreme Learning Machine
EMD	Empirical Mode Decomposition
EMS	Energy Management System

ERCOT	Electric Reliability Council of Texas
ESS	Energy Storage System
FLA	Facility Location Allocation
FMLA	Facility-Microgrid Location-Allocation
ID	Intra-Day
LSTM	Long Short-Term Memory
MAE	Mean Absolute Error
MILP	Mixed Integer Linear Programming
MINLP	Mixed Integer Non-Linear Programming
MMPA	Multi-Model Partitioning Algorithm
MMR	Minimax Regret
MSE	Mean Squared Error
MSLE	Mean Squared Logarithmic Error
PV	Photovoltaics
RNN	Recurrent Neural Network
SARIMA	Seasonal Auto-Regression Integrated Moving Average
SBV	Simplified Big Value
SCM	Supply Chain Management
SFMLA	Stochastic Facility Microgrid Location Allocation
TOU	Time of Use
VaR	Value at Risk

VPP	Virtual Power Plant
WT	Wind Turbines

ABSTRACT

Wind- and solar-based microgrid generation is a promising solution to reverse the climate change and achieve manufacturing sustainability. Virtual power plants (VPP) formed by a group of coordinated microgrid systems have the potential to accelerate the integration of variable renewable resources. We propose a facility-microgrid, location-allocation model to realize renewable and thermal cogeneration in smart factories and Industry 4.0. Under demand and supply uncertainty, the model jointly locates the factories and warehouse, assigns the transportation routes, and sizes wind turbines, photovoltaics, and energy storage for cost minimization. The model also performs operational planning for production, inventory, energy transactions, vehicle charging, and electricity and thermal cogeneration using combined heat and power. The proposed VPP planning model is demonstrated on multi-echelon supply chain networks using 11-year period, 2.3 million data. Several managerial insights are obtained. First, the experimental results show that the site with abundant renewables is opt for being the factory location despite of higher transportation and production cost. Second, the sizing of renewable microgrid is significantly influenced by time-of-use tariff or peaking price. Third, combined heat and power is proven to be a viable approach to streamline variable generation. Fourth, different decision-making criteria, such as value-at-risk and Minimax, may have huge impacts on the risk-averse planning. Future work can be focused on incorporating edge computing and vehicle-to-grid operations into the integration of renewable energy in smart factories.

1. INTRODUCTION AND LITERATURE REVIEW

1.1 Research Motivation and Background

To alleviate energy shortages and reduce carbon emissions, renewable-based energy technologies have seen the rapid development in the past decade. The US government targets 20% of electricity generated by wind in 2030 (DoE 2008). However, renewable energy sources like wind and solar also have their own shortcomings. For example, they are greatly affected by the weather condition and the power output is intermittent. Therefore, the impact on the power grid will cause reliability and security concern, especially when multiple renewable power sources generate at the same time. How to rationally regulate each source to ensure the reliable operation of the power grid and maximize the interests of all stakeholders becomes the main concern of variable generation technologies.

1.1.1 Load Forecasting

Load forecasting is one of the most effective ways to mitigate the aforementioned energy problem. Combining historical data with real-time weather conditions and multi-dimensional information such as time of day, the load demand can be effectively predicted. This allows the power system to adjust the dispatch plan in real time based on the forecasted demand. This aims to ensure power quality, reduce the reserve capacity, and save the operating cost of the power system. Effective forecasts also increase the market penetration rate of renewables sources and reduce the impact of power variability on the grid. Therefore, accurate load forecasting can minimize or mitigate the power shortage in transmission and distribution networks. Thanks to the rapid development in computing systems and machine learning algorithms in recent years, the application of

deep neural networks to load forecasting is becoming a powerful tool in long-term and short-term load prediction. For instance, recurrent neural network (RNN) is a type of machine learning algorithm for processing sequence data. In contrast to general neural networks, it can handle data that changes over time. Gradient explosion and gradient disappearance have been one of the most difficult problems in long-sequence training, and as a special type of RNN, long short-term memory (LSTM) can effectively solve them. For this reason, LSTM outperforms ordinary RNN in processing long-sequence data. This thesis uses existing or historical data to train a LSTM neural network to construct the prediction model, and then uses the trained model to further obtain the prediction results.

1.1.2 Virtual Power Plant

From the perspective of renewable power plants, effectively harnessing various clean energy resources and rationally dispatching the power can also improve the efficiency of the electric grid and increase the revenue of utility suppliers. Virtual power plant (VPP) is one of the new technologies to realize the intelligent distribution network. It refers to the integration of new generation, controllable loads and energy storage systems installed in the distribution grid as a special power plant. Through the distributed energy management system, a VPP system can actively participate in the operation of the grid in the day-ahead market. VPP is able to coordinate the smart grid and distributed energy resources, fully tap the value and benefits that distributed generating unit brings to the grid and end users.

As shown in Figure 1.1, in a VPP paradigm, renewables, controlled loads and energy storage systems are grouped into a unit, which can be seen as a special power

plant connected to the distribution grid and participating in its operation. Each unit is connected to the energy management system (EMS). In a smart grid with two-way communication capability, the EMS system can be used for unified dispatch and coordination of power generation, user consumption, and energy storage, so as to reduce generation losses, save greenhouse gas emissions, optimize resource utilization, control grid peak loads and improve power supply reliability.

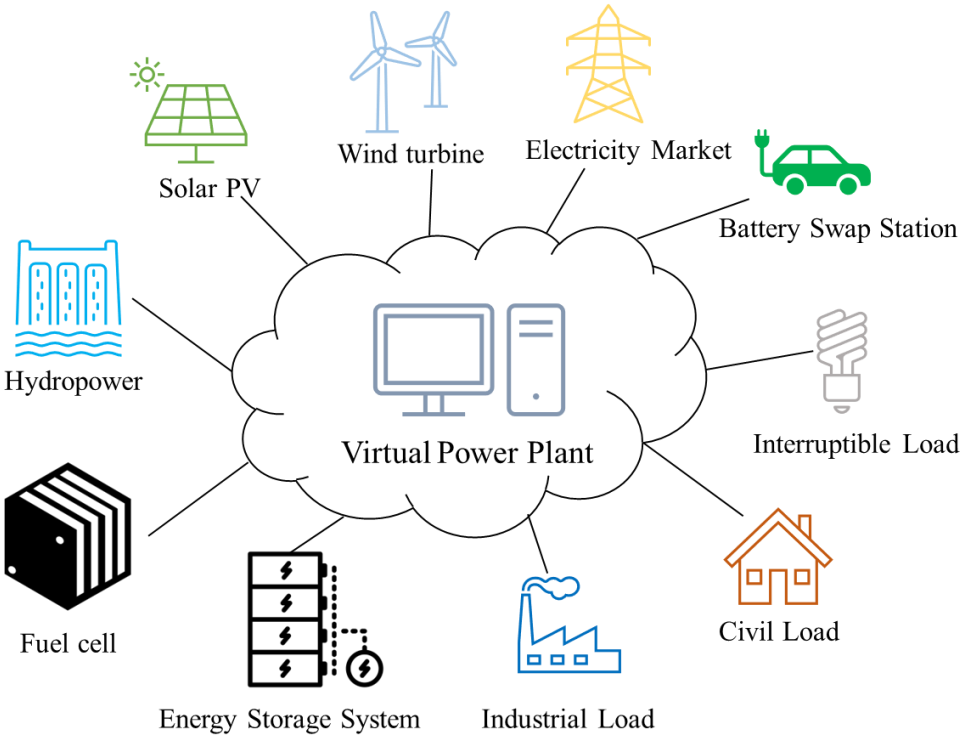


Figure 1.1 Virtual Power Plant

In this thesis research, a VPP with wind turbines, solar photovoltaics (PV), combined heat and power (CHP) and energy storage units is considered. In the first stage, we obtain the VPP electricity sales plan for the day-ahead market based on the demand data forecasted by LSTM. Then the rolling horizon algorithm is applied to the intraday market to obtain the most economical VPP generation schedule with electricity trading.

Meanwhile the balance between the supply and the demand for both thermal and electric energy is ensured. If the CHP runs at full capacity and still cannot meet the electricity demand, the VPP will purchase electric energy from the main grid.

1.1.3 Industry 4.0

Industry 4.0 is used interchangeably with the fourth industrial revolution and represents a new stage in the design, management and control of the industrial value chain. Figure 1.2 depicts the basic concept of Industry 4.0, which integrates the four basic elements, including smart factory, smart production, smart logistics, and smart energy. The decision making is supported through big data in the cloud. Users can control the whole industrial chain through one terminal. As an important guideline for modern industrial transformation, Industry 4.0 not only provides horizontal integration for the entire manufacturing sector through value networks, but also enables the factory edges to realize digital integration across the entire value chain and provides new ideas for vertical integration and networked manufacturing systems. In this process, we need to solve the following problems: How can physical network systems support long-term strategic operations, new value networks, and novel business models of enterprises? How can physical network systems enable end-to-end business processes including engineering workflows? How can physical network systems create flexible and reconfigurable manufacturing systems? Take the traditional manufacturing supply chain network as an example, information, materials and cash flow are the three basic elements that make up the traditional value chain. In this study, we attempt to integrate smart and clean energy into manufacturing and supply chain planning, break the barriers between energy market and product market, realize information interoperability and energy sharing through

unified or virtual power generation, and thus achieve vertical integration through manufacturing-energy nexus. The facility-microgrid location-allocation model provides an opportunity to consider the impact of the physical network on the subsequent production-inventory planning, logistics electrification, and transactive energy trading of the whole industrial chain at the beginning of the design.

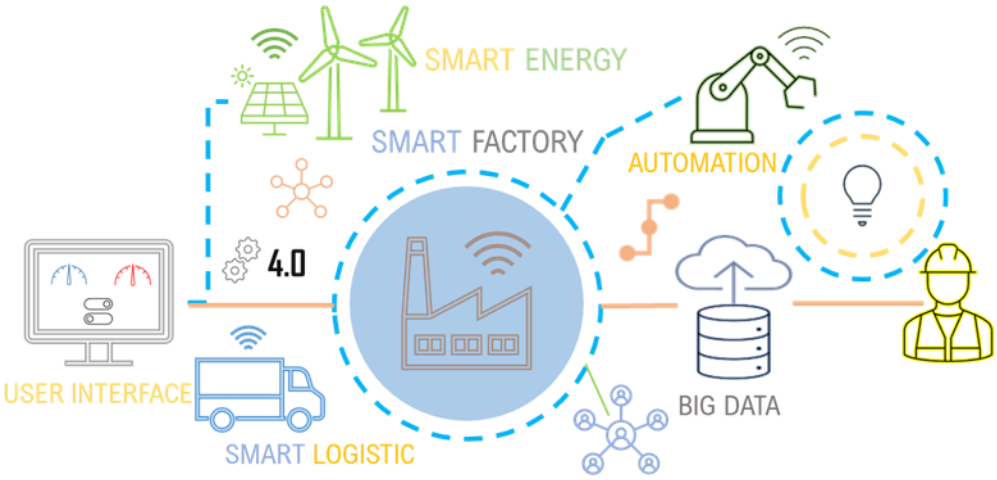


Figure 1.2 Industry 4.0

By applying VPP to smart factories, warehouses, and other business facilities, it meets the manufacturing industry's need for clean, flexible, reliable and sustainable energy through onsite renewable generation. The ultimate goal is to achieve zero carbon emissions across the industry. Also empowering the entire supply chain with four capabilities: interconnectivity, visibility, autonomy and predictive analytics, supported by real-time and historical information, to both effectively manage upstream suppliers and react faster to unforeseen events within the network.

1.2 Literature Review

1.2.1 Forecasting

Forecasting is an important task directly influencing the application of solar and wind energy. This can be addressed from three aspects. One is the prediction of solar radiation considering uncertain weather. The magnitude of solar radiation determines the amount of PV output power. Solar energy is one of the most important renewable sources, especially in the Middle East and Southern European countries with abundant sunshine hours (Kalogirou 2014). In recent years, a large amount of works using deep learning and weather parameters to predict solar radiation have been developed (Khatib et al., 2012; Inman et al., 2013; Sozen et al., 2004; Voyant et al., 2011). Predictive models to forecast future solar radiation are often constructed by inputting geographic and atmospheric information, such as latitude and longitude, ambient temperature and wind speed. Bilgili and Ozoren (2011) propose that the duration of sunshine, temperature and relative humidity are important meteorological parameters for predicting solar radiation. An artificial neural network (ANN) model based on the Bayesian framework called autocorrelation method is proposed by Lo´pez et al. (2005), which can be used to evaluate more relevant input parameters in the solar radiation model. The hybrid method based on auto-regressive integrated moving average (ARIMA) and time-delay neural network proposed by Ji and Chee (2011), has been successfully verified from a solar station in Singapore. Recently, a neural network model called extreme learning machine (ELM) is proposed by Huang et al. (2006), which has a very fast training speed because it is a multi-layer perceptron type of neural networks.

The second part of the forecasting is to predict the wind power generation.

According to the wind power curve, we can accurately determine the future wind generation in both short-term and long-term horizon. Theoretically speaking, natural meteorological rules determine the wind speed, and it has a strong regularity, which also provides the possibility of speed prediction. However, in the actual forecasting process, the wind speed changes with strong volatility, which could be non-stationary. The wind speed varies with location, altitude, and time. Therefore, to design a wind speed prediction model, many factors such as season, temperature, humidity, wind direction and air pressure must be considered. For this reason, the prediction of wind speed is very challenging. In recent years, many researchers have made a lot of contributions to wind speed prediction. Zhang et al. (2017) propose a wind speed forecasting model that integrates three different methods, i.e., adaptive neural network-based fuzzy inference system (ANFIS), the ensemble empirical mode decomposition (EEMD) and seasonal auto-regression integrated moving average (SARIMA). A basic neural network architecture that can predict wind speed is proposed by More and Deo (2003), and the feasibility of the model is also verified by experiments. A multi-step wind speed prediction model using the empirical mode decomposition (EMD) neural network is proposed by Guo et al. (2012) This model integrates several traditional neural networks to predict wind speed. The method is proven to be effective in the process of experimental verification.

The third forecasting part is the power demand or electricity load. Accurate power demand forecasting is very important to the operation of microgrid. It not only improves the utilization efficiency of energy storage system, but also avoids unnecessary costs caused by insufficient power supply. Therefore, improving the accuracy of power

demand forecasting can add many advantages to the microgrid system. The methods for demand forecast can be divided into two categories, one is traditional statistical methods, and the other is neural network models. For the first category, Soubdhan et al. (2016) apply the exponential smoothing and Kalman filters method for power load forecasting. Linear regression and autoregressive methods are also used in the prediction model of Javed et al. (2012). For the second category, neural network has received a lot of attention in recent years because of better accuracy than traditional statistical predictions. Multi-model partitioning algorithm (MMPA) proposed by Pappas et al. (2008) has achieved good results in short-term power demand forecasting. Ekonomou et al. (2016) propose an ANN model using wavelet denoising algorithm. The wavelet method can decompose the load data according to the frequency of the signal. Therefore, the wavelet method provides better model training for neural network, thus improving the accuracy of load forecasting.

1.2.2 VPP Model Formulation

In recent years, new mathematical models and design methods have been proposed, including simulations, energy generation management and the demand-side management coordination of generation and demand. The purpose of all these models is to maximize the efficiency of energy utilization, reduce user electricity costs and increase the revenue of the power plant based on the unique characteristics of renewables. In this area, a mathematical model is proposed by Zamarripa et al. (2011) to find the optimal level of production and storage to minimize operating costs by adding energy storage devices to meet uncertain energy needs. More recently, the mathematical model developed by Chen et al. (2013) aims to maximize the profit of a microgrid including

renewable power systems and energy storage systems. In addition, aiming to minimize the total operating cost, a mixed integer linear programming model (MILP) of energy production planning related to a residential microgrid-based energy supply chain network comprises multiple interconnected cogeneration systems is proposed by Kopanos et al. (2013). The common goal of these models is to minimize the operating cost of the power plant under the premise of satisfying the balance of supply and demand. In this process, various constraints in actual production such as production capacity, ramping limits and minimum startup and shutdown times are also considered. The large number of possible combinations of power generation units and consumption units in the grid makes it a very challenging optimization problem. There are also several models that focus on determining energy demand side management. Carrión and Arroyo (2006) present a discrete-time MILP model to minimize the energy cost of a given grid. According to energy prices and supply dynamics, Zondervan et al. (2010) propose a mixed integer non-linear programming (MINLP) model to optimize the production schedules for minimizing operating costs. A simulated annealing method proposed by Velik and Nicolay (2014) can maximize the profit of the power grid according to the variability of electricity prices in different time periods.

The appearance of peak power consumption is detrimental to energy suppliers and grid operators to some extent. This is because the existence of peak demand not only reduces the efficiency of the grid, but for users, the energy price often goes up significantly as well in peak hours. How to effectively prevent the occurrence of peaks is a major challenge to energy generation and demand management. The model developed by Vedova and Facchinetti (2012) can control the electricity consumption in real time

through advanced scheduling and power dispatching.

In addition, there are also a series of studies that focus on the management of both energy production and demand responses, mainly by optimizing production plans to adapt to the availability of utility grid energy. The continuous-time MILP model proposed by Nolde and Morari (2010) aims to minimize total energy consumption by adjusting the production schedule of steel plants, thereby reducing production costs. The program also introduces a penalty mechanism for power consumption that is not implemented in accordance with the power purchase contract. The optimization model applied on both the management and demand side mainly focuses on scheduling the production plan reasonably according to the energy price of different time periods. The discrete-time MILP model developed by Mitra et al. (2012) is to adjust the production plan according to the time-related electricity price plan. The demand response model proposed by Hadera et al. (2014) can effectively reduce the energy cost of steel plants. Similarly, an offline residential energy dispatch method based on the electricity pricing model is demonstrated by Mohsenian-Rad and León-García (2010).

Though significant amounts of efforts have been spent on the energy production-side management in recent years, the research in the VPP that combines the demand side and the production side, especially the cogeneration of microgrid and thermal energy, still deserves further investigation. The new VPP planning model not only achieves the balance of supply and demand, but also performs the peak shaving through CHP and microgrid cogeneration and energy storage operations, thereby maximizing the efficiency and utilization of renewable generating units. Along this line, a VPP model including a cogeneration scheme and an energy storage device is proposed by Koraki et al. (2018).

The rolling horizon algorithm applied in this model can optimize the working schedule of each device in the microgrid during the prediction period by predicting the future demand and renewable generation.

1.2.3 Supply Chain Facility Location-Allocation Model

In a traditional facility location-allocation (FLA) problem, we are given a set of customers that have a service or product demands and a set of candidate facilities partitioned into different levels or tiers. The goal is to determine where the facilities are opened or established at each level and allocating the existing customers to the facilities to meet the demands, while optimizing an objective function such as cost. The FLA problem is originally proposed by Cooper (1963). Since its inception, the FLA problem has received much attention in operations management community because of its computational challenges and broad applications. Some of the examples include network FLA problem (Hoseini Shekarabi et al., 2019, Ziaee and Choobineh, 2017), emergency logistics planning (Caunhye, Nie, Pokharel, 2012), and healthcare delivery (Zarrinpoor, Fallahnezhad, Pishvaeec, 2017), among others. In solving FLA problem, the customers' demands are often taken as the primary input for the problem. Deterministic demand profiles were adopted in early studies, yet most of the real-world demands tend to be stochastic. Hence the problem needs to be tackled in a more realistic way by incorporating uncertainties in demands. Several approaches have been proposed to address these uncertainties, including stochastic programming, simulation-based optimization, and minimization of the demand shortfall.

The FLA problem also has many intersections with the supply chain management (SCM) in terms of the strategic decisions on the locations for factories, warehouses or

distribution centers. For instance, Melo et al. (2009) review facility location models in the context of SCM and identify the design features that must be captured in order to be consistent with the strategic decisions. The authors also discuss the importance of having different types and capacities of facilities associated with supply chain planning. In fact, SCM models can be treated as an extended version of the FLA problem. Beside the strategic decision, SCM models also involve tactical and operational decisions on the production, procurement, inventory, transportation and routing. Therefore, the FLA problem can be treated as a simplified version of the supply chain network design problem because the former does not involve tactical and operational decisions.

In the past decade, SCM is seen a paradigm change as a result of renewable energy integration, transportation electrification, and microgrid or distributed power generation (Martin 2012; Huddleston 2015; Parker et al. 2019). Also known as onsite generation, a distributed generation (DG) system is formed by a group of distributed energy resources (DER) that act as a local power entity with respect to the main grid. Typical DER units include solar PV, wind turbines (WT), biogas fuel cells, CHP, and energy storage units. A growing number of firms, such as Honda, Walmart, and Apple, have installed WT and roof-top PV systems to power their energy-intensive facilities for attaining low-carbon operations (Stinpetru 2014; Ozment 2014). In fact, onsite generation is re-shaping the supply chain management landscape by transforming a traditional firm from passive electricity consumers to an active energy prosumer. An energy prosumer not only consumes but also to produce its own electricity in a DG realm (EIA 2019). However, distributed generation and prosumer energy have been rarely incorporated in existing FLA models or supply chain planning program.

1.3 Research Contributions

The contributions of this thesis are listed below:

(1) An RNN-based LSTM neural network model with lower validation loss is proposed to forecast time-series data, such as hourly wind speed, solar irradiance, and power demand. By adjusting the evaluation function, network structure and hyperparameters, each neural network layer can predict different types of time-series data either in short-term and long-term horizon. In this thesis, we will focus on power demand forecasting numerical experiments by using the trained neural network model.

(2) A novel VPP planning model is proposed for the design and operations of multi-echelon manufacturing supply chain networks. The new model brings together materials, information, cash and energy flows under a unified optimization framework. Particularly the model integrates product market and energy market through the joint decision on production, inventory and energy generation and sales under product demand and power supply uncertainty. Hence the classical 3-dimensdional supply design methodology is extended to 4-dimension with the integration of onsite generation.

(3) A facility-microgrid location-allocation model is proposed. This new model offers strategic decisions on the locations of factories and warehouses, and the sizing of WT, PV, and energy storage units. The model also makes operational planning for production, inventory, transportation, power generation, energy storage and trading with the main grid.

(4) The facility-microgrid location-allocation model is further covered into a stochastic optimization model. The results between the deterministic and the stochastic models are compared and analyzed, such as facility sites, microgrid sizing, and the operational-level decisions. Three different decision-making criteria are applied to analyze the optimal solution of the stochastic model, including value-at-risk, conditional-value-at-risk, and Minimax.

1.4 Thesis Outline

The remainder of the thesis is organized as follows. Chapter 2 concentrates on the application of deep neural networks on power load forecasting. In this chapter, a LSTM-based neural network model for power load forecasting is trained using 158,521 hourly data from the Electric Reliability Council of Texas (ERCOT). Several factors affecting the final results are also analyzed in the sensitivity analysis. Chapter 3 tests the feasibility of operating a VPP in a single microgrid setting. The VPP system model presented in a day-ahead and an intraday market, respectively. The purpose is to simulate real-life electricity market operation. Rolling horizon algorithm and real wind and weather data are used to test the feasibility of the VPP model. Chapter 4 introduces a multi-echelon, renewables-powered supply chain network design model. A facility-microgrid location-allocation model is proposed under product demand and energy supply uncertainty. The feasibility and scalability of the model are examined in two network instances. Key factors affecting the supply chain cost are identified and discussed through the sensitivity analysis. In Chapter 5, the facility-microgrid location-allocation model in Chapter 4 is transformed into a stochastic optimization. The optimal solution of the stochastic model

is evaluated in three different criteria, and the results are also compared with the deterministic solution.

2. NEURAL NETWORK ALGORITHMS FOR LOAD FORECASTING

2.1 Long Short-Term Memory (LSTM)

Recurrent neural networks (RNN) are distinguished from general neural networks in that they draw on the idea that "human cognition is based on past experience and memory". Compared with deep neural networks (DNN) and convolutional neural networks (CNN), the most special feature of RNN is that it has a memory function for the content of previous moment. The name is given because the current output of a sequence is also related to the previous moment's output. This is shown by the fact that the network remembers the previous information and applies it to the computation before the current output. That is, the nodes between the hidden layers are interconnected. The output of the input layer and the output of the hidden layer at the previous moment together form the input of the hidden layer at the current moment.

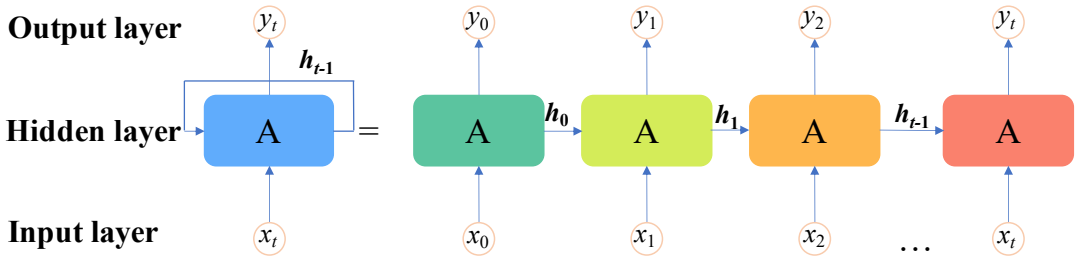


Figure 2.1 RNN Structure Diagram

Figure 2.1 shows a typical RNN network contains an input x, an output h, and a neural network unit A. Unlike ordinary neural networks, the unit of an RNN contains both outputs and inputs, while it also contains a self-looping link. This is the core of RNN: the information from the previous moment can be remembered and fed to the next moment. The right-hand side of the equal sign is the expanded form of the RNN. The initial input is x_0 and the output is y_0 and h_0. This means that the input to RNN at time t=0

is x_0 and the output is y_0. The state h_0 of the network neuron at t=0 is stored in A. When t=1, state h_1 of the network neuron at this time is determined by both the input x_1 at t=1 and the state h_0 of the neuron at t=0. The rest of the computation is the same until t reaches the end of the time series.

In the original RNN, the value of the hyperbolic tangent function of the network's input at t and the state of the neuron at t-1 together form the state of neuron A at time t. This value is both the output of the network at this moment and will also be the state of the network at the next moment. And this process of continuous transmission to the next stage is called RNN's forward propagation.

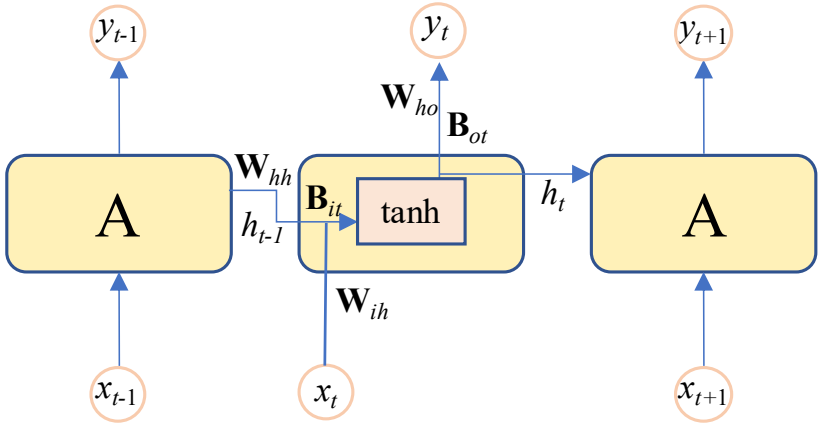


Figure 2.2 RNN Internal Structure Diagram

$\mathbf{W}_{ho}$ is the $l \times n$ weight matrix connecting n hidden layer units to l output layer units.

$\mathbf{W}_{ih}$ is the $n \times k$ weight matrix connecting k input units to n hidden layer units.

$\mathbf{W}_{hh}$ is the $n \times n$ weight matrix connecting n hidden layer units from time t-1 to time t.

$\mathbf{B}_{it}$ is the bias matrix of input operation.

$\mathbf{B}_{ot}$ is the bias matrix of output operation.

The calculation process of RNN described in Figure 2.2 is illustrated by the following equations:

$$h_t = f(W_{ih}x_t + W_{hh}h_{t-1} + B_{it}) \tag{2.1}$$

$$f(x) = tanh(x) = \frac{sinh(x)}{cosh(x)} = \frac{e^x - e^{-x}}{e^x + e^{-x}} \tag{2.2}$$

$$y_t = g(W_{hy}h_t + B_{ot}) \tag{2.3}$$

$$y_t = g\left(W_{hy}\left[f(W_{ih}x_t + W_{hh}h_{t-1} + B_{it})\right] + B_{ot}\right) \tag{2.4}$$

RNN is limited by the so-called short-term memory problems. For a sufficiently long sequence, it is difficult to pass information of an earlier time step to a later time step in RNN. Therefore, RNNs loses large amounts of important information at the beginning when processing a long sequence of data for prediction. This is mainly due to the disappearance of the gradient in the RNN during the backpropagation process. The gradient is used to update the weight of the neural network. The disappearance of the gradient means that the gradient decreases as time evolves. If the gradient value becomes very small, RNN will stop learning. Therefore, the network layer with little change of the gradient stops learning, and these layers usually belong to the earlier layers. Since these layers do not learn, what needs to be learned in longer sequences is hard to remember by RNN, hence the name short-term memory comes.

In order to avoid the weakness of the traditional RNN, in this study, we use its improved version, long short-term sequence memory networks, or commonly called the LSTM network. LSTM overcomes the above disadvantages of RNN and is able to analyze and learn the dependencies within long sequences. Hochreiter and Schmidhuber first proposed the LSTM in 1997, which has been refined and promoted in the research community. Analysis of long sequence data and the ability to retain critical information is the LSTM's core competency. All RNN are composed of one-by-one repeating chains of

neurons. Unlike the standard RNN which contains a simple repetitive module with only one tanh function layer, this LSTM has a similar chain structure and contains four neural network layers, and these four neural network layers are interconnected in a special way. The diagram of the internal structure is shown in Figure 2.3.

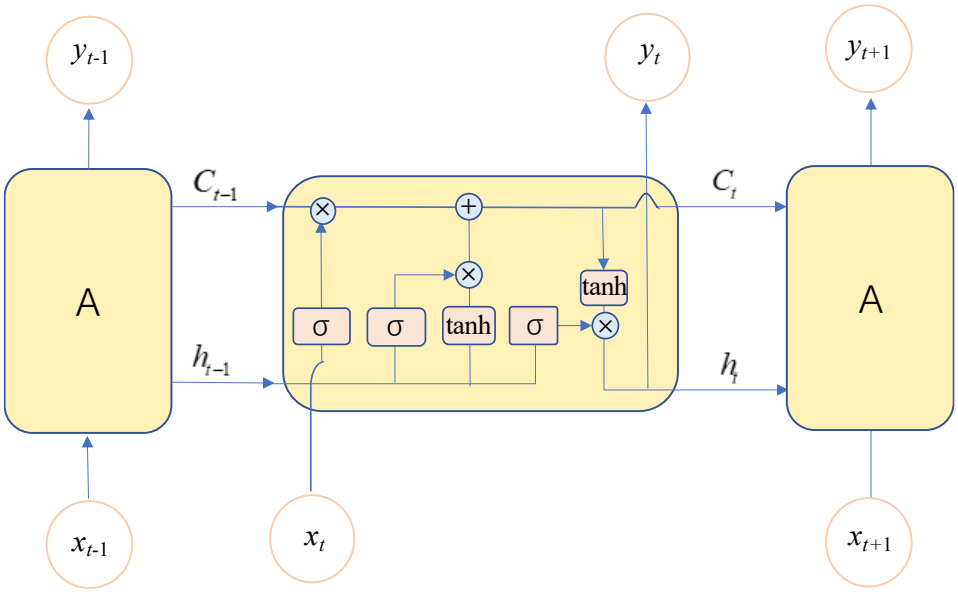


Figure 2.3 LSTM Internal Structure Diagram

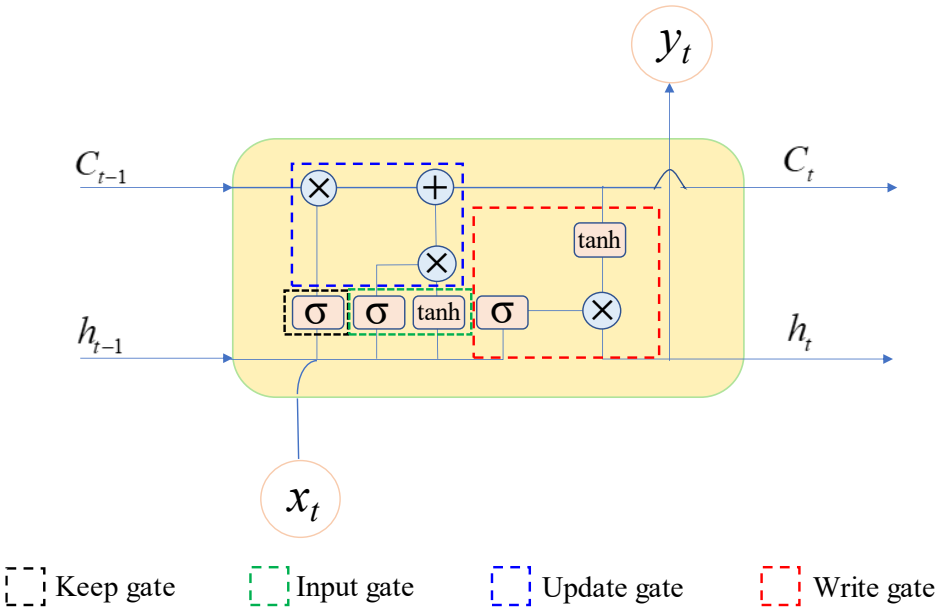


Figure 2.4 The Four Gates of the Model

For the LSTM in Figure 2.4, these four neural network layers are called keep gate, write gate, read gate, and update gate, respectively. It is through these gates that LSTM controls the amount of information transmitted. The upper-layer information C is only numerically transformed with the values of these gates during the transmission process and does not need to be matrix-multiplied with the entire network parameter **W**, hence avoiding gradient explosion or gradient disappearance that may occur when returning gradients.

The first step in the LSTM is to determine which state information needs to be discarded, this process is implemented by a sigmoid function layer called keep gate. This gate calculates the value of $h_{t\text{-}1}$ and x_t and outputs a number between 0 and 1, Then this number will be multiplied by the state at the previous moment $C_{t\text{-}1}$. Particularly 1 means "fully maintained" and 0 means "fully forgotten". The computation formula is given as follows (Hochreiter and Schmidhuber 1997),

$$sigmoid(t) = \frac{1}{1+e^{-t}} \tag{2.5}$$

$$f_t = sigmoid(W_f \cdot [h_{t-1}, x_t] + B_f) \tag{2.6}$$

The new information that can be saved in the unit state will be determined in the next step. First, the sigmoid layer called the "input gate" determines which values to be updated. Second, a vector of new candidate values $\tilde{C}_t$ is created by the tanh layer, which can be added to the state. The calculation formula is given by,

$$i_t = sigmoid(W_i \cdot [h_{t-1}, x_t] + B_i) \tag{2.7}$$

$$\tilde{C}_t = tanh(W_C \cdot [h_{t-1}, x_t] + B_C) \tag{2.8}$$

The old cell state $C_{t\text{-}1}$ will be updated to the new cell state C_t in the third step.

First, the old state C_t-1 is multiplied with f_t to discard the information to be forgotten. Then the candidate state $\tilde{C}_t$ is multiplied by 1- f_t to update the state.

$$C_t = f_t \times C_{t-1} + (1 - f_t) \times \tilde{C}_t \tag{2.9}$$

Finally, the output should be decided. The output is supposed to be based on the cell state, but it should be processed further. First, a sigmoid layer is run to determine which parts of the unit state should be output. Then the cell state is fed into tanh (limiting the value between -1 and 1) and the result is multiplied by the result of sigmoid gate so that the desired output is obtained.

$$O_t = sigmoid(W_o[h_{t-1}, x_t] + B_o) \tag{2.10}$$

$$h_t = O_t \times tanh(C_t) \tag{2.11}$$

In this study, we build a neural network model consisted of a layer of LSTM with a fully connected layer based on the Keras module (https://keras.io/), which is an open-source artificial neural network library written in Python for the design, debugging, evaluation, application, and visualization of deep learning models. The LSTM layer produces a 20-dimensional data, after passing through the fully connected layer. These data become a one-dimensional data sequence representing the one hour ahead forecasting result.

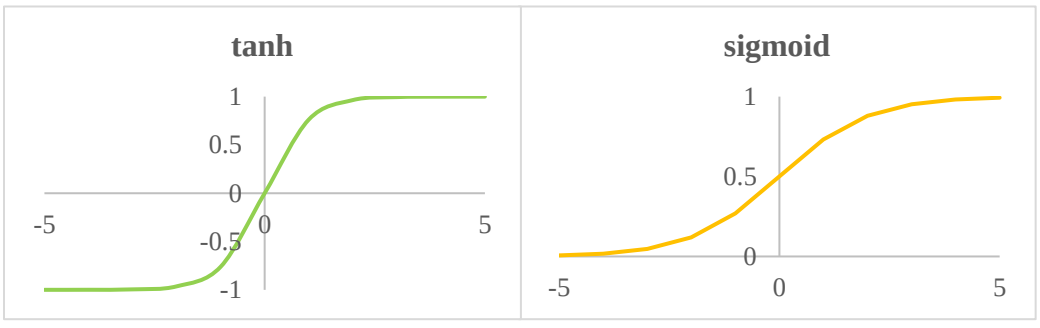


Figure 2.5 Tanh and Sigmoid Function

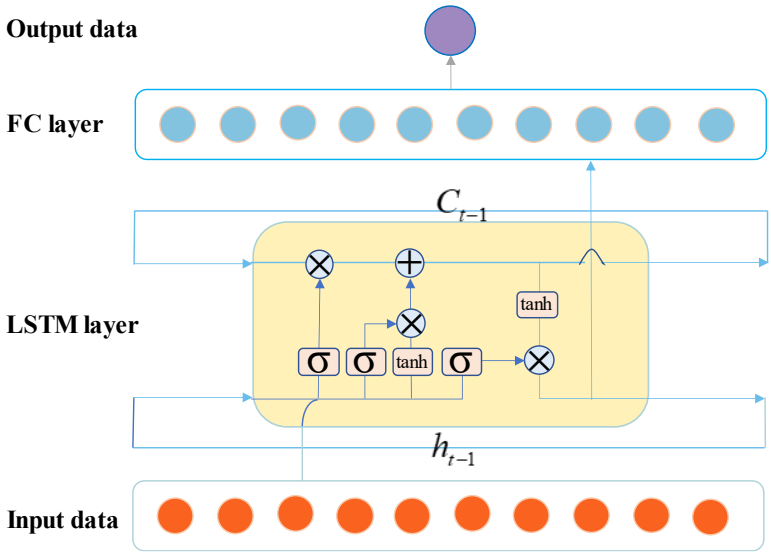


Figure 2.6 The Model Structure

2.2 Numerical Experiment

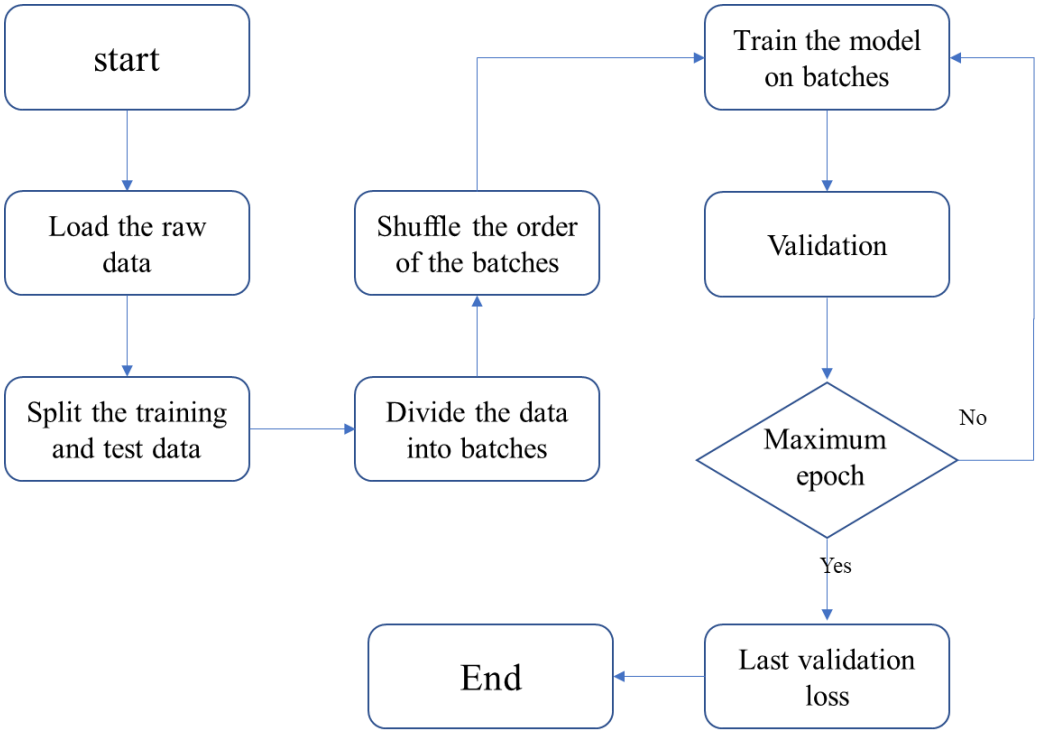


Figure 2.7 Forecasting Model Flowchart

The 18-year data set used in this study is from the ERCOT from January 1, 2002

to February 1, 2020. It is an hourly data set with a total of 158,521. In this data set, there are ten columns of data, the first column is the time stamp, the second to the ninth columns are the respective power load of the eight regions under the jurisdiction of ERCOT, and the last column is the sum of the power loads of the eight regions. The first 12 rows of data in the data set are shown in Table 2.1. Firstly, we need to normalize the data, importing the raw data into memory. Then, normalizing the raw data by subtracting the mean and then dividing by the standard deviation for each feature. The processed data conforms to the standard normal distribution, that is, the mean is 0 and the standard deviation is 1. There are two reasons for standardizing the raw data. First, removing the dimensions associated to the data. Hence different features can have the same scale and thus be comparable or weighted. Second, reducing the range of the initial data. If there exists a huge discrepancy between the data range of the initial data set, the data with a larger range will dominate those with a smaller range. For example, a data set with a range of 0 to 100 will dominate the data with of 0 to 1, resulting in biased outcome. The ultimate goal is to make each variable have the same effect on the analysis. In the second step, we split all the characterized data into training data and validation data, normally, 60% to 70% of the data is used for model training, and the remaining data are for testing purpose. Hence the first 95,000 of data in the dataset are training data and the last 63,521 records are used as validation data. The training dataset is used to train our model, and the validation data is used to test the trained model to generate loss feedback. Before entering the data into the model, we divided all the data into data batches, each batch has 256 pieces of data records to reduce the complexity of training. Then all the batches are shuffled according to a buffer size of 500 to increase the complexity between the input

and output data to reduce overfitting. During the training process, we use the Adam algorithm as our optimization algorithm. It optimizes the weight parameters and bias parameters to reduce the gap between the output value and the true value. We divide each epoch into 200 steps, executing 50 verifications at the end of each step, and using mean squared error (MSE) as our loss function to calculate the difference between the predicted value and the actual value. After 60 epochs, the validation loss is 0.0150.

Table 2.1 Part of the Dataset

Hour_End	COAST	EAST	'AR_WES'	NORTH	NORTH_C	OUTHER	SOUTH_C	WEST	ERCOT	Unit
2002/1/1 1:00	8331.47	1111.10	1094.05	995.30	10336.30	2165.01	4793.19	843.75	29670.16	MW
2002/1/1 2:00	8107.81	1091.48	1083.52	981.20	10178.05	2092.37	4766.92	835.49	29136.83	MW
2002/1/1 3:00	7890.72	1080.26	1085.04	971.31	10100.89	2042.08	4702.92	830.69	28703.91	MW
2002/1/1 4:00	7799.82	1079.73	1093.38	971.26	10081.57	2011.94	4669.06	835.07	28541.82	MW
2002/1/1 5:00	7815.97	1087.93	1106.65	982.54	10192.22	2002.49	4695.01	848.60	28731.41	MW
2002/1/1 6:00	7978.54	1101.93	1133.69	998.84	10402.11	2042.53	4777.18	874.84	29309.66	MW
2002/1/1 7:00	8133.22	1136.17	1169.70	1028.54	10655.38	2095.83	4945.76	923.41	30088.02	MW
2002/1/1 8:00	8136.47	1169.03	1219.35	1057.05	10881.09	2108.91	5052.62	975.94	30600.47	MW
2002/1/1 9:00	8088.58	1206.36	1226.70	1071.66	11287.13	2203.82	5155.20	992.50	31231.96	MW
2002/1/1 10:00	8254.43	1254.37	1248.63	1104.56	11721.67	2361.59	5375.23	1028.08	32348.55	MW
2002/1/1 11:00	8480.22	1267.46	1251.45	1114.90	11921.91	2465.14	5501.73	1040.43	33043.24	MW
2002/1/1 12:00	8646.21	1255.89	1240.02	1088.91	11827.44	2504.45	5501.57	1030.10	33094.59	MW

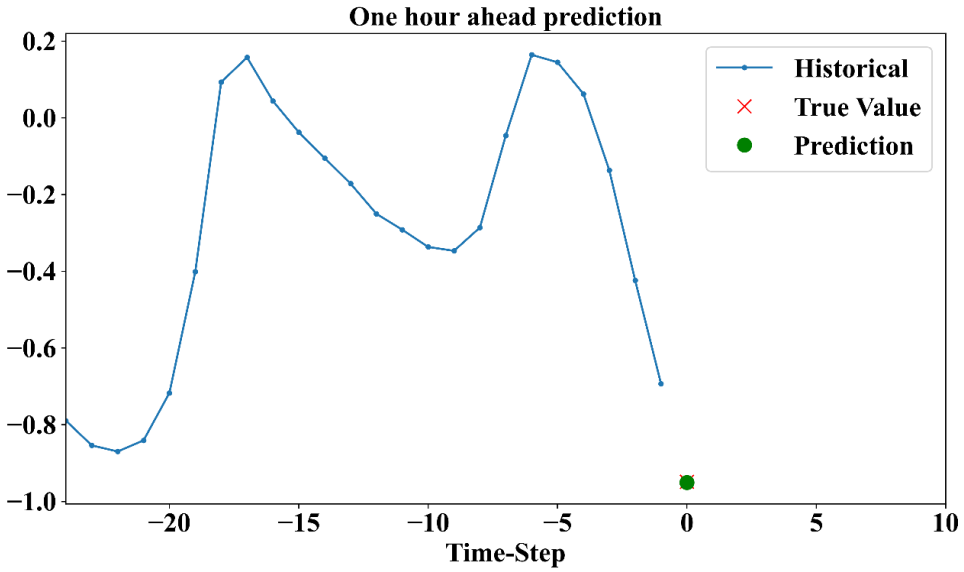


Figure 2.8 The Four Gates of the Model

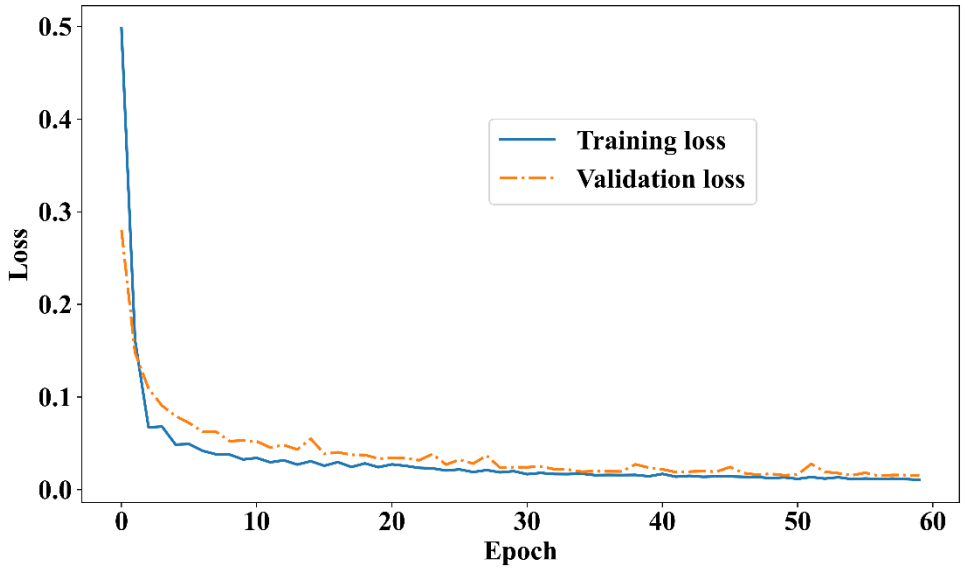


Figure 2.9 One Hour Ahead Prediction Result

2.3 Sensitivity Analysis

A sensitive analysis on the validation loss is performed. Two main factors are considered for the effect of validation loss. The first factor is the proportion of training data to the total data, and the second case is the effect of loss function on the validation loss. Normally using 60% - 70% of the total training data is expected to generate the best model, and for this reason, we set 60% as the benchmark. We add two more cases in sensitivity analysis with the training data being 75% and 50% of the total data, respectively.

For the second factor, mean absolute error (MSE) is used as our loss function in the benchmark study. It has the advantage of considering the average size of the error without considering its direction. However, because of the squared, the predicted value that deviates more from the true value will be penalized more severely than the predicted value that deviates less. In the sensitivity analysis we also add two cases for this type of factor, and the loss functions of the two cases are MAE and mean squared logarithmic

error (MSLE), respectively. MAE measures the average of the sum of the absolute differences between the predicted and the actual values. Like MSE, this measure also measures the magnitude of the error without considering the direction. As for MSLE, its penalty on underprediction is larger than overprediction, which is suitable for certain applications imposing larger underprediction losses. For instance, it is preferable to overpredict the power demand, because the consequence of generation shortage due to underprediction of load is much severer than overgeneration. The results are listed in Table 2.2.

Table 2.2 Sensitivity Analysis Results

Cases	Validation loss
Benchmark (training data 60%, MSE)	0.0150
Case 1 (training data 50%, MSE)	0.0191
Case 2 (training data 75%, MSE)	0.0176
Case 3 (training data 60%, MAE)	0.0932
Case 4 (training data 60%, MSLE)	0.2467

We can see from the results that 60% of training data and MSE evaluation function generate the lowest validation loss. Increasing or decreasing the percentage of training data will affect the final results. The MSE as the evaluation function is also the most suitable for the current model.

3. VIRTUAL POWER PLANTS PARTICIPATION IN ELECTRICITY MARKET

3.1 Background and Decision-making Algorithm

3.1.1 The VPP Introduction

Distributed power sources do not have sufficient capacity, flexibility and control to make the operation of power plants both cost-justified and technically feasible when operated in isolation, both in terms of management as well as market premise. However, these problems are solved when a group of distributed energy sources are integrated into a VPP. It can contribute to the overall operations of the grid by participating in the electricity market operations. A VPP is the equivalent of a generating station with a transmission system when participating in electricity market activities, such as: being responsible for setting generation schedules, limiting generation caps, controlling operating costs, etc. With these functions, an independent VPP can be in contact with other players in the power operation at any time and provide the appropriate services. While selling electricity through wholesalers. The concept of the VPP makes it possible to put distributed energy sources into grid operation on a large scale and also to provide services for the management of the distribution system.

The current electricity market is usually operated through a bidding process, in which power plants send their committed electricity sales and preferred prices to the day-ahead market (i.e., one day in advance) to participate in the electricity auction. VPP can also participate in the electricity market in the same way. However, unlike a centralized power plant, a VPP, as a microgrid, must first consider the power supply for its own load. Prior to participating in the auction of power in the next day market, the VPP must also

forecast its own power load of the next day. The projected energy surplus is then sold to the electricity market. This completes the day-ahead market operation. In the actual delivery day, VPP first delivers the planned power to the grid according to the plan. Subject to the fluctuation of renewables generation and power load, VPP needs to use CHP and energy storage devices to maintain its own energy demand, or even purchase from the main grid to meet its own power shortage. This completes the intraday market operation.

In the day-ahead market, we only need to use the LSTM model proposed in Chapter 2 to predict the weather conditions for the coming day, and then get the next day's power generation and the power load to get the estimated power sales. However, in the intraday market, we need to constantly adjust the efficiency of CHP and even the power trading with the main grid based on the real-time renewable's generation and the load in the microgrid, which requires a very large amount of computation, and a suitable algorithm is especially important due to the computational performance. The rolling horizon algorithm is used to perform this part of the computation.

3.1.2 Rolling Horizon Algorithm

As shown in Figure 3.1, given a scheduling horizon, the scheduling horizon in this research is 24 hours, and then given a prediction horizon and a control horizon. First, set the initial parameters of the system, such as the length of scheduling, prediction and control horizons, and the initial value of the energy storage system is zero, and also calculate the total number of iterations. The second step is to update uncertain parameters and the state of the system, such as the state of the energy storage device, and then solve the deterministic problem for the considered prediction horizon. Using the obtained

variable values calculates the operating cost of the system in this CH phase. Here we assume that the length of the control horizon is equal to the interval of data update, which is one hour. Until the entire scheduling horizon is iterated, we then terminate the algorithm. The sum of the optimal solutions of each control interval is the final solution of the entire scheduling horizon.

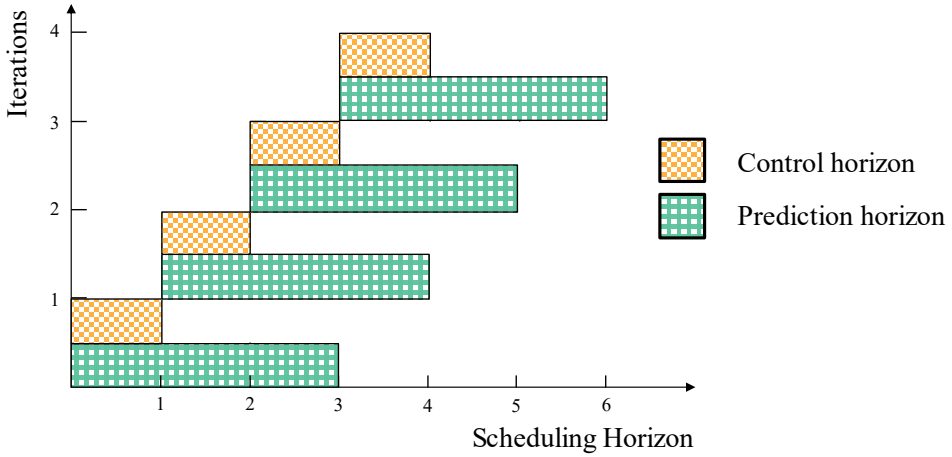


Figure 3.1 Rolling Horizon

3.2 Model Formulation

In this research the VPP system is comprised of CHP, WT, PV, and energy storage units for both electricity and thermal energy generation. As shown in Figure 3.2, the system consists of two models representing the two stages of the system's operations, namely the day-ahead model and the intraday model. The model parameters are summarized in Table 3.1. The decision variables are listed in Table 3.2.

Table 3.1 Notation for Model Parameters

Notation	Comments
T	Day-ahead planning horizon (h)
S	Number of scenarios of day-ahead renewable power generation forecasts.
p_s	Probability of occurrence for each scenario s
t	Horizon time (hour)
c^f	Fuel cost of CHP during interval t ($/MWh)
c^o	Operational cost of electrical storage unit during interval t ($/MWh)
ρ_t^{se}	Forecasted day-ahead market price per amount of energy ($/MWh)
$E_{\min}^{chp}$, $E_{\max}^{chp}$	Maximum and minimum electrical power injection of CHP unit (MW)
E_t^r	Electrical power injection of renewable energy sources (MW)
E_t^p , P_t^{th}	Total electrical and thermal load in VPP (MW)
S_t^e	Energy level of electrical storage unit (MWh)
η^{pt}	CHP heat-to-power ratio
$S_{\min}^e$, $S_{\max}^e$	Minimum and maximum energy level of electrical storage unit (MWh)
S_t^{th}	Energy level of thermal storage unit (MWh)
$S_{\min}^{th}$, $S_{\max}^{th}$	Minimum and Maximum energy level of thermal storage unit (MWh)
c^p	Penalty cost for intraday imbalances ($/MWh)

Table 3.2 Decision Variables of VPP Model

Notation	Comments
E_t^m	Active power trading in the day-ahead energy market (MW)
E_t^{chp}	Electrical power injection of CHP unit (MW)
E_t^b	Active power imbalance trading in intraday energy market (MW)
E_t^c , E_t^d	Electrical power charge and discharge unit (MW)
P_t^c , P_t^d	Thermal power charge and discharge unit (MW)

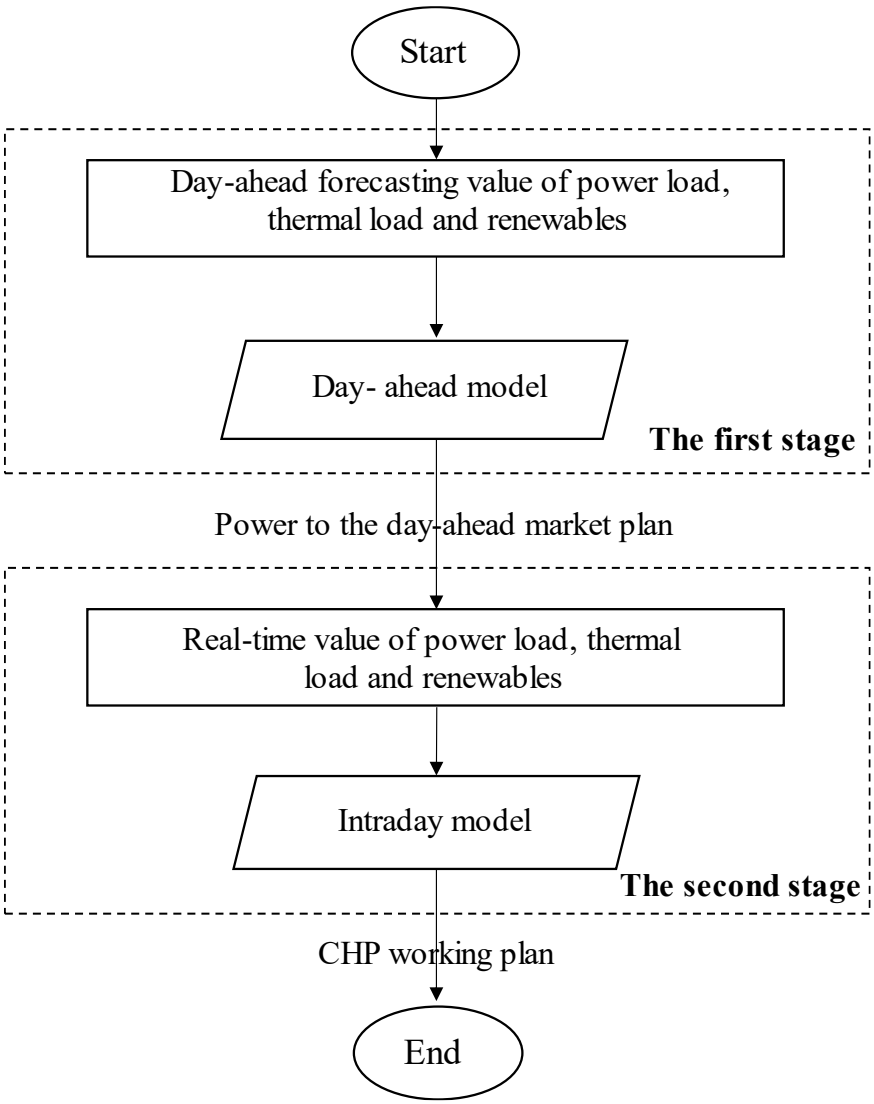


Figure 3.2 Flowchart of the Model

Model 3.1: Day-Ahead Market (Model DA)

Minimize:

$$f(E_t^{chp}, E_t^{ch}, E_t^{dc}, E_t^{m}) = \sum_{t=1}^{T} \left(c^{f} \cdot E_t^{chp} + c^{o} \cdot E_t^{c} + c^{o} \cdot E_t^{d} - \rho_t^{se} E_t^{m} \right) \tag{3.1}$$

Subject to:

$$E_t^{chp} + E_t^{r} + E_t^{d} - E_t^{c} - E_t^{m} = E_t^{p}, \qquad \forall t \tag{3.2}$$

$$\eta^{pt} \cdot E_t^{chp} + P_t^{d} - P_t^{c} = P_t^{th}, \qquad \forall t \tag{3.3}$$

$$S_t^e = S_{t-1}^e + E_t^c - E_t^d, \qquad \forall t \tag{3.4}$$

$$S_t^{th} = S_{t-1}^{th} + P_t^c - P_t^d, \qquad \forall t \tag{3.5}$$

$$S_{\min}^{th} \le S_t^{th} \le S_{\max}^{th}, \qquad \forall t \tag{3.6}$$

$$S_{\min}^{e} \le S_t^{e} \le S_{\max}^{e}, \qquad \forall t \tag{3.7}$$

$$E_{\min}^{chp} \le E_t^{chp} \le E_{\max}^{chp}, \qquad \forall t \tag{3.8}$$

$$E_t^m, E_t^c, E_t^d, P_t^d, P_t^c \ge 0, \qquad \forall t \tag{3.9}$$

$$S_0^{th}, \ \ S_0^e = 0 \ , \tag{3.10}$$

The cost of day-ahead market consists of CHP fuel cost, the operational cost of electric storage and the income from electricity to the day-ahead market, the day-ahead market cost is formulated as (3.1). Constraint (3.2) is the hourly electric power balance equation. It represents the amount of power generated by CHP, the amount of power provided by the storage device plus the amount of power generated by renewables, minus the amount of power supplied to the day-ahead market equals the load of VPP. Equation (3.3) is the hourly thermal power balance equation. All the thermal power produced minus the thermal stored equals the thermal load in the system. Constraint (3.4) is the constraint of the charging and discharging process. Constraint (3.5) is the charging and discharging process of the thermal storage units. Constraints (3.6) to (3.8) are the capacity constraint of the energy storage units. Constraint (3.9) is the sign constrain. Constraint (3.10) assumes that the initial energy of in the storage device is zero.

In this case, we use the generation data, the thermal and power load from Chapter 2. The electricity price, the fuel price, storage operation cost, the renewable generator capacity, CHP capacity and storage capacity are based on references (Despina et al. 2018;

EIA 2019). The ratio of electricity and heat generation of CHP is 1.21 to 1.

After the settlement of the day-ahead market, the system begins the planning for intraday operations, in which it first delivers power to the day-ahead market as planned, and then maintains the system's supply and demand balance through CHP and storage devices based on the updated projected renewables generation. If CHP cannot meet the power shortage, the VPP system purchases power E_t^b from the utility grid. In order to reduce the cost of the system, the primary goal of intraday planning is to minimize E_t^b, because larger E_t^b will significantly increase the system cost. The objective function of the intraday market model consists of the CHP fuel cost and the operating cost of the energy storage device, while the operating cost of the energy storage is dependent on the amount of electricity being transacted:

Model 3.2: Intra-Day Market Model (Model ID)

Minimize

$$f(E_t^{chp}, E_t^{ch}, E_t^{dc}, E_t^m, E_t^b) = \sum_{t=1}^{T} \left(c^f \cdot E_t^{chp} + c^o \cdot E_t^c + c^o \cdot E_t^d + c^p \cdot E_t^b - \rho_t^{se} E_t^m \right) \quad (3.11)$$

Subject to:

$$E_t^{chp} + E_t^r + E_t^d + E_t^b - E_t^c - E_t^m = E_t^p, \qquad \forall t \quad (3.12)$$

$$\eta^{pt} \cdot E_t^{chp} + P_t^d - P_t^c = P_t^{th}, \qquad \forall t \quad (3.13)$$

$$S_t^e = S_{t-1}^e + E_t^c - E_t^d, \qquad \forall t \quad (3.14)$$

$$S_t^{th} = S_{t-1}^{th} + P_t^c - P_t^d, \qquad \forall t \quad (3.15)$$

$$S_{\min}^{th} \le S_t^{th} \le S_{\max}^{th}, \qquad \forall t \quad (3.16)$$

$$S_{\min}^{e} \le S_t^{e} \le S_{\max}^{e}, \qquad \forall t \quad (3.17)$$

$$E_{\min}^{chp} \le E_t^{chp} \le E_{\max}^{chp}, \qquad \forall t \tag{3.18}$$

$$E_t^m, E_t^c, E_t^d, P_t^d, P_t^c \ge 0, \qquad \forall t \tag{3.19}$$

$$S_0^{th}, \ S_0^e = 0, \tag{3.20}$$

The intraday market cost is formulated in Equation (3.11). The difference between objective functions (3.11) and (3.1) is that Model ID also considers the cost of purchasing electricity from the grid based on the day-ahead model or Model DA. Equations (3.12) and (3.13) represent the hourly supply and demand balance of electrical and thermal energy within one day, respectively. Both take into account the total amount of energy generated and the amount sold to the day-ahead market. Constrains (3.14) to (3.20) are the same as Constraints (3.4) to (3.10) of the day-ahead model.

3.3 System Setting

The primary focus of this part is to determine the CHP operating schedule and the amount of power sold to the day-ahead market in each time period. After the internal supply and demand of the VPP is balanced in the day-ahead market, we input the power generation data of the day-ahead market decision into the second phase, i.e., the intraday market, to obtain the real-time operating schedule of the CHP and power purchase plan from the grid if necessary. Figures 3.3 shows the predicted and true values of renewables generation thermal load and power load for one day ahead, respectively.

Table 3.3 Data of the VPP Intra-Day Planning

Notation	Value	Unit
S	3	n/a
T	24	hour
c^f	44	$/MWh
c^o	2	$/MWh

$S_{\min}^{th}$	0	MWh
$S_{\max}^{th}$	135	MWh
$S_{\min}^{e}$	0	MWh
$S_{\max}^{e}$	90	MWh
$E_{\max}^{chp}$	135	MW
$E_{\min}^{chp}$	0	MW
η^{pt}	0.8	n/a

Table 3.4 Hourly Electricity Price (unit: $/MWh)

Hour	Selling price	Buying price
1	37	42
2	37	42
3	37	42
4	37	42
5	37	42
6	38	43
7	38	43
8	40	45
9	40	45
10	40	45
11	45	50
12	45	50
13	45	50
14	41	46
15	41	46
16	41	46
17	42	47
18	45	50
19	45	50
20	45	50
21	45	50
22	43	48
23	41	46
24	39	44

Table 3.5 Forecastion of Renewable Generation, Thermal and Power Load (unit: MW)

	Intraday	Day-ahead	Intra-day	Day-ahead	Intra-day	Day-ahead
hour	Renewable power		Thermal load		Electricity load	
1	183	155	79	84	197	199
2	163	155	62	70	161	171
3	142	155	83	73	188	192
4	176	165	79	76	197	195
5	177	175	75	79	183	183
6	199	180	70	76	192	210
7	172	185	75	68	205	190
8	208	225	62	56	262	259
9	235	215	49	40	224	237
10	201	220	37	36	270	265
11	219	230	38	37	271	263
12	265	245	44	34	275	264
13	260	235	42	33	240	189
14	265	210	32	38	185	185
15	255	195	33	36	199	214
16	240	165	55	53	278	270
17	180	175	59	60	264	264
18	150	170	65	71	275	278
19	151	165	99	89	279	283
20	161	155	86	82	295	295
21	143	155	75	80	289	270
22	146	155	75	75	270	206
23	151	155	78	81	231	233
24	168	155	72	75	156	174

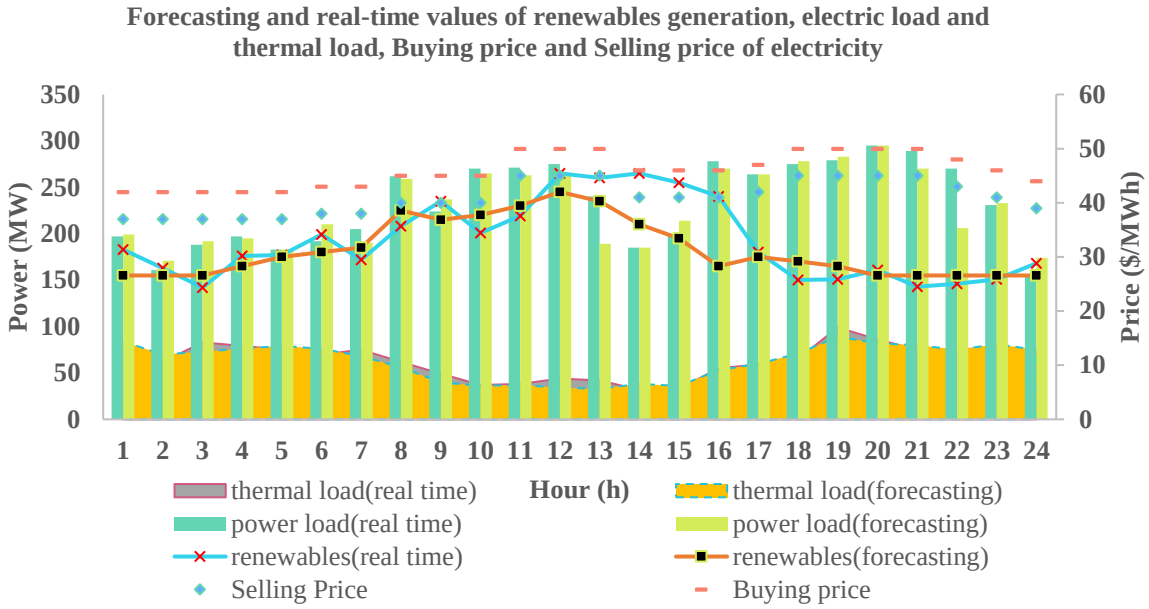


Figure 3.3 Input Data

3.4 Results and Discussion

Essentially day-ahead (DA) and intro-day (ID) models are deterministic models with only one scenario. The objective functions are to minimize the total VPP cost. The thermal storage system is assumed to have a relatively low cost compared with battery energy storage unit. By inputting the data in the Tables 3.3 to 3.5 (EIA 2019, Despina Koraki and Kai Strunz 2018, NREL 2019, ERCOT 2020), we solve Models 3.1 and 3.2 to schedule the daily CHP working schedule and electricity transaction scheme over 24 hours for the VPP system, respectively.

Model 3.1 or DA contains 194 decision variables and 98 constraints and is coded with Advanced Mathematical Programming Language (AMPL) software. CPLEX solver is used to search for the optimal CHP working schedule and power traded in the day-ahead market, electric charging and discharging amount in the storage unit for minimizing $f(E_t^{chp}, E_t^{ch}, E_t^{dc}, E_t^{m})$. The power traded in the day-ahead market serves as

input into the intraday model to minimize $f(E_t^{chp}, E_t^{ch}, E_t^{dc}, E_t^m, E_t^b)$. The intraday model also contains 194 decision variables and 98 constraints. The AMPL code is executed in Intel(R) Core (TM) i5-7200U CPU @ 2.5GHz, 4 Core(s), and 24 GB memory, 4 logical processor with running time of 0.016 second. The rolling horizon algorithm is employed to solve this model. The prediction and the control horizon are 3 hours and 1 hour, respectively. The minimum operation cost is $f(E_t^{chp}, E_t^{ch}, E_t^{dc}, E_t^m, E_t^b)$ =$66,510 per day. The results of decision variables are tabulated in Tables 3.6 and 3.7. A graphical representation of the results is further shown in Figure 3.4.

Table 3.6 Day-ahead Energy Planning (unit: MWh)

Time	E_t^m	E_t^{chp}	E_t^c	E_t^d	S_t^e	P_t^c	P_t^d	S_t^{th}
0	.	.	.	.	0	.	.	0
1	0	135	91	0	91	24	0	24
2	119	135	0	0	91	38	0	62
3	0	135	0	0	91	35	0	97
4	98	55.5	0	0	91	0	31.6	65.4
5	0	17	9	0	100	0	65.4	0
6	105	135	0	0	100	32	0	32
7	40	45	0	0	100	0	32	0
8	64	98	0	0	100	22.4	0	22.4
9	0	22	0	0	100	0	22.4	0
10	0	45	0	0	100	0	0	0
11	127	135	0	25	75	71	0	71
12	49.5	68.5	0	0	75	20.8	0	91.8
13	46	0	0	0	75	0	33	58.8
14	0	0	25	0	100	0	38	20.8
15	0	19	0	0	100	0	20.8	0
16	0	105	0	0	100	31	0	31
17	0	89	0	0	100	11.2	0	42.2
18	5.5	113.5	0	0	100	19.8	0	62
19	112	135	0	95	5	19	0	81
20	0	135	0	5	0	26	0	107
21	20	135	0	0	0	28	0	135
22	0	51	0	0	0	0	34.2	100.8
23	0	78	0	0	0	0	18.6	82.2
24	0	19	0	0	0	0	59.8	22.4

Table 3.7 Intra-day Energy Planning (Unit: MWh)

Time	E_t^{chp}	E_t^c	E_t^d	S_t^e	P_t^c	P_t^d	S_t^{th}	E_t^b
0	.	.	.	0	.	.	0	.
1	99	0	0	0	0	0	0	0
2	117	0	0	0	32	0	32	0
3	64	0	0	0	0	32	0	0
4	135	0	0	0	29	0	29	0
5	58	0	0	0	0	29	0	0
6	108	10	0	10	17	0	17	0
7	94	0	0	10	0	0	17	0
8	118	0	0	10	32	0	49	0
9	23	34	0	44	0	31	18	0
10	69	0	0	44	18	0	36	0
11	135	0	44	0	70	0	106	0
12	60	0	0	0	0	53	53	0
13	67	0	0	0	12	0	65	0
14	0	0	0	0	0	32	33	0
15	0	0	0	0	0	33	0	0
16	69	31	0	31	0	0	0	0
17	135	51	0	82	49	0	49	0
18	135	5	0	86	43	0	92	0
19	135	0	86	0	9	0	101	19
20	135	1	0	1	22	0	123	0
21	135	0	1	0	0	123	0	30
22	135	0	0	0	33	0	33	0
23	135	0	0	0	30	0	63	0
24	11	0	0	0	0	63	0	0

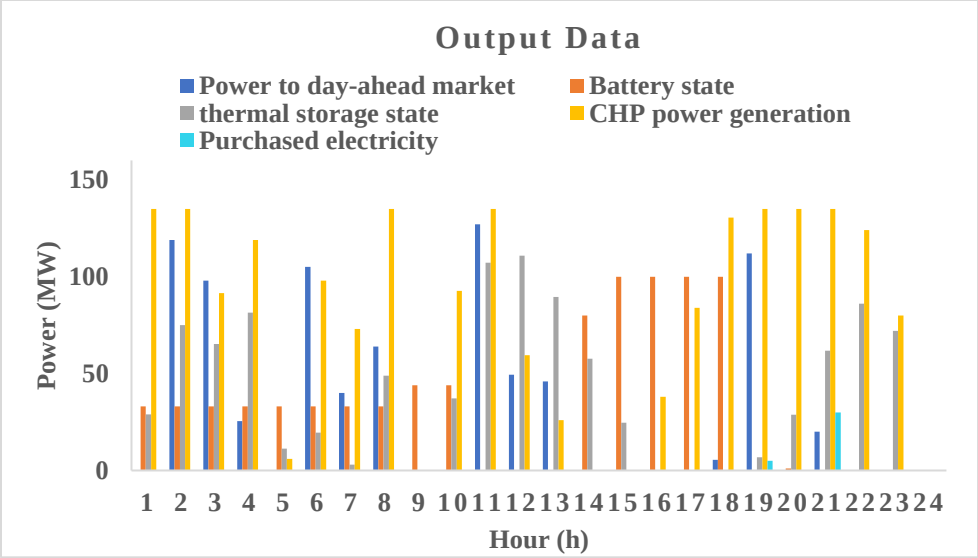


Figure 3.4 Results of Models

Tables 3.6 and 3.7 show the results of decision variables of Models 3.1 and 3.2, respectively. From the E_t^m column of Table 3.6 we can see that there are three peak periods for selling electricity, the first is from 1:00 a.m. to 8:00 a.m. This time is the low point of electricity consumption in the microgrid, and the system chooses to sell surplus electricity into the grid. The second time is from 11:00 am to 1:00 pm, and the third time period is from 6:00 pm to 9:00 pm. These two time periods are the peak of the microgrid's electricity consumption, but the system still chooses to sell electricity, both by turning on the CHP to the maximum and discharging all the electricity in the energy storage system, because the price of electricity in these two time periods is the highest and selling electricity at this time can be the most profitable for the system. From the column E_t^c and E_t^d of Table 3.6, we can find that the system has wisely chosen to charge the energy storage system after electricity consumption peak and when electricity prices are low, and to discharge during electricity consumption peak and when electricity prices are high. From the E_t^b column of Table 3.7, we can see that the only two purchases of

power from the main grid occurred at 7:00 and 9:00 pm, which are the peak hours of electricity consumption, while renewables generation was declining, indicating that the power demand in the microgrid could not be met during this time period, even if CHP is operating at maximum power. We can also conclude that because of the high price of power purchase, the system chooses as little power purchase as possible to reduce the cost of the microgrid. The model can reasonably manage energy storage system according to the real-time generation and power demand in the microgrid, hence improving the energy utilization efficiency. In order to test the influence of the prediction horizon and control horizon on the final results, a sensitivity analysis is performed. The results are obtained and shown in Table 3.8. As the prediction and control horizon becomes larger, the total cost becomes larger. It also shows instability because as the prediction horizon becomes larger, the accuracy of the input data decreases, which directly affects the final output, so there is no monotonicity trend from Case 2 to 4.

Table 3.8 Sensitivity Analysis

Case	Comments	Total cost ($)
1	Prediction horizon 3 hours, control horizon 1 hour	66,510
2	Prediction horizon 4 hours, control horizon 2 hour	79,001
3	Prediction horizon 6 hours, control horizon 3 hour	84,026
4	Prediction horizon 8 hours, control horizon 4 hour	74,847

4. FACILITY-MICROGRID LOCATION-ALLOCATION MODEL

4.1 Location-Allocation Model

4.1.1 Network Setting

Fixed charge model is a discrete location problem that has the objective to minimize total fixed cost of selecting candidate facilities and the variable costs like transportation. Fixed charge problem considering unit shipment cost between potential facilities to demand locations is originally formulated by Hirsch and Dantzig (1954). Costs in this model arise due to a set of demand point to be served by a set of location candidates (e.g., distribution center). Prior researchers use this model to solve location and allocation problem and its variants (Sule 1981, Nozick and Turnquist 2001b, Nozick and Turnquist 1998, Daskin 2008). Figure 4.1 shows a fixed charge mode implemented in a two-echelon supply chain network comprised of distribution centers (DC) and retail stores. Electric trucks are employed to ship the products from DC to the demand points of the stores.

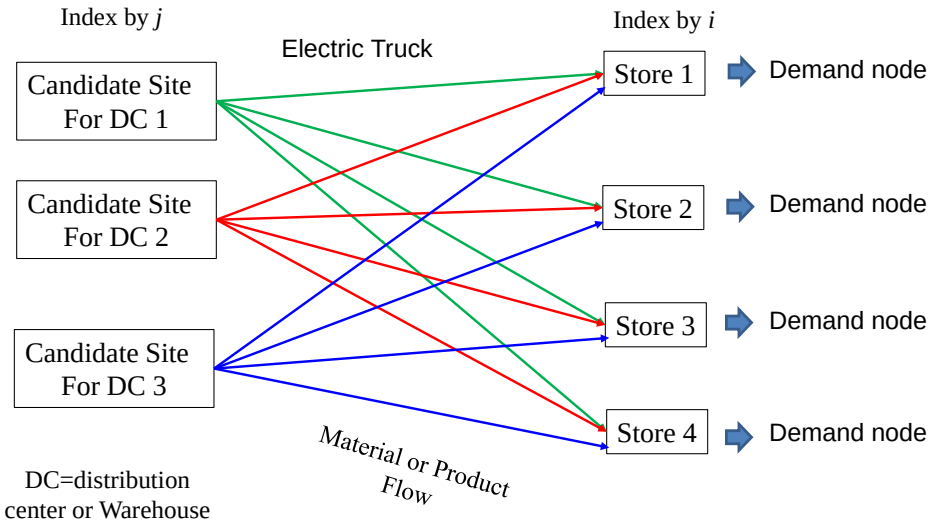


Figure 4.1 Location-Allocation in a DC-to-Retailor Network

Using a location-allocation problem in Figure 4.1 as example. Product demands are generated from the four retail stores. Demands could be quantified in daily, weekly, monthly or yearly basis. The decision variables are to establish the DC or warehouse in three candidate sites to meet the product demand. In this setting, there are three potential cases: establishing one DC only; establishing two DC; or establishing three DC.

4.1.2 Model Formulation

This fixed charge model with capacitated facility location problem is presented under a single sourcing constraint. It is a typical facility location allocation problem considering the demand of the nodes and the capacity of the established facility. The network is set for a problem with two echelons: demand side and facility sites. Typically, the inputs to the problem are the facility setup cost, the product transportation costs, customer demands, and supply capacities.

Table 4.1 Parameters and Variables for Model 4.1 or Fixed Charge Model

Notation	Comments
N	Number of candidate sites for opening DC, for n=1, 2, …, N.
S	Number of candidate sites for opening store, for s=1, 2, …, S.
F_n	Fixed cost of locating a facility at candidate site n.
c_{ns}	Shipping cost per unit distance per unit product between sites n and s.
q_s	Demand at retail store s.
d_{ns}	The distance from store s to DC facility site n.
γ_n	Capacity of the candidate DC site n.
u_n	1 if a DC facility is open at candidate site n, and 0 otherwise. Decision
v_{ns}	1 if demand at store s is served by DC at candidate site n, and 0 otherwise. Decision variable.

Model 4.1: Fixed Charge Model

Min:

$$f(\mathbf{u}, \mathbf{v}) = \sum_{n=1}^{N} F_n u_n + \sum_{s=1}^{S} \sum_{n=1}^{N} q_s c_{ns} d_{ns} v_{ns} \tag{4.1}$$

Subject to:

$$\sum_{n=1}^{N} v_{ns} = 1, \qquad \forall s \tag{4.2}$$

$$\sum_{s=1}^{S} q_s v_{ns} \le \gamma_n u_n, \qquad \forall n \tag{4.3}$$

$$v_{ns} \le u_n, \qquad \text{for } \forall\, n, \text{ and } \forall s \tag{4.4}$$

$$u_n \in \{0, 1\} \tag{4.5}$$

$$v_{ns} \in \{0, 1\} \tag{4.6}$$

The objective function (4.1) consists of two parts: the investment cost of opening facility, and the costs of production and transportation between DC and demand nodes (stores). Constraint (4.2) states that the total demand of node *s* is satisfied by one single DC. Constraint (4.3) states that the total amount of products shipped out of a DC should not exceed its capacity. Constraint (4.4) indicates that the product shipped from sites *n* to demand node *s* becomes possible only if a DC has opened in site *n*. Constraints (4.5) and (4.6) simply defines the binary integer nature of u_n and v_{ns}.

4.1.3 Numerical Experiments

We use the network in Figure 4.2 to perform a preliminary study:

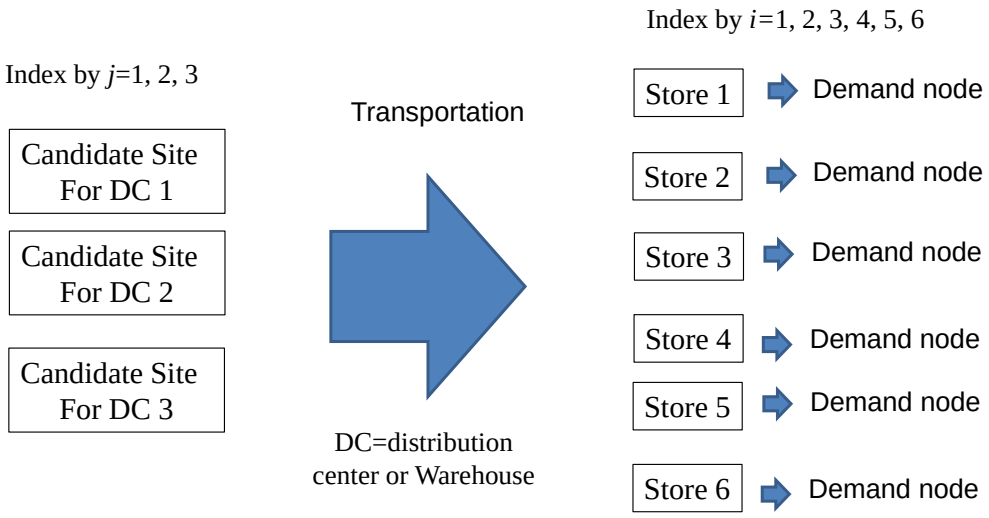


Figure 4.2 A Network with 3 Candidate DC Sites and 6 Demand Nodes

Table 4.2 shows the facility opening cost and the capacity of each site. Table 4.3 provides the unit ship cost per kilometer (km). The distance between site j and demand node s is given in Table 4.4. The customer demand data from individual demand nodes (or stores) is given in Table 4.5.

Table 4.2 Fixed Setup Cost and Capacity of the Candidate Sites

n	Fixed Setup cost F_n ($)	Capacity g_n (items/period)
1	3,500	300
2	7,600	420
3	10,658	550

Table 4.3 Unit Shipment Cost ($/item/km)

	Customers demand nodes s					
Candidate site n	s=1	s=2	s=3	s=4	s=5	s=6
1	19	16	13	19	15	18
2	12	10	11	22	17	16
3	13	12	17	12	8	10

Table 4.4 Distance Between Store *s* and DC Site *n* (unit: km)

	Customers demand node *s*					
Candidate site *n*	*s*=1	*s*=2	*s*=3	*s*=4	*s*=5	*s*=6
1	89	86	51	54	98	49
2	43	36	70	93	64	84
3	99	94	89	57	88	51

Table 4.5 Customer Demands of Stores

Store *s*	Demand q_s (units/period)
1	100
2	80
3	125
4	95
5	115
6	105

4.1.4 Results and Discussion

This model is coded with AMPL software. CPLEX solver is used to search for the optimal solution for minimizing the supply chain cost. All AMPL codes are executed in a PC with Intel(R) Core (TM) i5-7200U CPU @ 2.5GHz, 4 Core(s), 24 GB memory, and 4 Logical Processor. The total cost in this system is $384,523. All three candidate DCs are to be opened, and the specific transportation plan is shown in Table 4.6.

Table 4.6 Transportation Plan

	s=1	s=2	s=3	s=4	s=5	s=6
1	0	0	125	0	0	0
2	100	80	0	0	0	0
3	0	0	0	95	115	105

4.2 Two-Echelon Location-Allocation Model with Microgrid Integration

4.2.1 Nonlinear Model

In this section we expand the fixed charge model or Model 4.1 and formulate a location-allocation model with renewable microgrid integration. Particularly we jointly determine the location of the warehouse, and the capacity of microgrid installed in the warehouse. The microgrid is comprised of WT, PV and energy storage units, which are interconnected with main grid. This type of problem can be called facility-microgrid, location-allocation (FMLA) problem. Our study is among the first attempt to jointly site industrial facility and size renewable microgrid under supply and demand uncertainty for both products and energy. Denoted as Model 4.2, we present the model parameters and decision variables in Table 4.7.

Table 4.7 Parameters for Model 4.2

Notation	Comments
N	number of warehouse, for n=1, 2, .., N.
S	number of retail stores, for s=1, 2, .., S.
R	number of required production resources, for r=1, 2, .., R.
T	the number of power scheduling periods, for t=1, 2, …, T.
G	type of renewable generation, for g=1, 2, .., G.
π_{ins}	shipping cost of product i from warehouse n to store s ($/item/km).
D_s	demand for product in store s.
α	probability of meeting the customer product demand (e.g., 0.9 or
τ	time step size of power generation scheduling.
τ_{qk}	operating time of generation g at factory k in a production period.
τ_{qn}	operating time of generation g at warehouse n in a production period.

τ_{gs}	operating time of generation *g* at store *s* in a production period.
τ_p	time step size of a production period.
a_g	capacity cost of renewable generation *g* ($/MW).
d_{ES}	capacity cost of energy storage system ($/MWh).
b_{gn}	operation and maintenance cost of generation *g* at warehouse *n*
c_{gn}	carbon credits of generation *g* at warehouse *n* ($/MWh).
b_{ES}	energy storage system maintenance cost ($/MWh).
ϕ_g	capital recovery factor of generation *g*.
φ_{ES}	capital recovery factor of energy storage system.
λ_{gnjt}	capacity factor of generation *g* for warehouse *n* in period *j* at time *t*.
ρ^{se}_{kjt}	price of selling electricity from factory *k* in period *j* at time *t*
ρ^{bu}_{njt}	price of buying electricity by warehouse *n* in period *j* at time *t*
m_p	unit weight of product (kg/item).
e_{ik}	energy use for making one unit of product *i* at facility *k* (MWh/unit).
q_{EV}	e-truck (MWh/kg/km).
m_{EV}	e-truck self-weight (kg).
d_{ns}	distance between warehouse *n* and store *s* (km).
$\tilde{n}_{jtns}$	number of trips between warehouse *n* and store *s* in period *j* at time *t*.
τ_w	operating hours of warehouse *n* at time *t*.
$P_{ng}^{\max}$	maximum power capacity of generation *g* in warehouse *n* (MW).
F_n	fixed cost of locating a warehouse at candidate site *n*.
γ_n	capacity of the candidate warehouse site *n*
d_{ns}	the distance from warehouse site *n* to store site *s*.
π_{ns}	unit product shipment cots between warehouse *n* and store *s* (unit:
L_n	the power demand of warehouse in location *n*.

Table 4.8 Decision Variables for Model 4.2

Notation	Comments
$\hat{u}_n$	1 if a warehouse is located at site *j*, and 0 otherwise. Decision variable.
$\hat{v}_{ns}$	1 if demand at store *s* is served by warehouse at candidate site *j*, and 0 otherwise. Decision variable.
P^c_{gn}	power capacity of generation *g* at warehouse *n* (MW).
B^c_n	capacity of Energy Storage System (ESS) at warehouse *n* (MWh).
B_{nt}	energy stored in ESS at warehouse *n* in period at time *t* (MWh).
E^{se}_{kt}	energy sold from factory *k* at time *t* (MWh).
E^{bu}_{nt}	energy purchased by warehouse *n* from the grid at time *t* (MWh).

Model 4.2 is also called facility microgrid location-allocation (FMLA) and is formulated as a two-echelon problem with DC and retail stores. The objective is to minimize the cost comprised of opening warehouse, shipping, installation of WT, PV and ESS units, and generation asset maintenance, carbon credits, and utility bills, and revenue of selling surplus energy to the main grid. Note that the model is formulated over one year horizon with T=8,760 hours. In the current model, we also assume the demands of the stores are the annual demand.

Model 4.2: Facility-Microgrid Location-Allocation (FMLA)

Minimize:

$$\begin{aligned} f(\hat{\mathbf{u}},\hat{\mathbf{v}},\mathbf{P}^c,\mathbf{B}^c,\mathbf{E}) = & \sum_{n=1}^{N} F_n \hat{u}_n + \sum_{n=1}^{N}\sum_{s=1}^{S} D_s \pi_{ns} d_{ns} \hat{v}_{ns} \\ & + \sum_{g=1}^{G}\sum_{n=1}^{N} \phi_g a_g P_{gn}^c \hat{u}_n + \sum_{t=1}^{T}\sum_{g=1}^{G}\sum_{n=1}^{N} \tau_{gn}(b_g - c_g)\lambda_{tgn} P_{gn}^c \hat{u}_n \\ & + (\varphi_{ES} d_{ES} + b_{ES}) \sum_{n=1}^{N} B_n^c \hat{u}_n + \sum_{n=1}^{N}\sum_{t=1}^{T} (\rho_{nt}^{bu} E_{nt}^{bu} - \rho_{nt}^{se} E_{nt}^{se}) \hat{u}_n \end{aligned} \tag{4.7}$$

Subject to:

$$\sum_{n=1}^{N} \hat{v}_{ns} = 1, \qquad \forall\, s \tag{4.8}$$

$$\sum_{s=1}^{S} D_s \hat{v}_{ns} \le \gamma_n \hat{u}_n, \qquad \forall n \tag{4.9}$$

$$\hat{v}_{ns} \le \hat{u}_n, \qquad \forall\, n, \text{ and } \forall\, s \tag{4.10}$$

$$\begin{aligned} & \tau_w L_n \hat{u}_n + \frac{1}{T} m_p q_{EV} \sum_{s=1}^{S} d_{ns} D_s \hat{v}_{ns} + \frac{1}{T} 2 m_{EV} q_{EV} \sum_{s=1}^{S} d_{ns} \hat{v}_{ns} \\ & + B_{nt} \hat{u}_n - B_{n,t-1} \hat{u}_n + E_{nt}^{se} \hat{u}_n - E_{nt}^{bu} \hat{u}_n = \sum_{g=1}^{G} \tau_{gn} \lambda_{tgn} P_{gn}^c \hat{u}_n \end{aligned}, \qquad \forall t, \text{ and } \forall n \tag{4.11}$$

$$0 \le P_{gn}^c \le P_g^{\max}, \qquad \forall g, \text{ and } \forall n \tag{4.12}$$

$$0 \le B_{nt} \le B_n^c, \qquad \forall t, \text{ and } \forall n \tag{4.13}$$

$$B_{n,0}, B_{n,T} = B_n^c, \qquad \forall n \tag{4.14}$$

$$E_{nt}^{bu}, E_{nt}^{se} \ge 0, \qquad \forall t, \text{ and } \forall n \tag{4.15}$$

$$B_n^c \ge 0, \qquad \forall n \tag{4.16}$$

$$B_{nt} \ge 0, \qquad \forall t, \text{ and } \forall n \tag{4.17}$$

$$\hat{u}_n \in \{0, 1\}, \qquad \forall n \tag{4.18}$$

$$\hat{v}_{ns} \in \{0, 1\}, \qquad \forall\, n, \text{ and } \forall\, s \tag{4.19}$$

Objective function (4.7) aims to minimize the annualized cost comprised of establishing warehouse, product shipment, installation of WT, PV and ESS units, and maintenance, carbon credits, and utility bills, and revenue of selling surplus energy to the main grid. Constraints (4.8) to (4.10) are associated with the classical location-allocation planning model. Constraint (4.11) is the energy balance equation in the warehouse. If a warehouse is set up at site *n*, the hourly electricity demand, the forward electric transportation, the stored energy, and the energy transaction between microgrid and main grid are offset by onsite microgrid generation. Constraint (4.12) defines the lower and upper limits of output power of generation *g*. Constraint (4.13) state that the energy stored in ESS should not exceed its capacity limit. Constraint (4.14) state that all ESS units are full at the beginning and the end of the planning horizon. Constraints (4.15) to (4.19) simply define the non-negativity of the decision variables.

4.2.2 Basic Big-Value Method for Model 4.2

Model 4.2 belongs to the mixed-integer nonlinear programming problem because of multiplication terms such as $P_{gn}^c \hat{u}_n$ and $B_n^c \hat{u}_n$. Hence, the big-value transformation is

adopted to convert the original model into an equivalent linear formulation. The working principle of such conversion is briefly described below.

If *x* and *y* are two decision variables with *x* being binary integer, and *y* being non-negative continuous variable. A continuous variable *z* is introduced to replace *xy*, namely $z = xy$. Then all the possible results of *xy* can be expressed by the following equivalent constraints:

$$\begin{cases} z \le Mx \\ z \le y \\ z \ge y - M(1-x) \\ z \ge 0 \end{cases} \tag{4.20}$$

where *M* is an arbitrary large positive value with $y < M$. Let us take the example of $P^c_{gn}\hat{u}_n$ where $\hat{u}_n$ is binary and $P^c{}_{gn}$ is non-negative continuous variable. According to the above big-value method, $P^c_{gn}\hat{u}_n$ can be transformed into the following constraint set,

$$\begin{cases} z_{gn} \le M\hat{u}_n \\ z_{gn} \le P^c_{gn} \\ z_{gn} \ge P^c_{gn} - M(1-\hat{u}_n) \\ z_{gn} \ge 0 \end{cases} \tag{4.21}$$

Similarly, the big-value method can be applied to $B_{nt}\hat{u}_n$, $E^{se}_{nt}\hat{u}_n$ and $E^{bu}_{nt}\hat{u}_n$. Before we apply the big-value transformation, let us rewrite constraint (4.11) as follows:

$$\hat{u}_n\left(\sum_{g=1}^{G}\tau_{gn}\lambda_{tgn}P^c_{gn} - B_{nt} + B_{n,t-1} - E^{se}_{nt} + E^{bu}_{nt}\right) = \tau_w L_n \hat{u}_n + \frac{1}{T}m_p q_{EV}\sum_{s=1}^{S} d_{ns}D_s\hat{v}_{ns} + \frac{1}{T}2m_{EV}q_{EV}\sum_{s=1}^{S} d_{ns}\hat{v}_{ns}\ ,$$

$$\forall t, \text{ and } \forall n \tag{4.22}$$

According to equation (4.20), we define

$$\omega_{nt} = x_n y_{nt} = \hat{u}_n\left(\sum_{g=1}^{G}\tau_{gn}\lambda_{tgn}P^c_{gn} - B_{nt} + B_{n,t-1} - E^{se}_{nt} + E^{bu}_{nt}\right), \quad \forall t, \text{ and } \forall n \tag{4.23}$$

Where:

$$x_n = \hat{u}_n \,, \tag{4.24}$$

$$y_{nt} = \sum_{g=1}^{G} \tau_{gn} \lambda_{tgn} P_{gn}^{c} - B_{nt} + B_{n,t-1} - E_{nt}^{se} + E_{nt}^{bu} \,, \tag{4.25}$$

Now constraint (4.22) can be transformed into five linear constraints as following:

$$\omega_{nt} = \tau_w L_n \hat{u}_n + \frac{1}{T} m_p q_{EV} \sum_{s=1}^{S} d_{ns} D_s \hat{v}_{ns} + \frac{1}{T} 2 m_{EV} q_{EV} \sum_{s=1}^{S} d_{ns} \hat{v}_{ns} \,, \tag{4.26}$$

$$\omega_{nt} \le M \hat{u}_n \,, \tag{4.27}$$

$$\omega_{nt} \le \sum_{g=1}^{G} \tau_{gn} \lambda_{tgn} P_{gn}^{c} - B_{nt} + B_{n,t-1} - E_{nt}^{se} + E_{nt}^{bu} \,, \tag{4.28}$$

$$\omega_{nt} \ge \sum_{g=1}^{G} \tau_{gn} \lambda_{tgn} P_{gn}^{c} - B_{nt} + B_{n,t-1} - E_{nt}^{se} + E_{nt}^{bu} - M(1 - \hat{u}_n) \,, \tag{4.29}$$

$$\omega_{nt} \ge 0 \,, \tag{4.30}$$

Finally, replacing constraint (4.11) with (4.26) to (4.30), Model 4.2 becomes a mixed-integer linear optimization model, denoted as Model FMLA-2BBV where BBV represents basic big-value.

Model 4.3: FMLA-2BBM:

Minimize:

$$\begin{aligned} f(\hat{\mathbf{u}}, \hat{\mathbf{v}}, \mathbf{P}^c, \mathbf{B}^c, \mathbf{E}) = & \sum_{n=1}^{N} F_n \hat{u}_n + \sum_{n=1}^{N} \sum_{s=1}^{S} D_s \pi_{ns} d_{ns} \hat{v}_{ns} \\ & + \sum_{g=1}^{G} \sum_{n=1}^{N} \phi_g a_g P_{gn}^{c} + \sum_{t=1}^{T} \sum_{g=1}^{G} \sum_{n=1}^{N} \tau_{gn} (b_g - c_g) \lambda_{tgn} P_{gn}^{c} \\ & + (\varphi_{ES} d_{ES} + b_{ES}) \sum_{n=1}^{N} B_n^c + \sum_{n=1}^{N} \sum_{t=1}^{T} (\rho_{nt}^{bu} E_{nt}^{bu} - \rho_{nt}^{se} E_{nt}^{se}) \end{aligned} \tag{4.31}$$

Subject to:

$$\sum_{n=1}^{N} \hat{v}_{ns} = 1 \,, \qquad \forall\, s \tag{4.32}$$

$$\sum_{s=1}^{S} D_s \hat{v}_{ns} \le \gamma_n \hat{u}_n , \qquad \forall n \tag{4.33}$$

$$\hat{v}_{ns} \le \hat{u}_n , \qquad \forall\, n, \text{ and } \forall\, s \tag{4.34}$$

$$\omega_{nt} = \tau_w L_n \hat{u}_n + \frac{1}{T} m_p q_{EV} \sum_{s=1}^{S} d_{ns} D_s \hat{v}_{ns} + \frac{1}{T} 2 m_{EV} q_{EV} \sum_{s=1}^{S} d_{ns} \hat{v}_{ns} , \qquad \forall\, n, \text{ and } \forall\, t \tag{4.35}$$

$$\omega_{nt} \le M \hat{u}_n , \qquad \forall\, n, \text{ and } \forall\, t \tag{4.36}$$

$$\omega_{nt} \le \sum_{g=1}^{G} \tau_{gn} \lambda_{tgn} P_{gn}^{c} - B_{nt} + B_{n,t-1} - E_{nt}^{se} + E_{nt}^{bu} , \qquad \forall\, n, \text{ and } \forall\, t \tag{4.37}$$

$$\omega_{nt} \ge \sum_{g=1}^{G} \tau_{gn} \lambda_{tgn} P_{gn}^{c} - B_{nt} + B_{n,t-1} - E_{nt}^{se} + E_{nt}^{bu} - M(1-\hat{u}_n) , \qquad \forall\, n, \text{ and } \forall\, t \tag{4.38}$$

$$\omega_{nt} \ge 0 , \qquad \forall\, n, \text{ and } t \tag{4.39}$$

$$0 \le P_{gn}^{c} \le P_{g}^{\max} , \qquad \forall g, \text{ and } \forall n \tag{4.40}$$

$$0 \le B_{nt} \le B_{n}^{c} , \qquad \forall t, \text{ and } \forall n \tag{4.41}$$

$$B_{n,0}, B_{n,T} = B_{n}^{c} , \qquad \forall n \tag{4.42}$$

$$E_{nt}^{bu}, E_{nt}^{se} \ge 0 , \qquad \forall t, \text{ and } \forall n \tag{4.43}$$

$$B_{n}^{c} \ge 0 , \qquad \forall n \tag{4.44}$$

$$B_{nt} \ge 0 , \qquad \forall t, \text{ and } \forall n \tag{4.45}$$

$$\hat{u}_n \in \{0, 1\}, \qquad \forall n \tag{4.46}$$

$$\hat{v}_{ns} \in \{0, 1\}, \qquad \forall\, n, \text{ and } s \tag{4.47}$$

4.2.3 Simplified Big-Value Method for Model 4.2

We further present a simplified way of using big-value method to transform Model 4.2 into a mixed-integer linear program. The new model is called simplified big-value model, denoted as Model FMLA-2SBV.

Model 4.4 FMLA-2SBV

Minimize:

$$f(\hat{\mathbf{u}},\hat{\mathbf{v}},\mathbf{P}^c,\mathbf{B}^c,\mathbf{E}) = \sum_{n=1}^{N} F_n \hat{u}_n + \sum_{n=1}^{N}\sum_{s=1}^{S} D_s \pi_{ns} d_{ns} \hat{v}_{ns} + \sum_{g=1}^{G}\sum_{n=1}^{N} \phi_g a_g P_{gn}^c + \sum_{t=1}^{T}\sum_{g=1}^{G}\sum_{n=1}^{N} \tau_{gn}(b_g - c_g)\lambda_{tgn} P_{gn}^c + (\varphi_{ES} d_{ES} + b_{ES}) \sum_{n=1}^{N} B_n^c + \sum_{n=1}^{N}\sum_{t=1}^{T} (\rho_{nt}^{bu} E_{nt}^{bu} - \rho_{nt}^{se} E_{nt}^{se}) \quad (4.48)$$

Subject to:

$$\sum_{n=1}^{N} \hat{v}_{ns} = 1, \qquad \forall\, s \quad (4.49)$$

$$\sum_{s=1}^{S} D_s \hat{v}_{ns} \le \gamma_n \hat{u}_n, \qquad \forall n \quad (4.50)$$

$$\hat{v}_{ns} \le \hat{u}_n, \qquad \forall\, n, \text{ and } s \quad (4.51)$$

$$\tau_w L_n \hat{u}_n + \frac{1}{T} m_p q_{EV} \sum_{s=1}^{S} d_{ns} D_s \hat{v}_{ns} + \frac{1}{T} 2 m_{EV} q_{EV} \sum_{s=1}^{S} d_{ns} \hat{v}_{ns} + B_{nt} - B_{n,t-1} + E_{nt}^{se} - E_{nt}^{bu} = \sum_{g=1}^{G} \tau_{gn} \lambda_{tgn} P_{gn}^c,$$

$$\forall t, \text{ and } \forall n \quad (4.52)$$

$$B_n^c \le M \hat{u}_n, \qquad \forall g, \text{ and } \forall n \quad (4.53)$$

$$B_n^c \le M \hat{u}_n \qquad \forall n \quad (4.54)$$

$$E_{nt}^{se} \le M \hat{u}_n, \qquad \forall t, \text{ and } \forall n \quad (4.55)$$

$$0 \le P_{gn}^c \le P_g^{\max}, \qquad \forall g, \text{ and } \forall n \quad (4.56)$$

$$0 \le B_{nt} \le B_n^c, \qquad \forall t, \text{ and } \forall n \quad (4.57)$$

$$B_{n0}, B_{nT} = B_n^c \qquad \forall n \tag{4.58}$$

$$E_{nt}^{bu}, E_{nt}^{se} \geq 0, \qquad \forall t, \text{ and } \forall n \tag{4.59}$$

$$B_n^c \geq 0, \qquad \forall n \tag{4.60}$$

$$B_{nt} \geq 0, \qquad \forall t, \text{ and } \forall n \tag{4.61}$$

$$\hat{u}_n \in \{0, 1\}, \qquad \forall n \tag{4.62}$$

$$\hat{v}_{ns} \in \{0, 1\}, \qquad \forall\, n, \text{ and } \forall s \tag{4.63}$$

In this model, the big-value method is only used to constrain the variables, instead of applying the big-value method to the entire constraint as in Model FMLA-2BBV. The variables constrained by the big-value method can also be applied to the constraints, thereby improving the computational efficiency.

4.3 Three-Echelon Location-Allocation Model with Microgrid Integration

4.3.1 Problem Setting

In this section we expand the two-echelon FMLA model to three-echelon supply chain networks comprised factories, warehouses and retail stores. Particularly we jointly determine the location of factories, warehouse, and microgrid systems to realize transactive energy operations. Each microgrid system is comprised of WT, PV and energy storage devices. All microgrid systems are interconnected with main grid, together powering the supply chain facilities. The model parameters and decision variables of the three-echelon supply chain network are summarized in Tables 4.9 and 4.10, respectively.

Without loss of generality, Figure 4.1 shows the network structure with three candidate locations for factories, DC, and microgrid systems. It is worth mentioning that

in our setting, the demand of a store is fulfilled by one warehouse. However, the products in a warehouse can be provided by more than one factory.

Table 4.9 Parameters for Three-Echelon FMLA Model

Notation	Definition
K	number of candidate factory sites, for k=1, 2, ..., K.
N	number of candidate warehouse sites, for n=1, 2, ..., N.
S	number of retail stores, for s=1, 2, ..., S.
G	type of renewable generation, for g=1, 2, ..., G.
R	number of required production resources, for r=1, 2, ..., R.
T	number of power scheduling periods, for t=1, 2, …, T.
π_{ikn}	unit shipping cost of product i from factory k to warehouse n ($/item/km).
π_{ins}	unit shipping cost of product i from warehouse n to store s ($/item/km).
D_{ijns}	demand for product i of store s to warehouse n in period j.
α	probability of meeting the product demand (e.g., 0.9 or 0.95).
τ_p	time step size of a production planning period.
τ	time step size of power generation scheduling.
τ_{gk}	operating time of generation g at factory k in a production period.
τ_{gn}	operating time of generation g at warehouse n in a production period.
τ_{gs}	operating time of generation g at store s in a production period.
τ_w	operating hours of warehouse n at time t.
a_g	capacity cost of renewable generation g ($/MW).
d_{ES}	capacity cost of energy storage device ($/MWh).
b_{gk}	operation and maintenance cost of generation g at factory k ($/MWh).
b_{gn}	operation and maintenance cost of generation g at warehouse n ($/MWh).
c_{gk}	carbon credits of generation g at factory k ($/MWh).
c_{gn}	carbon credits of generation g at warehouse n ($/MWh).
b_{ES}	maintenance cost of energy storage device ($/MWh).
ϕ_g	capital recovery factor of generation g.
φ_{ES}	capital recovery factor of energy storage system.
λ_{gkjt}	capacity factor of generation g for factory k in period j at time t.
λ_{gnjt}	capacity factor of generation g for warehouse n in period j at time t.
ρ^{se}_{kjt}	price of selling electricity from factory k in period j at time t ($/MWh).
ρ^{se}_{njt}	price of selling electricity from warehouse n in period j at time t ($/MWh).
ρ^{bu}_{kjt}	price of buying electricity by factory k in period j at time t ($/MWh).
ρ^{bu}_{njt}	price of buying electricity by warehouse n in period j at time t ($/MWh).
m_i	unit weight of product i (kg/item).
e_{ik}	energy use for making one unit of product i at facility k (MWh/unit).
q_{EV}	e-truck energy intensity rate (MWh/kg/km).
m_{EV}	e-truck self-weight (kg).

n_{knjt}	number of trips between factory *k* and warehouse *n* in period *j* at time *t*.
$\hat{n}_{ijns}$	number of trips between warehouse *n* and store *s* in period *j* at time *t*.
$P_{gk}^{\max}$	maximum capacity installation of generation *g* in factory *k* (MW).
$P_{gn}^{\max}$	maximum capacity installation of generation *g* in warehouse *n* (MW).
F_k	annualized cost of opening a factory in location *k*.
$\hat{F}_n$	annualized cost of opening a warehouse in location *n*.
p_{ijk}	cost of making one unit of product *i* in period *j* at factory *k* ($/item).
h_{ijn}	holding cost of product *i* in period *j* at warehouse *n* ($/item/period).
b_{ijn}	backorder cost of product *i* in period *j* at warehouse *n* ($/item).
γ_n	warehouse capacity in site *n*.
d_{kn}	distance from factory site *k* to warehouse site *n* (km)
$\hat{d}_{ns}$	distance from warehouse site *n* to store site *s* (km)
L_n	power demand of warehouse in location *n*.
w_{ikr}	resource *r* consumed for making one unit of product *i* at factory *k*.
W_{jkr}	total available production resource *r* in period *j* at factory *k*.

Table 4.10 Decision Variables of Three-Echelon FMLA Model

Notation	Definition
u_k	1 if a factory is located at site *k*, and 0 otherwise.
v_{ijkn}	1 if product *i* made by factory *k* is shipped to warehouse *n* in period *j*, and 0 otherwise.
$\hat{u}_n$	1 if a warehouse is located at site *n*, and 0 otherwise.
$\hat{v}_{ins}$	1 if demand *i* at store *s* is served by warehouse at site *n*, and 0 otherwise. Decision variable.
x_{ijkn}	The amount of product *i* made by factory *k* in period *j* and shipped to warehouse *n*.
$\hat{x}_{ijns}$	The amount of product *i* shipped from warehouse *n* to store *s* in period *j*.
y_{ijn}	inventory of product *i* in period *j* at warehouse *n*.
z_{ijn}	backorders of product *i* in period *j* at warehouse *n*.
P^c_{gk}	power capacity of generation *g* at factory *k* (MW).
P^c_{gn}	power capacity of generation *g* at warehouse *n* (MW).
B^c_k	capacity of energy storage device at factory *k* (MWh).
B^c_n	capacity of energy storage device at warehouse *n* (MWh).
B_{kt}	energy stored in ESS at factory *k* in period at time *t* (MWh).
B_{nt}	energy stored in ESS at warehouse *n* in period at time *t* (MWh).
E^{se}_{kt}	energy sold from factory *k* at time *t* (MWh).
E^{se}_{nt}	energy sold from warehouse *n* at time *t* (MWh).
E^{bu}_{kt}	energy bought by factory *k* from the grid at time *t* (MWh).
E^{bu}_{nt}	energy bought by warehouse *n* from the grid at time *t* (MWh).

4.3.2 Nonlinear Facility-Microgrid Location-Allocation Model

The goal of the FMLA model is to minimize the supply chain cost comprised of setup and operations of factories, warehouse, transportation and microgrid systems. The microgrid system cost consists of initial capital, maintenance and operations, utility energy bills, carbon credits, and revenue of selling energy to the main grid. The last two items are indeed the incomes to the supply chain. The objective function incorporating all these cost items is given as follows.

A. The objective function of the 3-Echelon FMLA Model

Model 4.5: FMLA1

Minimize:

$$
\begin{aligned}
&f_1(\mathbf{u},\hat{\mathbf{u}},\mathbf{v},\hat{\mathbf{v}},\mathbf{x},\mathbf{y},\mathbf{z},\mathbf{P}^c,\mathbf{B}^c,\mathbf{E}) \\
&=\sum_{k=1}^{K} F_k u_k+\sum_{i=1}^{I}\sum_{j=1}^{J}\sum_{k=1}^{K}\sum_{n=1}^{N} x_{ijkn}\, p_{ijk}\, v_{ijkn}+\sum_{i=1}^{I}\sum_{j=1}^{J}\sum_{k=1}^{K}\sum_{n=1}^{N} x_{ijkn}\,\pi_{ikn}\, d_{kn}\, v_{ijkn} \\
&+\sum_{n=1}^{N}\hat{F}_n\hat{u}_n+\sum_{i=1}^{I}\sum_{j=1}^{J}\sum_{n=1}^{N} h_{ijn}\, y_{ijn}+\sum_{i=1}^{I}\sum_{j=1}^{J-1}\sum_{n=1}^{N} b_{ijn}\, z_{ijn}+\sum_{i=1}^{I}\sum_{j=1}^{J}\sum_{n=1}^{N}\sum_{s=1}^{S}\hat{x}_{ijns}\,\pi_{ins}\, d_{ns}\,\hat{v}_{ins} \\
&+\sum_{g=1}^{G}\sum_{k=1}^{K}\phi_g\, a_g\, P^c_{gk}\, u_k+\sum_{j=1}^{J}\sum_{t=1}^{T}\sum_{g=1}^{G}\sum_{k=1}^{K}\tau_{gk}\,(b_g-c_g)\,\lambda_{jgkt}\, P^c_{gk}\, u_k \qquad (4.64) \\
&+(\varphi_{ES}\, d_{ES}+b_{ES})\sum_{k=1}^{K} B^c_k u_k+\sum_{j=1}^{J}\sum_{t=1}^{T}\sum_{k=1}^{K}(\rho^{bu}_{jkt}\, E^{bu}_{jkt}-\rho^{se}_{jkt}\, E^{se}_{jkt})\,u_k \\
&+\sum_{g=1}^{G}\sum_{n=1}^{N}\phi_g\, a_g\, P^c_{gn}\hat{u}_n+\sum_{j=1}^{J}\sum_{t=1}^{T}\sum_{g=1}^{G}\sum_{n=1}^{N}\tau_{gn}\,(b_g-c_g)\,\lambda_{jgnt}\, P^c_{gn}\hat{u}_n \\
&+(\varphi_{ES}\, d_{ES}+b_{ES})\sum_{n=1}^{N} B^c_n\hat{u}_n+\sum_{j=1}^{J}\sum_{t=1}^{T}\sum_{n=1}^{N}(\rho^{bu}_{jtn}\, E^{bu}_{jtn}-\rho^{se}_{jtn}\, E^{se}_{jtn})\,\hat{u}_n
\end{aligned}
$$

The first two lines of Equation (4.64) capture the location and allocation costs of factories and warehouse. The remaining lines are associated with the costs of microgrid systems installed in factories and warehouse sites. Note that u_k and $\hat{u}_n$ are the binary decision variables, representing whether a plant or warehouse is open in site *k* or *n*, respectively. Meanwhile, v_{knij} is the binary decision variable, representing whether

Product *i* made by plant *k* is shipped to warehouse *n* in period *j*. Similarly, $\hat{v}_{nsi}$ is the binary decision variable, representing product *i* requested by Store *s* is served by the warehouse in site *n*. Lastly, **x**, **y** and **z** are the decision vectors, standing for production, inventory, and backorders in each period of the planning horizon.

The location-allocation of microgrid system involve both strategic and operational decisions. Strategic decisions include the siting and sizing of WT, PV and ESS units, which is captured by decision variable $\boldsymbol{P}^c$ and $\boldsymbol{B}^c$, respectively. The operational decisions include B_{kt} and B_{nt}, representing the hourly energy stored in ESS unit in factory *k* and warehouse *n* at time *t*, respectively. $E^{se}{}_{kt}$ and $E^{se}{}_{nt}$ are the decision variables, representing the energy sold to the grid from factory *k* and warehouse *n* at time *t*, respectively. Finally, $E^{bu}{}_{kt}$ and $E^{bu}{}_{nt}$ are the decision variables, representing the energy purchased from the grid by factory *k* and warehouse *n* at time *t*, respectively.

It is worth mentioning that objective function (4.64) involves stochastic wind and solar generation manifested as random capacity factor (CF). Particularly λ_{jgkt} is the CF of generation *g* in factory *k* at time *t*, and λ_{jgnt} is the CF of generation *g* in warehouse *n* at time *t*. Hence the actual output power is $\lambda_{jgkt}\, P^c{}_{gk}$ where $P^c{}_{gk}$ is the capacity of generation *g* in factory *k*. Same interpretation can be applied to warehouses. To make the problem tractable, hourly CF values are estimated based on 11-year climate data of the candidate location. It is worth noting that we use the mean CF in Chapter 4, and in Chapter 5 we use different CF values per scenario for the stochastic model.

There are three types of constraints: facility location, production-inventory balance, and energy demand and supply balance. These constraints are presented below.

B. Constraints of Facility Location

$$\sum_{n=1}^{N} \hat{v}_{ins} = 1, \qquad \forall i, \text{ and } \forall s \tag{4.65}$$

$$\sum_{s=1}^{S} \hat{x}_{ijns} \le \gamma_{in} \hat{u}_n, \qquad \forall i, \forall j, \text{ and } \forall n \tag{4.66}$$

$$\sum_{k=1}^{K} x_{ijkn} \le \gamma_{in} \hat{u}_n, \qquad \forall i, \forall j, \text{ and } \forall n \tag{4.67}$$

$$\hat{v}_{ins} \le \hat{u}_n, \qquad \forall\, i, \forall n, \text{ and } \forall s \tag{4.68}$$

$$v_{ijkn} \le u_k \hat{u}_n, \qquad \forall i, \forall j, \forall k, \text{ and } \forall n \tag{4.69}$$

$$u_k,\ \hat{u}_n \in \{0, 1\}, \qquad \forall k, \text{ and } \forall n \tag{4.70}$$

$$v_{ijkn},\ \hat{v}_{ins} \in \{0, 1\}, \qquad \forall i, \forall j, \forall k, \forall n, \text{ and } \forall s \tag{4.71}$$

Constraint (4.65) indicates that a demand node (retail store) is served by only one warehouse. Constraints (4.66) and (4.67) define the capacity of a warehouse if it is opened in a particular site. Constraints (4.68) show that the product shipping between two facilities are possible only if the upper stream warehouse is opened. Constraints (4.69) indicates that the product shipping between factory and warehouse are possible only if both facilities are open at the same time. Constraints (4.70) and (4.71) simply states the binary nature of decision variables.

C. Constraints of Production-Inventory Balance

$$\sum_{k=1}^{K} x_{i1kn} v_{i1kn} + y_{i0n} - y_{i1n} + z_{i1n} = \sum_{s=1}^{S} \hat{x}_{i1ns}, \qquad \text{for } j = 1, \forall i, \text{ and } \forall n \tag{4.72}$$

$$\sum_{k=1}^{K} x_{ijkn} v_{ijkn} + y_{ij-1n} - y_{ijn} - z_{ij-1n} + z_{ijn} = \sum_{s=1}^{S} \hat{x}_{ijns}, \quad \text{for } j = 2, 3, \ldots, J\text{-}1, \forall i, \text{ and } \forall n \tag{4.73}$$

$$\sum_{k=1}^{K} x_{iJkn} v_{iJkn} + y_{iJ-1n} - y_{iJn} - z_{iJ-1n} = \sum_{s=1}^{S} \hat{x}_{iJns}, \qquad \text{for } j = J, \forall i, \text{ and } \forall n \tag{4.74}$$

$$\Pr\left\{\hat{x}_{ijns} \geq D_{ijs}\right\} \geq \alpha, \qquad \forall i, \forall j, \forall n, \text{ and } \forall s \tag{4.75}$$

$$\sum_{i=1}^{I}\sum_{n=1}^{N} w_{ikr} x_{ijkn} \leq W_{jkr} u_k, \qquad \forall j, \forall k, \text{ and } \forall r \tag{4.76}$$

$$y_{i0n} = 0, \qquad \forall i, \text{ and } \forall n \tag{4.77}$$

Constraints (4.72) to (4.74) are the production-inventory balance equations between factories and warehouses for each product and period. Constraint (4.75) is the chance constraint and states that for given product *i* in period *j*, the demand of store *s* must be satisfied at 100×*a*% confidence level. Constraint (4.76) represents the production resource constraint, such as labor and machine hours available in each period. Constraint (4.77) assumes the initial inventory is zero. Direct solving the chance constraint (4.75) is difficult. For normal demand with mean $E[D_{ijs}]$ and variance $Var(D_{ijs})$, the original chance constraint can be converted a deterministic counterpart as follows:

$$\hat{x}_{ijns} \geq E[D_{ijs}] + Z_\alpha \sqrt{Var(D_{ijs})}, \qquad \forall i, \forall j, \text{ and } \forall s \tag{4.78}$$

Where, Z_a is the *Z*-value of the standard normal distribution.

D. Energy Balance Constraints

$$\begin{aligned}&\sum_{i=1}^{I}\sum_{n=1}^{N}(e_{ik} + q_{EV} d_{kn} m_i) x_{ijkn}^t + q_{EV}\sum_{i=1}^{I}\sum_{n=1}^{N} n_{jknt} d_{kn} m_{EV} v_{ijkn} \\ &+\left(B_{jkt} - B_{jk,t-1} + E_{jkt}^{se} - E_{jkt}^{bu}\right) u_k = \sum_{g=1}^{G} \tau_{gk} \lambda_{gjkt} P_{gk}^c u_k\end{aligned}, \quad \forall j, \forall k, \text{ and } \forall t \tag{4.79}$$

$$\begin{aligned}&\tau_w L_n \hat{u}_n + q_{EV}\sum_{k=1}^{K}\sum_{i=1}^{I} n_{jknt} d_{kn} m_{EV} v_{ijkn} + q_{EV}\sum_{i=1}^{I}\sum_{s=1}^{S} \hat{d}_{ns} m_i \hat{x}_{ijns}^t \\ &+2q_{EV}\sum_{i=1}^{I}\sum_{s=1}^{S} \hat{n}_{jnst} \hat{d}_{ns} m_{EV} \hat{v}_{ins} + \left(B_{jnt} - B_{jn,t-1} + E_{jnt}^{se} - E_{jnt}^{bu}\right)\hat{u}_n = \sum_{g=1}^{G} \tau_{gn} \lambda_{gjnt} P_{gn}^c \hat{u}_n\end{aligned}, \forall j, \forall n, \text{ and } \forall t \tag{4.80}$$

$$x_{ijkn}^t = \frac{x_{ijkn}}{T}, \qquad \forall i, \ \forall j, \forall k, \forall n, \text{ and } \forall t \tag{4.81}$$

$$\hat{x}_{ijns}^{t} = \frac{\hat{x}_{ijns}}{T}, \qquad \forall i,\ \forall j, \forall n, \forall s, \text{ and } \forall t \qquad (4.82)$$

$$0 \le B_{jkt} \le B_k^c u_k \qquad \forall j, \forall k, \text{ and } \forall t \qquad (4.83)$$

$$0 \le B_{jnt} \le B_n^c \hat{u}_n, \qquad \forall j, \forall n, \text{ and } \forall t \qquad (4.84)$$

$$B_{jk0} = B_{j-1,kT}, \qquad \text{for } j = 2, 3, \ldots, J, \text{ and } \forall k \qquad (4.85)$$

$$B_{jn0} = B_{j-1,nT}, \qquad \text{for } j = 2, 3, \ldots, J, \text{ and } \forall n \qquad (4.86)$$

$$B_{1k0} = B_{JkT} = B_k^c \qquad \text{for } j=1 \text{ and } J, t=0 \text{ and } T, \text{ and } \forall k \qquad (4.87)$$

$$B_{1n0} = B_{JnT} = B_n^c, \qquad \text{for } j=1 \text{ and } J, t=0 \text{ and } T, \text{ and } \forall n \qquad (4.88)$$

$$0 \le P_{gk}^c, P_{gn}^c \le P_{\max}^c, \qquad \forall g, \forall k, \text{ and } \forall n \qquad (4.89)$$

$$E_{jkt}^{bu}, E_{jkt}^{se} \ge 0, \qquad \forall j, \forall k, \text{ and } \forall t \qquad (4.90)$$

$$E_{jnt}^{bu}, E_{jnt}^{se} \ge 0, \qquad \forall j, \forall n, \text{ and } \forall t \qquad (4.91)$$

$$B_k^c, B_n^c \ge 0, \qquad \forall k, \text{ and } \forall n \qquad (4.92)$$

$$B_{jkt}, B_{jnt} \ge 0, \qquad \forall j, \forall k, \forall n, \text{ and } \forall t \qquad (4.93)$$

$$x_{ijkn}, \hat{x}_{ijns}, y_{ijn}, z_{ijn} \in \{0,1,2....\}, \qquad \forall i, \forall j, \forall k, \forall n, \text{ and } \forall t \qquad (4.94)$$

Constraint (4.79) is the hourly energy balance equation in factory. For factory *k*, the hourly electricity demand, the forward electric transportation, the stored energy, and the transactive energy between onsite generation and main grid are offset by the microgrid. Similarly, constraint (4.80) defines the hourly energy balance at warehouses and retail stores, respectively. Constraints (4.81) and (4.82) convert the strategic production decision into hourly production rate, and *T* is the number of hours per period. Constraints (4.83) and (4.84) state that the energy stored in ESS should not exceed its

capacity limit. Constraints (4.85) and (4.86) stipulates the energy continuity, that is the initial state of ESS in the current period must equals the state of the last hour of the previous period. Constraint (4.87) and (4.88) state that the ESS units are full at the beginning and the end of the planning horizon. Constraint (4.89) defines the lower and upper limits of output power of generation *g*. Constraints (4.90) to (4.93) simply define the non-negativity of the decision variables. Finally, constraint (4.94) states the non-negative integers of the decision variables.

4.3.3 Transformation to Linear Optimization Models

Basic Big-Value Reformulation

Now we apply basic big-Value reformulation method to Constraint (4.79), and the resulting linear constraints are given as follows:

$$\omega_{jkt} = \sum_{i=1}^{I}\sum_{n=1}^{N}(e_{ik} + q_{EV} d_{kn} m_i) x_{ijkn}^{t} + \sum_{i=1}^{I}\sum_{n=1}^{N} q_{EV} n_{jknt} d_{kn} m_{EV} v_{ijkn}, \qquad \forall j, \forall k, \text{ and } \forall t \qquad (4.95)$$

$$\omega_{jkt} \le M u_k, \qquad \forall j, \forall k, \text{ and } \forall t \qquad (4.96)$$

$$\omega_{jkt} \le \sum_{g=1}^{G} \tau_{gk} \lambda_{gjkt} P_{gk}^{c} - B_{jkt} + B_{jk,t-1} - E_{jkt}^{se} + E_{jkt}^{bu}, \qquad \forall j, \forall k, \text{ and } \forall t \qquad (4.97)$$

$$\omega_{jkt} \ge \sum_{g=1}^{G} \tau_{gk} \lambda_{gjkt} P_{gk}^{c} - B_{jkt} + B_{jk,t-1} - E_{jkt}^{se} + E_{jkt}^{bu} - M(1-u_k), \qquad \forall j, \forall k, \text{ and } \forall t \qquad (4.98)$$

$$\omega_{jkt} \ge 0, \qquad \forall j, \forall k, \text{ and } \forall t \qquad (4.99)$$

Also, we apply basic big-Value reformulation method to Constraints (4.80), and the resulting linear constraints are given as follows:

$$\hat{\omega}_{jnt} = \tau_w L_n \hat{u}_n + q_{EV} \sum_{i}^{I}\sum_{k=1}^{K} n_{jknt} d_{kn} m_{EV} v_{ijkn} + q_{EV} \sum_{i=1}^{I}\sum_{s=1}^{S} \hat{d}_{ns} m_i \hat{x}_{ijns}^{t} + 2 q_{EV} \sum_{i=1}^{I}\sum_{s=1}^{S} \hat{n}_{jnst} \hat{d}_{ns} m_{EV} \hat{v}_{ins}$$

$$\forall j, \forall n, \text{ and } \forall t \qquad (4.100)$$

$$\hat{\omega}_{jnt} \le M \hat{u}_n, \qquad \forall j, \forall n, \text{ and } \forall t \qquad (4.101)$$

$$\hat{\omega}_{jnt} \le \sum_{g=1}^{G} \tau_{gn} \lambda_{gjnt} P_{gn}^{c} - B_{jnt} + B_{jn,t-1} - E_{jnt}^{se} + E_{jnt}^{bu}, \qquad \forall j, \forall n, \text{ and } \forall t \qquad (4.102)$$

$$\hat{\omega}_{jnt} \ge \sum_{g=1}^{G} \tau_{gn} \lambda_{gjnt} P_{gn}^{c} - B_{jnt} + B_{jn,t-1} - E_{jnt}^{se} + E_{jnt}^{bu} - M(1-\hat{u}_{n}), \quad \forall j, \forall n, \text{ and } \forall t \qquad (4.103)$$

$$\hat{\omega}_{jnt} \ge 0, \qquad \forall j, \forall n, \text{ and } \forall t \qquad (4.104)$$

Constraints (4.72) to (4.74) are transformed into linear constraints as follows:

$$\sum_{k=1}^{K} x_{i1kn} + y_{i0n} - y_{i1n} + z_{i1n} = \sum_{s=1}^{S} \hat{x}_{i1ns}, \qquad \text{for } j = 1, \forall i, \text{ and } \forall n \qquad (4.105)$$

$$\sum_{k=1}^{K} x_{ijkn} + y_{ij-1n} - y_{ijn} - z_{ij-1n} + z_{ijn} = \sum_{s=1}^{S} \hat{x}_{ijns}, \qquad \text{for } j = 2, 3, \ldots, J\text{-}1, \forall i, \text{ and } \forall n \qquad (4.106)$$

$$\sum_{k=1}^{K} x_{iJkn} + y_{iJ-1n} - y_{iJn} - z_{iJ-1n} = \sum_{s=1}^{S} \hat{x}_{iJns}, \qquad \text{for } j = J, \forall i, \text{ and } \forall n \qquad (4.107)$$

In this method, two additional constraints must be added to ensure that products can only be shipped on an opened transit line.

$$x_{ijkn} - M v_{ijkn} \le 0, \qquad \forall\, i, \forall j, \forall k, \text{ and } \forall n \qquad (4.108)$$

$$\hat{x}_{ijns} - M \hat{v}_{ins} \le 0, \qquad \forall\, i, \forall j, \forall n, \text{ and } \forall s \qquad (4.109)$$

After applying the basic big-value method, the original FMLA1 model can be transformed into a mixed integer linear model as follows:

Model 4.6: FMLA2

Minimize:

$$
\begin{aligned}
& f_2(\mathbf{u},\hat{\mathbf{u}},\mathbf{v},\hat{\mathbf{v}},\mathbf{x},\mathbf{y},\mathbf{z},\mathbf{P}^c,\mathbf{B}^c,\mathbf{E}) \\
&= \sum_{k=1}^{K} F_k u_k + \sum_{i=1}^{I}\sum_{j=1}^{J}\sum_{k=1}^{K}\sum_{n=1}^{N} x_{ijkn} p_{ijk} + \sum_{i=1}^{I}\sum_{j=1}^{J}\sum_{k=1}^{K}\sum_{n=1}^{N} x_{ijkn}\pi_{ikn} d_{kn} \\
&+ \sum_{n=1}^{N} \hat{F}_n \hat{u}_n + \sum_{i=1}^{I}\sum_{j=1}^{J}\sum_{n=1}^{N} h_{ijn} y_{ijn} + \sum_{i=1}^{I}\sum_{j=1}^{J-1}\sum_{n=1}^{N} b_{ijn} z_{ijn} + \sum_{i=1}^{I}\sum_{j=1}^{J}\sum_{n=1}^{N}\sum_{s=1}^{S} \hat{x}_{ijns}\pi_{ins} d_{ns} \\
&+ \sum_{g=1}^{G}\sum_{k=1}^{K} \phi_g a_g P_{gk}^c + \sum_{j=1}^{J}\sum_{t=1}^{T}\sum_{g=1}^{G}\sum_{k=1}^{K} \tau_{gk}(b_g - c_g)\lambda_{gjkt} P_{gk}^c + (\phi_{ES} d_{ES} + b_{ES}) \sum_{k=1}^{K} B_k^c \qquad (4.110) \\
&+ \sum_{j=1}^{J}\sum_{t=1}^{T}\sum_{k=1}^{K} (\rho_{jkt}^{bu} E_{jkt}^{bu} - \rho_{jkt}^{se} E_{jkt}^{se}) \\
&+ \sum_{g=1}^{G}\sum_{n=1}^{N} \phi_g a_g P_{gn}^c + \sum_{j=1}^{J}\sum_{t=1}^{T}\sum_{g=1}^{G}\sum_{n=1}^{N} \tau_{gn}(b_g - c_g)\lambda_{gjnt} P_{gn}^c + (\phi_{ES} d_{ES} + b_{ES}) \sum_{n=1}^{N} B_n^c \\
&+ \sum_{j=1}^{J}\sum_{t=1}^{T}\sum_{n=1}^{N} (\rho_{jnt}^{bu} E_{jnt}^{bu} - \rho_{jnt}^{se} E_{jnt}^{se})
\end{aligned}
$$

Subject to:

Constraints (4.65) to (4.68)

Constraints (4.70) and (4.71)

Constraints (4.76) to (4.78)

Constraints (4.81) to (4.109)

Simplified Big-Value Reformulation

After applying the big-Value method, objective function (4.64) can be simplified into a mixed integer linear model. Therefore, the new model, denoted as FMLA3, can be formulated as follows:

Model 4.7: FMLA3

Minimize:

$$
\begin{aligned}
& f_3(\mathbf{u}, \hat{\mathbf{u}}, \mathbf{v}, \hat{\mathbf{v}}, \mathbf{x}, \mathbf{y}, \mathbf{z}, \mathbf{P}^c, \mathbf{B}^c, \mathbf{E}) \\
& = \sum_{k=1}^{K} F_k u_k + \sum_{i=1}^{I}\sum_{j=1}^{J}\sum_{k=1}^{K}\sum_{n=1}^{N} x_{ijkn} p_{ijk} + \sum_{i=1}^{I}\sum_{j=1}^{J}\sum_{k=1}^{K}\sum_{n=1}^{N} x_{ijkn}\pi_{ikn} d_{kn} \\
& + \sum_{n=1}^{N} \hat{F}_n \hat{u}_n + \sum_{i=1}^{I}\sum_{j=1}^{J}\sum_{n=1}^{N} h_{ijn} y_{ijn} + \sum_{i=1}^{I}\sum_{j=1}^{J-1}\sum_{n=1}^{N} b_{ijn} z_{ijn} + \sum_{i=1}^{I}\sum_{j=1}^{J}\sum_{n=1}^{N}\sum_{s=1}^{S} \hat{x}_{ijns}\pi_{ins} d_{ns} \\
& + \sum_{g=1}^{G}\sum_{k=1}^{K} \phi_g a_g P_{gk}^c + \sum_{j=1}^{J}\sum_{t=1}^{T}\sum_{g=1}^{G}\sum_{k=1}^{K} \tau_{gk}(b_g - c_g)\lambda_{gjkt} P_{gk}^c + (\phi_{ES} d_{ES} + b_{ES}) \sum_{k=1}^{K} B_k^c \qquad (4.111) \\
& + \sum_{j=1}^{J}\sum_{t=1}^{T}\sum_{k=1}^{K} (\rho_{jkt}^{bu} E_{jkt}^{bu} - \rho_{jkt}^{se} E_{jkt}^{se}) \\
& + \sum_{g=1}^{G}\sum_{n=1}^{N} \phi_g a_g P_{gn}^c + \sum_{j=1}^{J}\sum_{t=1}^{T}\sum_{g=1}^{G}\sum_{n=1}^{N} \tau_{gn}(b_g - c_g)\lambda_{gjnt} P_{gn}^c + (\phi_{ES} d_{ES} + b_{ES}) \sum_{n=1}^{N} B_n^c \\
& + \sum_{j=1}^{J}\sum_{t=1}^{T}\sum_{n=1}^{N} (\rho_{jnt}^{bu} E_{jnt}^{bu} - \rho_{jnt}^{se} E_{jnt}^{se})
\end{aligned}
$$

Subject to

Constraints (4.65) to (4.68)

Constraints (4.70) and (4.71)

Constraints (4.76) to (4.78)

Constraints (4.81) to (4.94)

Constraints (4.105) to (4.109)

$$
\begin{aligned}
& \sum_{i=1}^{I}\sum_{n=1}^{N} (e_{ik} + q_{EV} d_{kn} m_i) x_{ijkn}^t + q_{EV} \sum_{i=1}^{I}\sum_{n=1}^{N} n_{jknt} d_{kn} m_{EV} v_{ijkn} \\
& + B_{jkt} - B_{jk,t-1} + E_{jkt}^{se} - E_{jkt}^{bu} = \sum_{g=1}^{G} \tau_{gk} \lambda_{gjkt} P_{gk}^c
\end{aligned}
\quad , \quad \forall j, \forall k, \text{ and } \forall t \qquad (4.112)
$$

$$
P_{gk}^c \le M\hat{u}_k , \qquad \forall g \text{ and } \forall k \qquad (4.113)
$$

$$
B_k^c \le M\hat{u}_k \qquad \forall k \qquad (4.114)
$$

$$
E_{kt}^{se} \le M\hat{u}_k , \qquad \forall k \text{ and } \forall t \qquad (4.115)
$$

$$E_{kt}^{bu} \le M\hat{u}_k, \qquad \forall k \text{ and } \forall t \tag{4.116}$$

$$\begin{aligned}&\tau_w L_n \hat{u}_n + q_{EV}\sum_{i=1}^{I}\sum_{k=1}^{K} n_{jknt} d_{kn} m_{EV} v_{ijkn} + q_{EV}\sum_{i=1}^{I}\sum_{s=1}^{S} \hat{d}_{ns} m_i \hat{x}_{ijns}^{t} \\ &+2q_{EV}\sum_{i=1}^{I}\sum_{s=1}^{S} \hat{n}_{jnst} \hat{d}_{ns} m_{EV} \hat{v}_{ins} + B_{jnt} - B_{jn,t-1} + E_{jnt}^{se} - E_{jnt}^{bu} = \sum_{g=1}^{G} \tau_{gn} \lambda_{gjnt} P_{gn}^{c},\end{aligned} \qquad \forall j, \forall n, \text{ and } \forall t \tag{4.117}$$

$$P_{gn}^{c} \le M\hat{u}_n, \qquad \forall g, \text{ and } \forall n \tag{4.118}$$

$$B_n^{c} \le M\hat{u}_n, \qquad \forall n \tag{4.119}$$

$$E_{nt}^{se} \le M\hat{u}_n, \qquad \forall n, \text{ and } \forall t \tag{4.120}$$

$$E_{nt}^{bu} \le M\hat{u}_n, \qquad \forall t, \text{ and } \forall n \tag{4.121}$$

4.4 Numerical Experiments

4.4.1 Network Setting

A three-tier manufacturing supply chain system in Figure 4.3 is used to demonstrate the three models. Denoted as 4F-2W-4S, the network is comprised four candidate factory locations and two candidate warehouse locations, while the four stores are pe-opened. The distribution of these candidate locations and the distance between adjacent cities are shown in Figure 4.3 factory candidate locations 1, 2, 3 and 4 are placed in Phoenix, Reno, Yuma, Tucson, respectively. Las Vegas and Los Angeles are the warehouse candidate locations. Four fixed stores are in Salt Lake City, San Jose, Sacramento and San Francisco, respectively.

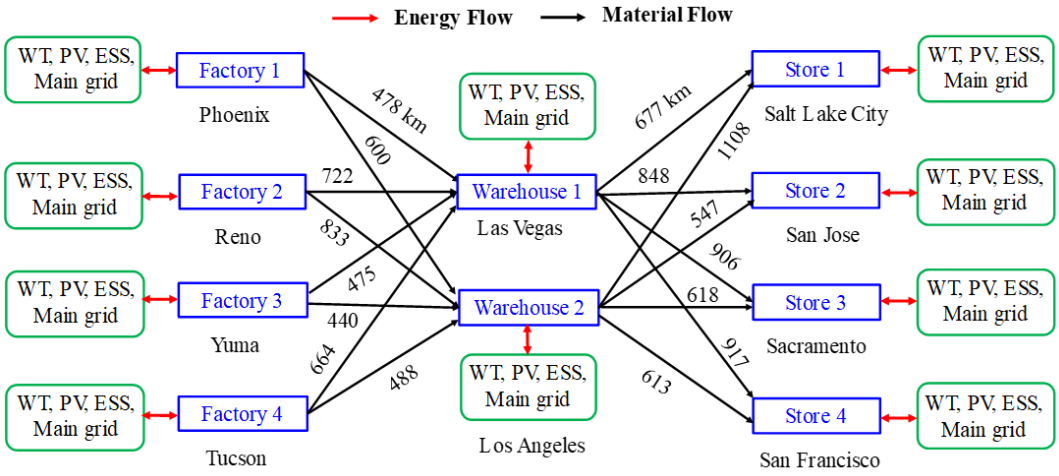


Figure 4.3 Candidate Locations for Supply Chain Facilities and Microgrid

Two products need to be produced, and both can be made in four candidate factories. The production planning is carried out on a weekly basis over 52 weeks (i.e., one year). We assume that the weekly product demand of the four stores follows the normal distribution shown in Table 4.11. In addition, the demand in each store must be satisfied with α=100% confidence. Product-specific parameters such as production cost, holding cost, energy use, and resource consumption are listed in Table 4.12. The available machine and labor hours per week in each factory are shown in Tables E1 and E2 of the Appendix E.

Table 4.11 Weekly Product Demand of the 4F-2W-4S Network

	Product A		Product B	
	Mean	Standard Deviation	Mean	Standard Deviation
Store 1	250	35	200	40
Store 2	350	42	300	57
Store 3	180	45	160	30
Store 4	220	40	190	40

Table 4.12 Parameters for Production Planning in FMLA Problem

Item	Notation	Product A (i=1)	Product B (i=2)	Unit
Energy use	e_i	0.9	1.2	MWh/item
Production cost	p_i	400	600	$/item
Holding cost	h_i	16	24	$/item/week
Backorder cost	b_i	75	100	$/item
Shipping cost	π_i	0.05	0.08	$/item/km
Labor hour	w_{i1}	16	24	hour/item
Machine hour	w_{i2}	100	200	hour/item
Product weight	m_i	3	4	kg/item

Table 4.13 Parameters for Microgrid System in FMLA Problem

Item	Notation	Value	Unit	Notation	Value	Unit
WT	a_g	1.5	$M/MW	w_v	5000	kg
WT	b_g	12	$/MWh	q_v	1.19×10^{-7}	MWh/kg/km
WT	c_g	0	$/MWh	T	168	Hour/period
WT/PV	ϕ_g	0.0802	n/a	n_{jkn}	1	trip/week
PV	a_g	1.9	$M/MW	$\hat{n}_{jns}$	1	trip/week
PV	b_g	4	$/MWh	τ_w	1	hour
PV	c_g	10	$MWh	$P^c{}_{max}$	20	MW
ESS	b_{ES}	0	$/MWh	τ_{gk}, τ_{gn}, τ_{gs}	1	hour
ESS	d_{ES}	0.4	$M/MWh	$\rho^{bu}{}_{jkt}$, $\rho^{bu}{}_{jnt}$, $\rho^{bu}{}_{jst}$	70	$/MWh
ESS	ϕ_{ES}	0.1295	n/a	$\rho^{se}{}_{jkt}$, $\rho^{se}{}_{jnt}$, $\rho^{se}{}_{jst}$	50	$/MWh

Some renewables-related input data is further provided in Table 4.13, such as WT, PV, ESS, e-trucks and utility pricing. These data are adopted or estimated based on the reports from National Renewable Energy Laboratory (Stehly et al. 2018; Fu et al. 2018a; Fu et al. 2018b). The capital recovery factor of WT and PV, ϕ_g is estimated based on a 20-year lifetime with an annual discount rate of 5%. For the capital recovery factor of ESS, ϕ_{ES} is estimated based on its 10-year lifetime with an annual discount rate of 5%. All Factories and warehouse operate in 24 hours a day and 7 days a week (i.e., 24/7 mode), and the electric load of a factory depends on the hourly production rate of

Products A and B. It is assumed that warehouses have a relatively stable load of 7 MW. Table 4.14 (Ortiz-Astorquiza 2018, Alizadeh 2019) lists the fixed setup cost and energy consumption and warehouse capacity of all candidate facilities.

Table 4.14 Setup Cost, Energy Demand and Capacity of Facilities

Candidate Location	Facility	Annualized Setup Cost ($)	Energy Demand (MW)	Capacity
Phoenix	Factory 1	40,000,000	n/a	n/a
Reno	Factory 2	45,000,000	n/a	n/a
Yuma	Factory 3	35,000,000	n/a	n/a
Tucson	Factory 4	42,000,000	n/a	n/a
Las Vegas	Warehouse 1	20,000,000	7	2,000
Los Angeles	Warehouse 2	25,000,000	7	2,000

4.4.2 Results and Discussion

Models FMLA1, FMLA2 and FMLA3 are solved separately to schedule the weekly production over one-year period. These models are coded with Advanced AMPL software. Gurobi solver is used to search for the optimal solution for minimizing the supply chain cost. All AMPL codes are executed in a PC with Intel(R) Core (TM) i5-7200U CPU @ 2.5GHz, 4 Core(s), 24 GB memory, and 4 Logical Processor. The number of variables and constraints of the three models given by AMPL are tabulated in Table 4.15.

Table 4.15 The Size of Three Optimization Models

Model type	Model	Number of Variables	Number of Constraints
Non-Linear Model	FMLA1	162,184	109,130
Basic Big-value Model	FMLA2	214,600	267,210
Simplified Big-value Model	FMLA3	162,184	214,812

Table 4.16 compares the computation time and the solution results of the three models. Model FMLA1 yields the least cost of $178,927,112, but it requires the longest computation time of 5694.5s. Model FMLA2 has the fastest solution time of 137.4s, but it also has the worst solution of $178,936,445, which is 0.005% higher than the non-linear model. The solution time of Model FMLA3 is 287.6s, which is compatible to FMLA2. The optimal cost of FMLA3 is $178,931,575. This is only 0.003% higher than the nonlinear model (i.e., FMAL1). Therefore, Model FMLA3 is preferred because it can generate a high-quality solution with much smaller computation time.

Table 4.16 Optimal Cost and Computation Time of Three Models

Model	Objective Function ($)	Cost Difference ($)	Relative Difference in %	Computation Time (s)
FMLA1	178,927,112	0	0	5694.5
FMLA2	178,936,445	9,333	0.005	137.4
FMLA3	178,931,575	4,463	0.003	287.6

The three models yield the same location choice for factories and warehouses. Two factories are to be opened: one in Yuma and the other in Tucson. Only one warehouse is needed and opened in Los Angeles. The result is summarized in Table 4.17.

Table 4.17 Decisions on Facility Location and Allocation

Candidate Location	Facility	Solution	Open
Phoenix	Factory 1	0	no
Reno	Factory 2	0	no
Yuma	Factory 3	1	yes
Tucson	Factory 4	1	yes
Las Vegas	Warehouse 1	1	yes
Los Angeles	Warehouse 2	0	no

In terms of energy storage, the optimal solutions given by the three models show that there is no installation for ESS in all factories and warehouses. For the sizing of WT

and PV, the results of the three models are shown in Table 4.18, and their results are almost identical.

Table 4.18 Microgrid Allocation of Three Method Models

Model	Microgrid	Factory 3	Factory 4	Warehouse 1
FMLA1	WT	0	0	3.19
	PV	0	10.36	7.12
	ESS	0	0	0
FMLA2	WT	0	0	3.2
	PV	0	10.35	7.12
	ESS	0	0	0
FMLA3	WT	0	0	3.20
	PV	0	10.36	7.12
	ESS	0	0	0

Figures 4.4 and 4.5 show the decisions on **x**, **y** and **z** of Products A and B based on Model FMLA1. Similar results hold for other two models. Since the backorder cost is relatively high for both products, the model returns a solution with small amounts of backorders.

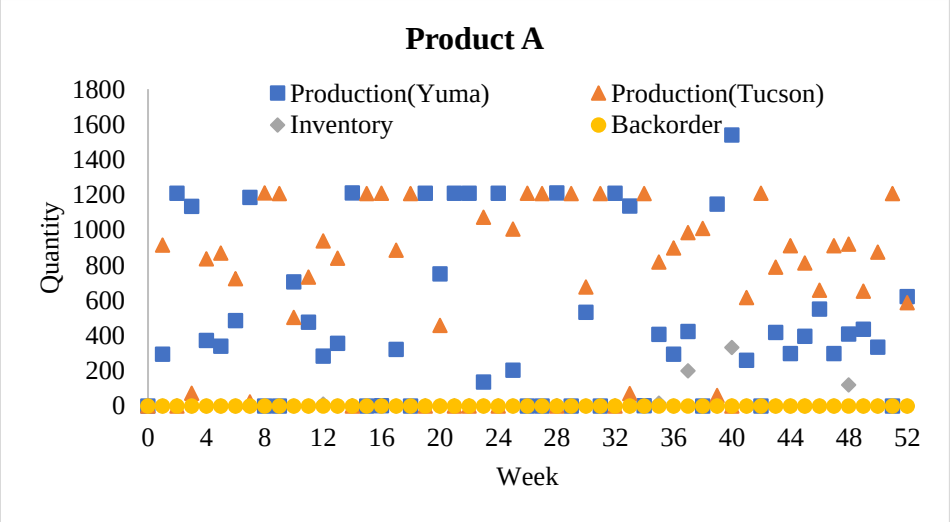


Figure 4.4 Production, Inventory, and Backorder of Product A

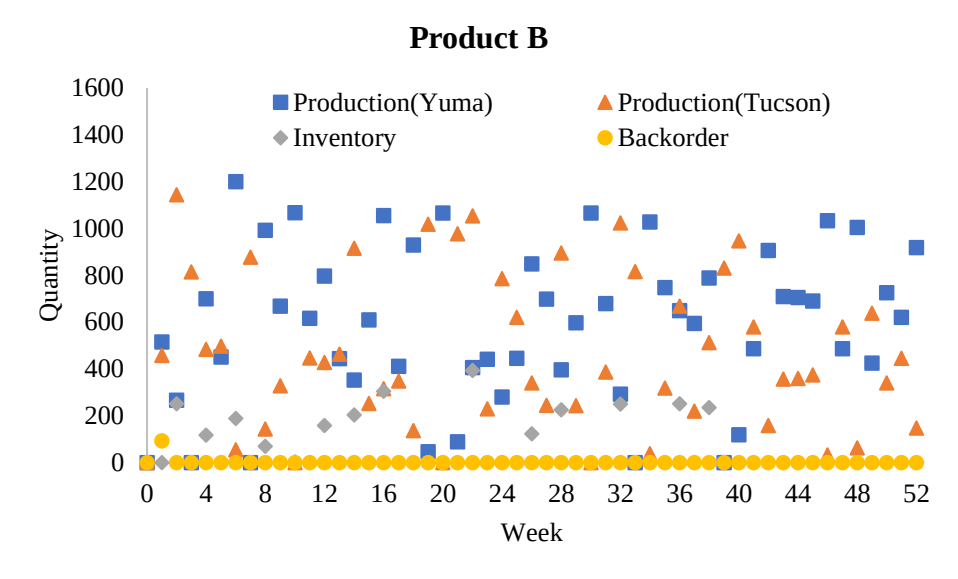


Figure 4.5 Production, Inventory, and Backorder of Product B

Figures 4.6 and 4.7 show the hourly energy bought from and sold to the grid for the factory in over fifteen weeks and in Week 10, respectively. The factory can engage two-way energy trading because of the onsite WT and PV generation. Figures 4.8 and 4.9 show the energy flow of Factory 3 in Yuma and Warehouse 1 in Las Vegas, respectively. The factory in Yuma leverage grid power for facility operations because of no microgrid installation. The variation of the power demand is due to the fact that the production varies in each period, causing the change in energy use. The warehouse in Las Vegas chooses to install WT and PV due to high wind and solar CF, and the power deficit is met by the main grid. Meanwhile, in days with higher wind or solar generation, the excess energy can be sold to the main grid via the transactive market.

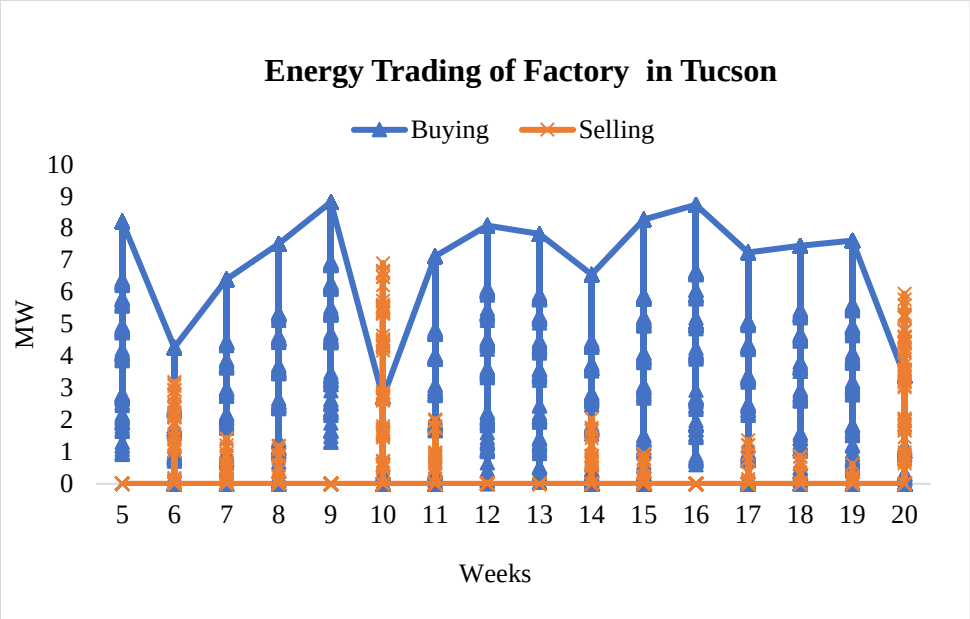


Figure 4.6 Prosumer Hourly Energy Trading of Factory 4 in Week 10

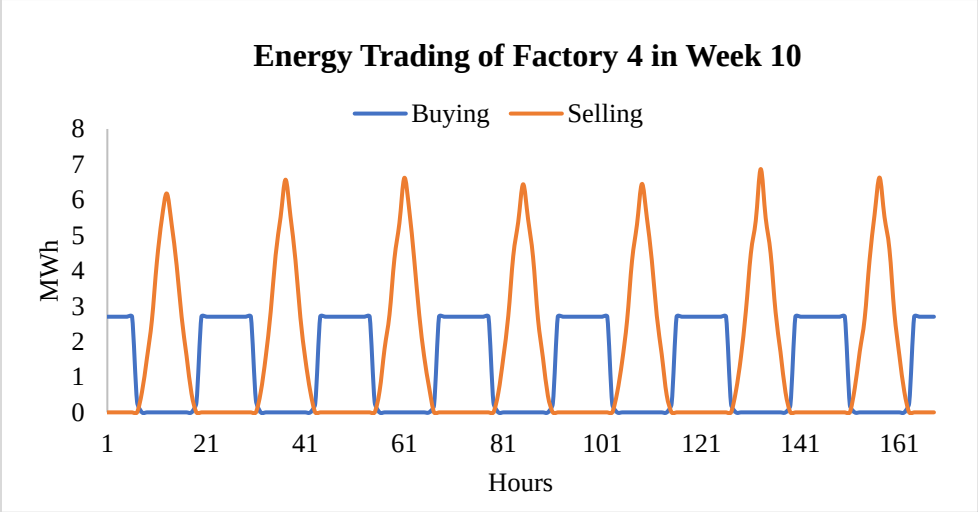


Figure 4.7 Prosumer Hourly Energy Trading of Factory 4 in Weeks 5 to 20

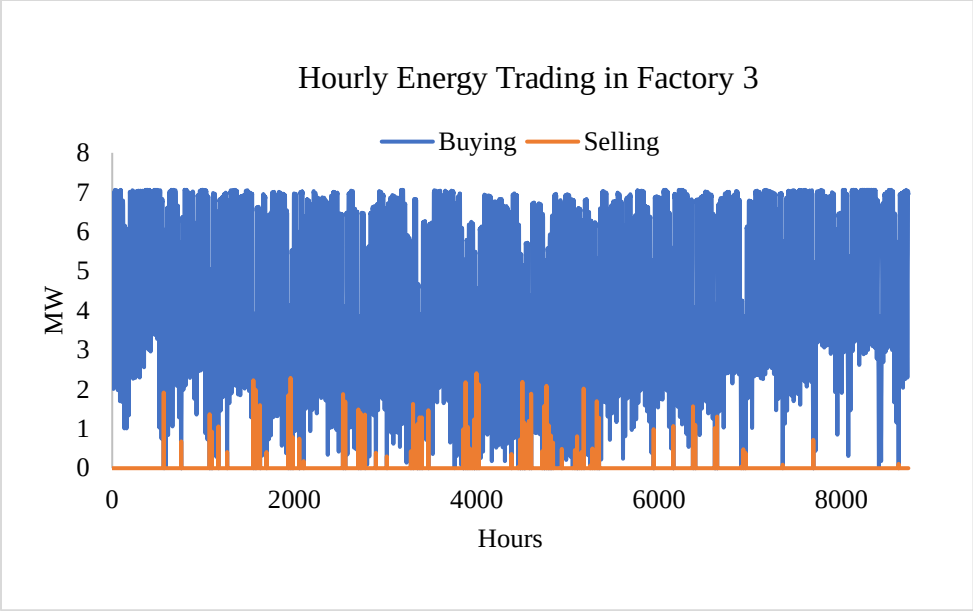


Figure 4.8 Prosumer Hourly Energy Trading of Factory 3

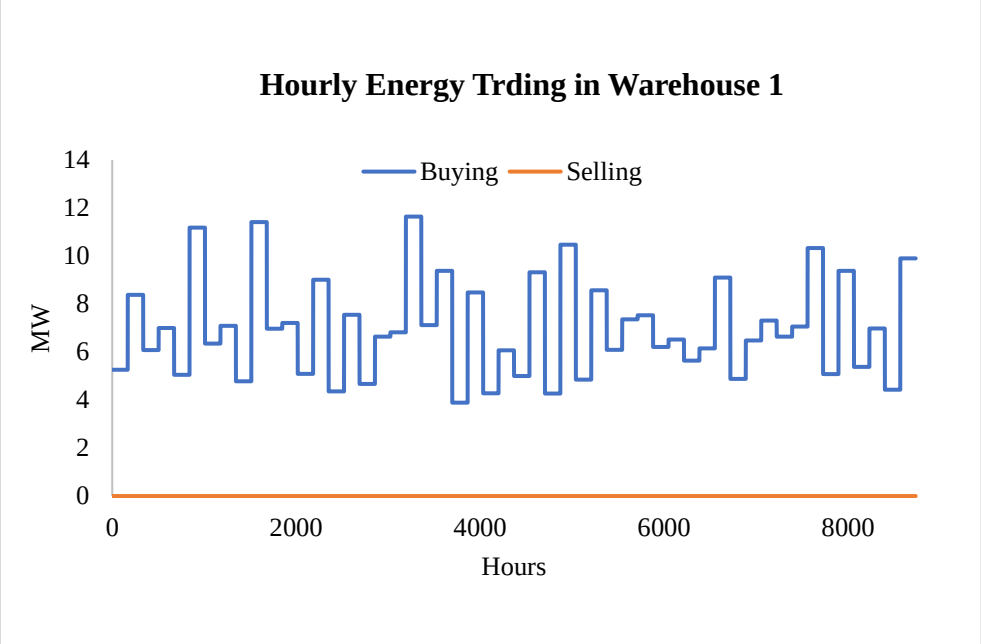


Figure 4.9 Prosumer Hourly Energy Trading of Warehouse 1

4.5 Sensitivity Analysis

4.5.1 Sensitivity Analysis on Production Planning

We made a sensitivity analysis of the model from the aspects of holding and backorder cost, product energy use, and unit production cost to investigate the influence of these aspects on the model. Compared with the benchmark value in Table 4.12 the variation of holding and backorder costs of Product A and B is ±50% and ±100%, and the variation of product energy use is ±25%, ±50% and ±100%, The variation of unit production cost is ±15%, ±25% and ±50%, a total of 17 scenarios are analyzed. The results are listed in Table 4.19. In terms of holding and backorder cost, the impact on the supply chain cost is nominal, ranging from -0.06% to 0.04%. If product energy use changes by ±100%, the total cost changes by ±4.76% compared with the benchmark cost. If the unit production cost change by ±15%, the total supply chain cost varies by ±4.9%. It is anticipated that the unit production cost has the largest impact on the supply chain cost. Overall, the production decisions based on Model FMLA1 are robust, regardless of the variations in holding and backorder cost, product energy use, or unit production cost.

Table 4.19 Sensitivity Analysis on Production Planning

Scenarios	Comment	Total cost ($)	Difference ($)	Relative Difference (%)
1	Benchmark	178,931,575	0.00	0.00%
2	Increase h_i50%	178,968,974	37,399	0.02%
3	Decrease h_i 50%	178,892,522	-39,052	-0.02%
4	Increase h_i 100%	179,002,927	71,352	0.04%
5	Decrease h_i 100%	178,828,867	-102,707	-0.06%
6	Increase b_i 50%	178,936,180	4,605	0.00%
7	Decrease b_i 50%	178,923,717	-7,857	0.00%
8	Increase b_i 100%	178,940,827	9,252	0.01%
9	Decrease b_i 100%	178,819,825	-111,749	-0.06%
10	Increase e_i 25%	181,059,959	2,128,383	1.19%

11	Decrease e_i 25%	176,802,877	-2,128,697	-1.19%
12	Increase e_i 50%	183,188,020	4,256,445	2.38%
13	Decrease e_i 50%	174,673,994	-4,257,581	-2.38%
14	Increase e_i 100%	187,442,590	8,511,015	4.76%
15	Decrease e_i 100%	170,416,121	-8,515,454	-4.76%
16	Increase p_i 15%	187,692,312	8,760,737	4.90%
17	Decrease p_i 15%	170,170,614	-8,760,960	-4.90%

4.5.2 Sensitivity Analysis on Microgrid Sizing

Several microgrid parameters including energy selling price, buying price, time-of-use (TOU) rate, and cost of WT, PV and ESS units are changed to examine their impacts on the supply chain cost. We compare 14 difference cases with the benchmark, and the results are shown in Table 4.20. There are three observations made from the sensitivity analysis data. I assume that cases with a difference of less than 1% from benchmark's results in the results of the sensitivity analysis indicate that the case has a small impact on total cost, while cases with a difference of more than 1% from benchmark have a larger impact on total cost.

- First, by comparing Case 3 to 5 with Case 1 (i.e., benchmark), when the electricity purchase price increases, the total cost goes up significantly, indicating that the electricity purchase price has a greater impact on the system.
- Second, from the result of Case 9 to 11, reducing the ESS cost does not significantly lower the total supply chain cost. We can conclude that the ESS unit can streamline the variable power generation, but the cost saving is minimum in grid-tied microgrid operation.
- Third, Cases 12 to 15 show that the installation cost of PV and WT has a significant impact on the total expenditure of the supply chain system.

Table 4.20 Sensitivity Analysis on Microgrid Sizing

Case	Comments	Total cost ($)	Cost Difference ($)	Difference (%)
1	Benchmark	178,931,575	0.00	0.00
2	Energy selling price increase 25%	178,879,948	-51,627	-0.03
3	Energy purchase price increase 25%	180,969,274	2,037,699	1.14
4	Energy purchase price increase 50%	182,551,163	3,619,587	2.02
5	Energy purchase price increase 100%	185,101,461	6,169,887	3.45
6	Buy: 70/MWh (10am-9pm), $35/MWh (10pm-9am), Sell:50/MWh (10am-9pm), $25/MWh (10pm-9am)	175,821,518	-3,110,057	-1.74
7	Buy: $140/MWh (10am-9pm), $70/MWh (10pm-9am), Sell: $100/MWh (10am-9pm), $50/MWh (10pm-9am)	178,485,720	-445,854	-0.25
8	Buy: $140/MWh (10am-9pm), $70/MWh (10pm-9am), Sell: $50/MWh (10am-9pm), $50/MWh (10pm-9am)	181,064,071	2,132,495	1.19
9	$0.01M/MWh for battery cost	178,870,627	-60,948	-0.03
10	$0.05M/MWh for battery cost	178,931,413	-162	0.00
11	$0.1M/MWh for battery cost	178,931,460	-115	0.00
12	$1.5M/MW for PV	177,786,537	-1,145,038	-0.64
13	$1M/MW for PV	175,401,335	-3,530,240	-1.97
14	$0.5M/MW for PV	172,995,424	-5,936,151	-3.32
15	$1M/MW for WT	177,924,628	-1,006,947	-0.56

4.5.3 Model Scalability

Production Planning

To examine the scalability, Model FMLA is implemented in a larger supply chain network with 20-facility. The 8F-4W-8S network is comprised of eight factories, four warehouses, and eight stores. The eight factories are located in Phoenix, Reno, Yuma and Tucson, Salt Lake, San Jose, Sacramento, San Francisco, respectively. The four warehouses are located in Las Vegas and Los Angeles, and two other virtual cities, respectively. All eight stores are in virtual cities. All microgrids are connected with the main grid. Table 4.21 shows the distances between the factories and the warehouses and between the warehouses and the stores.

Table 4.21 Distance between the Facilities (km)

Factory	W1	W2	W3	W4	W1	W2	W3	W4	Store
F1	478	600	462	856	1105	444	473	705	S1
F2	722	833	682	457	869	929	729	1028	S2
F3	475	440	533	1044	583	608	1060	958	S3
F4	664	488	1038	626	1018	659	846	1003	S4
F5	677	1108	833	660	745	505	925	1020	S5
F6	848	547	529	1072	1010	737	562	477	S6
F7	906	618	558	797	518	607	712	733	S7
F8	917	613	611	453	742	586	661	762	S8

Table 4.22 Weekly Product Demand of the 8F-4W-8S Network

	Product A		Product B	
Store	Mean	Standard Deviation	Mean	Standard Deviation
1	250	35	200	40
2	350	42	300	57
3	180	45	160	30
4	220	40	190	40
5	331	36	212	37

6	203	41	206	34
7	225	37	225	34
8	320	38	187	31

Table 4.23 Setup Cost, Energy Demand, and Capacity of New Candidate Locations

Facilities	Annualized setup cost ($)	Energy demand (MW)	Facility Capacity
Factory 4	44,000,000	n/a	n/a
Factory 5	38,000,000	n/a	n/a
Factory 6	35,000,000	n/a	n/a
Factory 7	38,000,000	n/a	n/a
Warehouse 3	21,000,000	6.5	2,000
Warehouse 4	26,000,000	7.5	2,000

Each factory can make Products A and B to meet the aggregate demand from the retail stores. Table 4.22 shows the mean and standard deviation of the weekly demand of eight stores. The availability of weekly labor and machine hours in each factory is shown in Tables C1 and C2 of Appendix C. Table 4.23 indicates the Setup cost, energy demand, and warehouse capacity of several newly added candidate locations. For this 8F-4W-8S network, factories will be opened in Yuma, San Jose, Sacramento and San Francisco among the eight factory candidate locations, and the warehouse will be opened in the first and third candidates of four warehouse candidate locations. In this network, there are 332,720 decision variables and 436,312 constraints. The total cost yielded by FMLA3 is $344,791,648. Figures 4.10 to figure 4.13 show the weekly production of Products A and B in eight factories, as well as the inventory and backorders in four warehouses, respectively.

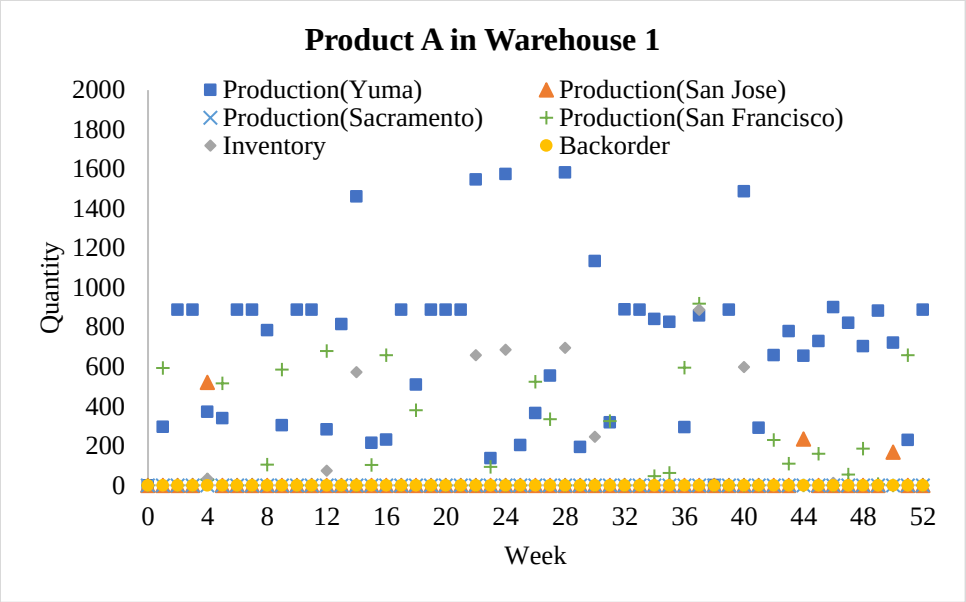


Figure 4.10 Production and Inventory Planning Product A in Warehouse 1

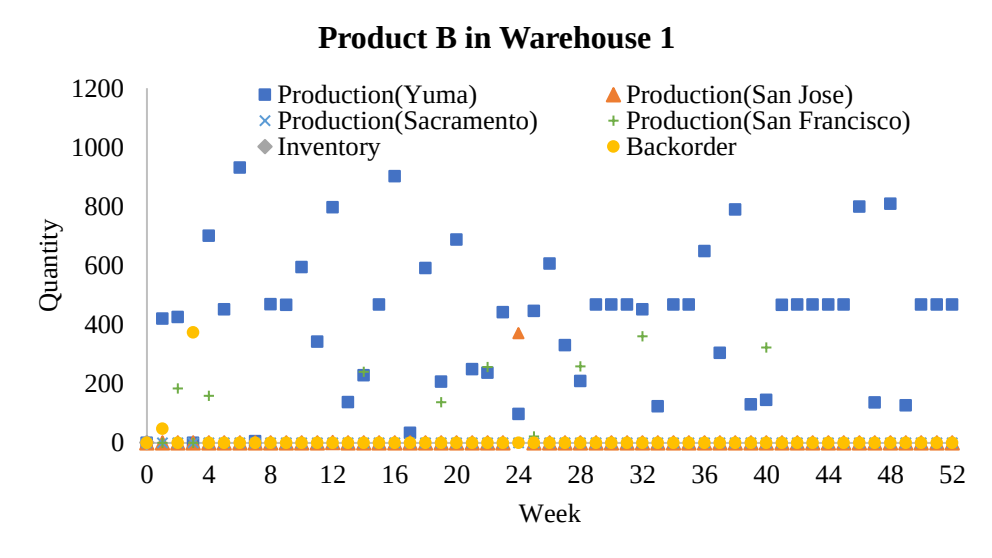


Figure 4.11 Production and Inventory Planning Product B in Warehouse 1

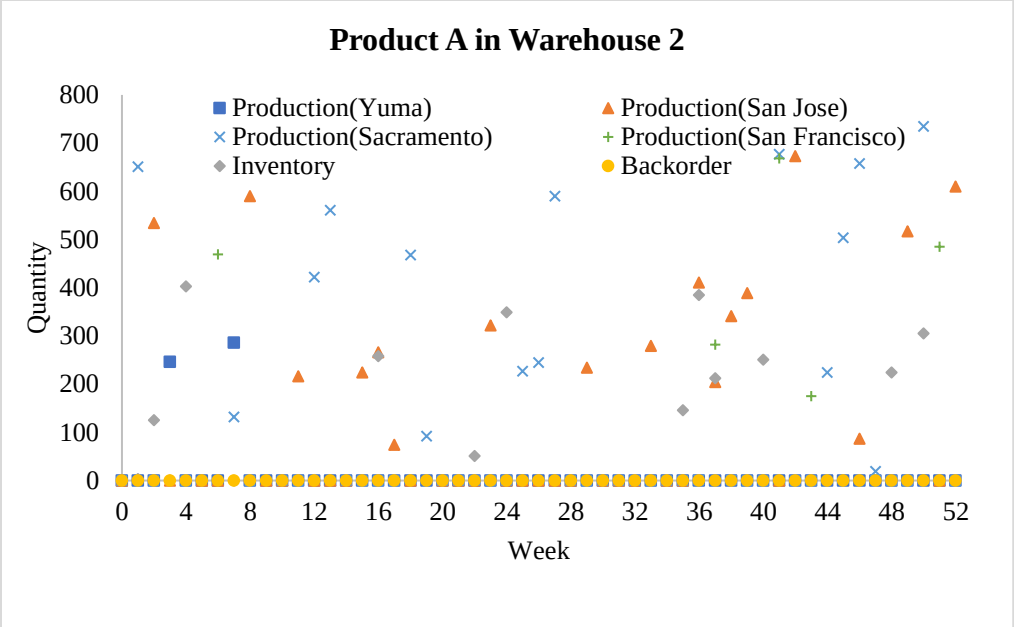


Figure 4.12 Production and Inventory Planning Product A in Warehouse 2

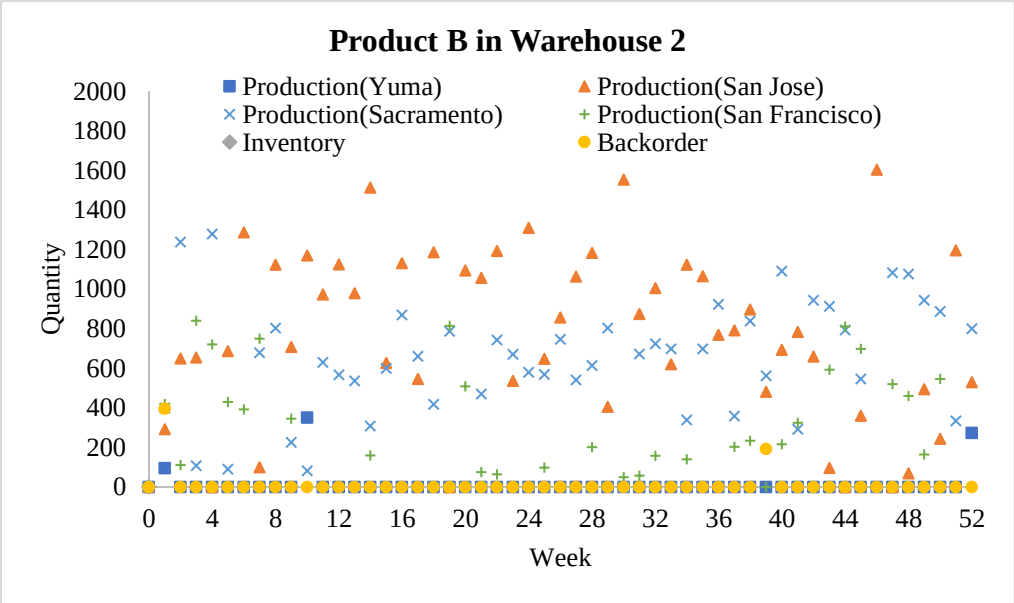


Figure 4.13 Production and Inventory Planning Product B in Warehouse 2

Microgrid Sizing

The results of WT, PV and ESS sizing for each facility are presented in Table 4.24. Factory 8 in San Francisco installs 20 MW WT. Warehouse 1 in Las Vegas installs

3.19 MW WT and 7.09 MW PV, and Warehouse 3 installs 20 MW WT. Other facilities opt for no microgrid installation and are powered by the main grid.

Table 4.24 Microgrid Allocation of the 8F-4W-8S Network

Item	Factory				Warehouse	
	3	6	7	8	1	3
WT(MW)	0	0	0	20	3.19	20
PV(MW)	0	0	0	0	7.09	0
ESS (MW)	0	0	0	0	0	0

5. FACILITY-MICROGRID LOCATION ALLOCATION FOR RISK AVERSE DESIGN

5.1 Introduction

While renewable generation is an effective solution to the climate change crisis, their instability also makes the system design and operations challenging. For example, during the design of a renewables-based microgrid, it is necessary to consider the type of renewables and installation capacity in relation to the energy demand, wind speed, solar irradiance and electricity price of the facility site. To streamline the intermittency, we may consider whether it is necessary to add ESS and what the storage capacity is needed to balance energy supply and demand as well as to maximize the efficiency of energy utilization.

Among the various uncertainties, climate conditions such as wind speed and sunshine state are of particular importance. In the previous section, we leverage the concept of cap CF to model the impact of weather conditions on renewable generation. We can obtain the weather statistics of a region based on historical meteorological data, such as the mean and variance of the CF, but we still do not know the exact CF at a particular time instance in the future. By converting the deterministic model into a stochastic model, we can mimic the real situation as close as possible.

In this chapter, we convert the models in Chapter 4 into the stochastic programming model. In the conversion process, we assume that the CF is a random parameter, and all other parameters are deterministic or known. By generating new data through simulation based on historical data, we obtain a series of scenarios and the probability of occurrence of each scenario. We solve the stochastic facility-microgrid

location-allocation model and can obtain a more realistic optimal solution based on CF scenarios and different occurrence probabilities.

In the deterministic optimization model, since the input data are all known, the optimal solution is also a deterministic value. However, compared with the deterministic optimization, the optimal solution of a stochastic optimization model only represents the best solution in the current scenario. It may not be the globally optimal solution that exactly matches the reality of all possible scenarios or situations. This requires us to evaluate the results according to the different criteria. The commonly used decision-making criteria include Expectation Value, MiniMin, Minimax, Value-at-Risk (VaR), Conditional Value-at-Risk (CVaR), Minimax Regret (MMR). In this chapter we focus on comparing the solution results derived from VaR, CVaR and Minimax.

Whether it is VaR, CVaR or Minimax, the optimal solution is evaluated after considering the results of all scenarios. VaR and CVaR need to give the result based on a certain confidence level. In contrast, Minimax takes the maximum result of all scenarios as the final optimal solution. Therefore, this criterion is also one of the most pessimistic and, of course, the most risk-averse. Compared with Minimax arbitrary selection method, VaR allows decision-maker to obtain the final result at certain confidence level. On the other hand, the results given by the VaR only consider the values within the confidence interval, and do not consider the conditions beyond the confidence level. Therefore, VaR is a relatively optimistic criterion, and the degree of risk-averse is not strong. CVaR is proposed to address the weakness of VaR by improving or fully considering the situations outside the confidence level. Hence the results are more convincing, and the risk-averse ability is much stronger than VaR. All three methods have their own

advantages and disadvantages, we will be able to achieve the best results by choosing the appropriate criteria according to the actual situation.

5.2 Model Formulation

Table 5.1 summarizes the model parameter, and Table 5.2 lists the decision variables.

Table 5.1 Parameters for Stochastic Model

Notation	Definition
K	number of candidate factory sites, for k=1, 2, ..., K.
N	number of candidate warehouse sites, for n=1, 2, ..., N.
S	number of retail stores, for s=1, 2, ..., S.
G	type of renewable generation, for g=1, 2, ..., G.
R	number of required production resources, for r=1, 2, ..., R.
T	number of power scheduling periods, for t=1, 2, …, T.
W	number of wind and solar capacity factor scenarios, for w=1, 2, …, W
π_{ikn}	unit shipping cost of product i from factory k to warehouse n ($/item/km).
π_{ins}	unit shipping cost of product i from warehouse n to store s ($/item/km).
D_{ijs}	demand for product i of store s in period j.
α	probability of meeting the product demand.
β_w	probability of wind and solar generation scenario w at factories
τ_p	time step size of a production planning period.
τ_{gk}	operating time of generation g at factory k in a production period.
τ_{gn}	operating time of generation g at warehouse n in a production period.
τ_{gs}	operating time of generation g at store s in a production period.
τ_w	operating hours of warehouse n at time t.
a_g	capacity cost of renewable generation g ($/MW).
d_{ES}	capacity cost of energy storage device ($/MWh).
b_{gk}	operation and maintenance cost of generation g at factory k ($/MWh).
b_{gn}	operation and maintenance cost of generation g at warehouse n ($/MWh).
c_{gk}	carbon credits of generation g at factory k ($/MWh).
c_{gn}	carbon credits of generation g at warehouse n ($/MWh).
b_{ES}	maintenance cost of energy storage device ($/MWh).
ϕ_g	capital recovery factor of generation g.
φ_{ES}	capital recovery factor of energy storage system.
$\lambda_{\omega gjkt}$	capacity factor of generation g for factory k in period j at time t of scenario ω.
$\lambda_{\omega gjnt}$	capacity factor of generation g for warehouse n in period j at time t of scenario ω.
ρ^{se}_{jkt}	price of selling electricity from factory k in period j at time t ($/MWh).

ρ^{se}_{jnt}	price of selling electricity from warehouse *n* in period *j* at time *t* ($/MWh).
ρ^{bu}_{jkt}	price of buying electricity by factory *k* in period *j* at time *t* ($/MWh).
ρ^{bu}_{jnt}	price of buying electricity by warehouse *n* in period *j* at time *t* ($/MWh).
m_i	unit weight of product *i* (kg/item).
e_{ik}	energy use for making one unit of product *i* at facility *k* (MWh/unit).
q_{EV}	e-truck energy intensity rate (MWh/kg/km).
m_{EV}	e-truck self-weight (kg).
n_{jknt}	number of trips between factory *k* and warehouse *n* in period *j* at time *t*.
$\hat{n}_{jnst}$	number of trips between warehouse *n* and store *s* in period *j* at time *t*.
$P_{gk}^{\max}$	maximum capacity installation of generation *g* in factory *k* (MW).
$P_{gn}^{\max}$	maximum capacity installation of generation *g* in warehouse *n* (MW).
F_k	annualized cost of opening a factory in location *k*.
$\hat{F}_n$	annualized cost of opening a warehouse in location *n*.
p_{ijk}	cost of making one unit of product *i* in period *j* at factory *k* ($/item).
h_{ijn}	holding cost of product *i* in period *j* at warehouse *n* ($/item/period).
b_{ijn}	backorder cost of product *i* in period *j* at warehouse *n* ($/item).
γ_{in}	warehouse capacity for product *i* at warehouse site *n*.
d_{kn}	distance from factory site *k* to warehouse site *n* (km)
$\hat{d}_{ns}$	distance from warehouse site *n* to store site *s* (km)
L_n	power demand of warehouse in location *n*.
w_{ikr}	resource *r* consumed for making one unit of product *i* at factory *k*.
W_{jkr}	total available production resource *r* in period *j* at factory *k*.

Table 5.2 Decision Variables of Stochastic Model

Notation	Definition
u_k	1 if a factory is opened at site *k*, and 0 otherwise.
v_{ijkn}	1 if product *i* made by factory *k* is shipped to warehouse *n* in period *j*, and 0 otherwise.
$\hat{u}_n$	1 if a warehouse is opened at site *n*, and 0 otherwise.
$\hat{v}_{ins}$	1 if demand *i* at store *s* is served by warehouse at site *n*, and 0 otherwise.
x_{ijkn}	The amount of product *i* made by factory *k* in period *j* and shipped to warehouse *n*.
$\hat{x}_{ijns}$	The amount of product *i* shipped from warehouse *n* to store *s* in period *j*.
y_{ijn}	inventory of product *i* in period *j* at warehouse *n*.
z_{ijn}	backorders of product *i* in period *j* at warehouse *n*.
P^c_{gk}	installed capacity of generation *g* at factory *k* (MW).
P^c_{gn}	installed capacity of generation *g* at warehouse *n* (MW).
B^c_k	installed capacity of energy storage device at factory *k* (MWh).
B^c_n	installed capacity of energy storage device at warehouse *n* (MWh).
B_{jkt}	energy stored in ESS at factory *k* in period *j* at time *t* (MWh).
B_{jnt}	energy stored in ESS at warehouse *n* in period *j* at time *t* (MWh).

E^{se}_{jkt}	energy sold from factory *k* in period *j* at time *t* (MWh).
E^{se}_{jnt}	energy sold from warehouse *n* in period *j* at time *t* (MWh).
E^{bu}_{jkt}	energy bought by factory *k* from the grid in period *j* at time *t* (MWh).
E^{bu}_{jnt}	energy bought by warehouse *n* from the grid in period *j* at time *t* (MWh).

In this stochastic optimization model, we assume that wind speed and solar irradiance are random parameters, corresponding to the CF of both WT and solar PV in the model. based on this assumption, the objective function is converted into Equation (5.1), and for constraints, we only need to convert Equations (4.112) and (4.117) of Chapter 4 into Equations (5.16) and (5.21), respectively. All other constraints remain the same. The optimal solution obtained from this stochastic optimization model will be the expectation of all scenarios. The stochastic optimization model is described as follows:

Model 5.1 SFMLA (Stochastic Facility-Microgrid Location-Allocation Model)

Minimize:

$$
\begin{aligned}
&C_D(\mathbf{u},\hat{\mathbf{u}},\mathbf{v},\hat{\mathbf{v}},\mathbf{x},\mathbf{y},\mathbf{z},\mathbf{P}^c,\mathbf{B}^c,\mathbf{E}) \\
&=\sum_{k=1}^{K}F_k u_k+\sum_{i=1}^{I}\sum_{j=1}^{J}\sum_{k=1}^{K}\sum_{n=1}^{N}x_{ijkn}p_{ijk}+\sum_{i=1}^{I}\sum_{j=1}^{J}\sum_{k=1}^{K}\sum_{n=1}^{N}x_{ijkn}\pi_{ikn}d_{kn} \\
&+\sum_{n=1}^{N}\hat{F}_n\hat{u}_n+\sum_{i=1}^{I}\sum_{j=1}^{J}\sum_{n=1}^{N}h_{ijn}y_{ijn}+\sum_{i=1}^{I}\sum_{j=1}^{J-1}\sum_{n=1}^{N}b_{ijn}z_{ijn}+\sum_{i=1}^{I}\sum_{j=1}^{J}\sum_{n=1}^{N}\sum_{s=1}^{S}\hat{x}_{ijns}\pi_{ins}d_{ns} \\
&+\sum_{g=1}^{G}\sum_{k=1}^{K}\phi_g a_g P^c_{gk}+\sum_{j=1}^{J}\sum_{t=1}^{T}\sum_{g=1}^{G}\sum_{k=1}^{K}\sum_{\omega=1}^{\Omega}\beta_\omega\tau_{gk}(b_g-c_g)\lambda_{\omega gjkt}P^c_{gk} \\
&+(\phi_{ES}d_{ES}+b_{ES})\sum_{k=1}^{K}B^c_k+\sum_{j=1}^{J}\sum_{t=1}^{T}\sum_{k=1}^{K}(\rho^{bu}_{jkt}E^{bu}_{jkt}-\rho^{se}_{jkt}E^{se}_{jkt}) \\
&+\sum_{g=1}^{G}\sum_{n=1}^{N}\phi_g a_g P^c_{gn}+\sum_{j=1}^{J}\sum_{t=1}^{T}\sum_{g=1}^{G}\sum_{n=1}^{N}\sum_{\omega=1}^{\Omega}\beta_\omega\tau_{gn}(b_g-c_g)\lambda_{\omega gjnt}P^c_{gn} \\
&+(\phi_{ES}d_{ES}+b_{ES})\sum_{n=1}^{N}B^c_n+\sum_{j=1}^{J}\sum_{t=1}^{T}\sum_{n=1}^{N}(\rho^{bu}_{jnt}E^{bu}_{jnt}-\rho^{se}_{jnt}E^{se}_{jnt})
\end{aligned}
\tag{5.1}
$$

Where:

w is the wind and solar generation scenarios for *w* =1, 2, …, W

b_w is the probability of generation capacity value of $l_{\omega gjkt}$ for generation g at factory k at time t in period j.

$$\sum_{\omega=1}^{\Omega} \beta_{\omega} = 1 \tag{5.2}$$

Subject to:

Constraints (5.3) to (5.40) below

A. Constraints of Facility Location

$$\sum_{k=1}^{K} x_{ijkn} \le \gamma_{in} \hat{u}_n, \qquad \forall i, \forall j, \text{ and } \forall n \tag{5.3}$$

$$\sum_{s=1}^{S} \hat{x}_{ijns} \le \gamma_{in} \hat{u}_n, \qquad \forall i, \forall j, \text{ and } \forall n \tag{5.4}$$

$$\sum_{n=1}^{N} \hat{v}_{ins} = 1, \qquad \forall i, \text{ and } \forall s \tag{5.5}$$

$$\hat{v}_{ins} \le \hat{u}_n, \qquad \forall\, i, \forall n, \text{ and } \forall s \tag{5.6}$$

$$u_k,\ \hat{u}_n \in \{0, 1\}, \qquad \forall k, \text{ and } \forall n \tag{5.7}$$

$$v_{ijkn},\ \hat{v}_{ins} \in \{0, 1\}, \qquad \forall i, \forall j, \forall k, \forall n, \text{ and } \forall s \tag{5.8}$$

Constraints (5.3) and (5.4) define the capacity of a warehouse if it is opened in a particular site. Constraint (5.5) indicates that a demand node (retail store) is served by only one warehouse or known as “dedicated warehouse” service. Constraints (5.6) show that the product shipping between a warehouse and a store is possible only if the upper stream warehouse is opened. Constraints (5.7) and (5.8) simply states the binary nature of decision variables.

B. Constraints of Production-Inventory Balance

$$\sum_{k=1}^{K} x_{i1kn} + y_{i0n} - y_{i1n} + z_{i1n} = \sum_{s=1}^{S} \hat{x}_{i1ns}\,, \qquad \text{for } j = 1,\ \forall i, \text{ and } \forall n \qquad (5.9)$$

$$\sum_{k=1}^{K} x_{ijkn} + y_{ij-1n} - y_{ijn} - z_{ij-1n} + z_{ijn} = \sum_{s=1}^{S} \hat{x}_{ijns}\,, \qquad \text{for } j = 2, 3, \ldots, J\text{-}1,\ \forall i, \text{ and } \forall n \qquad (5.10)$$

$$\sum_{k=1}^{K} x_{iJkn} + y_{iJ-1n} - y_{iJn} - z_{iJ-1n} = \sum_{s=1}^{S} \hat{x}_{iJns}\,, \qquad \text{for } j = J,\ \forall i, \text{ and } \forall n \qquad (5.11)$$

$$x_{ijkn} - M v_{ijkn} \le 0, \qquad \forall\ i, \forall j,\ \forall k, \text{ and } \forall n \qquad (5.12)$$

$$\hat{x}_{ijns} - M \hat{v}_{ins} \le 0, \qquad \forall\ i, \forall j,\ \forall n, \text{ and } \forall s \qquad (5.13)$$

$$\sum_{i=1}^{I} \sum_{n=1}^{N} w_{ikr} x_{ijkn} \le W_{jkr} u_k\,, \qquad \forall j,\ \forall k, \text{ and } \forall r \qquad (5.14)$$

$$y_{i0n} = 0, \qquad \forall i, \text{ and } \forall n \qquad (5.15)$$

$$\sum_{n=1}^{N} \hat{x}_{ijns} \ge E[D_{ijs}] + Z_\alpha \sqrt{Var(D_{ijs})}, \qquad \forall i,\ \forall j, \text{ and } \forall s \qquad (5.16)$$

Where, Z_a is the Z-value of the standard normal distribution.

C. Energy Balance Constraints

Balance for factory

$$\sum_{i=1}^{I} \sum_{n=1}^{N} (e_{ik} + q_{EV} d_{kn} m_i) x_{ijkn}^{t} + q_{EV} \sum_{i=1}^{I} \sum_{n=1}^{N} n_{jknt} d_{kn} m_{EV} v_{ijkn} + B_{jkt} - B_{jk,t-1} + E_{jkt}^{se} - E_{jkt}^{bu} = \sum_{g=1}^{G} \sum_{\omega=1}^{\Omega} \beta_\omega \tau_{gk} \lambda_{\omega gjkt} P_{gk}^{c}\,,$$

$$\forall j,\ \forall k, \text{ and } \forall t \qquad (5.17)$$

$$P_{gk}^{c} \le M \hat{u}_k\,, \qquad \forall g, \text{ and } \forall k \qquad (5.18)$$

$$B_k^{c} \le M \hat{u}_k\,, \qquad \forall k \qquad (5.19)$$

$$E_{kt}^{se} \le M \hat{u}_k\,, \qquad \forall k, \text{ and } \forall t \qquad (5.20)$$

$$E_{kt}^{bu} \le M \hat{u}_k\,, \qquad \forall k, \text{ and } \forall t \qquad (5.21)$$

Balance for warehouse

$$\tau_w L_n \hat{u}_n + q_{EV} \sum_{i=1}^{I} \sum_{k=1}^{K} n_{jknt} d_{kn} m_{EV} v_{ijkn} + q_{EV} \sum_{i=1}^{I} \sum_{s=1}^{S} \hat{d}_{ns} m_i \hat{x}^t_{ijns} + 2q_{EV} \sum_{i=1}^{I} \sum_{s=1}^{S} \hat{n}_{jnst} \hat{d}_{ns} m_{EV} \hat{v}_{ins} + B_{jnt} - B_{jn,t-1}$$
$$+ E^{se}_{jnt} - E^{bu}_{jnt} = \sum_{g=1}^{G} \sum_{\omega=1}^{\Omega} \tau_{gn} \lambda_{\omega gjnt} P^c_{gn},$$

$\forall j, \forall n,$ and $\forall t$ (5.22)

$P^c_{gn} \le M\hat{u}_n,$ $\forall g,$ and $\forall n$ (5.23)

$B^c_n \le M\hat{u}_n,$ $\forall n$ (5.24)

$E^{se}_{nt} \le M\hat{u}_n,$ $\forall n,$ and $\forall t$ (5.25)

$E^{bu}_{nt} \le M\hat{u}_n,$ $\forall t,$ and $\forall n$ (5.26)

Other Balances

$x^t_{ijkn} = \frac{x_{ijkn}}{T}$, $\forall i,\ \forall j, \forall k, \forall n,$ and $\forall t$ (5.27)

$\hat{x}^t_{ijns} = \frac{\hat{x}_{ijns}}{T}$, $\forall i,\ \forall j, \forall n, \forall s,$ and $\forall t$ (5.28)

$0 \le B_{jkt} \le B^c_k u_k$ $\forall j, \forall k,$ and $\forall t$ (5.29)

$0 \le B_{jnt} \le B^c_n \hat{u}_n$, $\forall j, \forall n,$ and $\forall t$ (5.30)

$B_{jk0} = B_{j-1,kT}$, for j =2, 3,…, J, and $\forall k$ (5.31)

$B_{jn0} = B_{j-1,nT}$, for j =2, 3,…, J, and $\forall n$ (5.32)

$B_{1k0} = B_{JkT} = B^c_k$ for j=1 and J, t=0 and T, and $\forall k$ (5.33)

$B_{1n0} = B_{JnT} = B^c_n,$ for j=1 and J, t=0 and T, and $\forall n$ (5.34)

$0 \le P^c_{gk}, P^c_{gn} \le P^c_{\max}$, $\forall g, \forall k,$ and $\forall n$ (5.35)

$E^{bu}_{jkt}, E^{se}_{jkt} \geq 0$, $\forall j$, $\forall k$, and $\forall t$ (5.36)

$E^{bu}_{jnt}, E^{se}_{jnt} \geq 0$, $\forall j$, $\forall n$, and $\forall t$ (5.37)

$B^{c}_{k}, B^{c}_{n} \geq 0$, $\forall k$, and $\forall n$ (5.38)

$B_{jkt}, B_{jnt} \geq 0$, $\forall j$, $\forall k$, $\forall n$, and $\forall t$ (5.39)

$x_{ijkn}, \hat{x}_{ijns}, y_{ijn}, z_{ijn} \in \{0,1,2....\}$, $\forall i$, $\forall j$, $\forall k$, $\forall n$, and $\forall t$ (5.40)

5.3 Value at Risk (VaR)

5.3.1 Mathematical Formulation

VaR is a measure of an investment's risk of loss. Under normal market conditions, it estimates how much a group of investments may lose with a given probability over a set period of time (for example, one month or a year). Firms and regulators in the financial industry typically use VaR to measure the amount of assets needed to cover the possible losses. VaR does provide an evaluation criterion for risk-averse decision-makers by taking into account the probability of various scenarios. However, VaR does not provide us with a decision process, in other words, the values of the variables and the optimal solutions can only be given by the stochastic optimization model, and VaR only provides the decision maker with a way to evaluate the optimal solutions from another perspective. The final result does not change the optimal solutions and values of the variables given by the stochastic optimization model. As shown in Figure 5.1, given $\varphi \in$ [0, 1] the VaR_{φ} corresponds to the φ^{th} quantile of the objective value of the scenarios. That is, VaR represents a threshold that exceeds the optimal solution, and the probability of that value occurring is (1-φ) 100%. Further, when φ becomes larger, the value of VaR also increases for the cost minimization problem we are addressing. This also means that

the results we obtain are more resistant to risk, because the probability of exceeding this value becomes smaller. When φ is 0 or (1-φ)100%=100%. we actually obtain the Minimax of all scenario results. The following model describes the process by which I obtain the minimum VaR:

Model 5.2

Min：

$$VaR_{\varphi} \tag{5.41}$$

Subject to:

$$C(\mathbf{u},\hat{\mathbf{u}},\mathbf{v},\hat{\mathbf{v}},\mathbf{x},\mathbf{y},\mathbf{z},\mathbf{P}^{c},\mathbf{B}^{c},\mathbf{E}|\omega)-VaR_{\varphi}\le M\delta_{\omega}, \qquad \forall\omega \tag{5.42}$$

$$\sum_{\omega=1}^{\Omega}\beta_{\omega}\delta_{\omega}\le 1-\varphi \tag{5.43}$$

Equation (5.44) indicates that our objective function is to find the minimum VaR with a confidence level of φ, and $C(\mathbf{u},\hat{\mathbf{u}},\mathbf{v},\hat{\mathbf{v}},\mathbf{x},\mathbf{y},\mathbf{z},\mathbf{P}^{c},\mathbf{B}^{c},\mathbf{E}|\omega)$ in the constraint (5.45) denotes the minimum cost when scene ω occurs, here δ_{ω} is a binary decision variable. If the cost exceeds VaR, then δ_{ω} =1. Otherwise, δ_{ω} =0. Finally, M is an arbitrary large value.

The main drawback of VaR is that it can only reflect the minimum loss with a certain probability but cannot give the loss beyond this probability. That is, when we apply VaR as a criterion, our attention is focused on the regular risks that can be managed with a distribution close to a certain probability, while ignoring the tail risks.

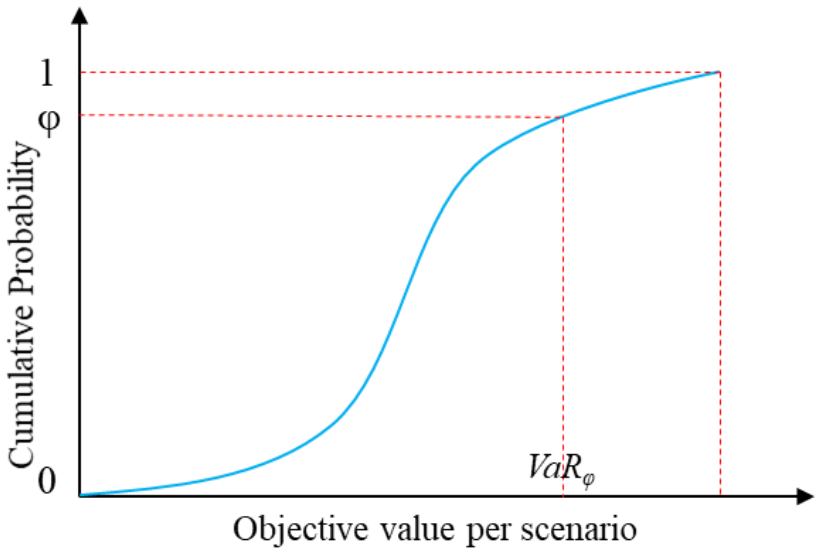


Figure 5.1 Graphical Illustration of VaR

5.3.2 Algorithm Description

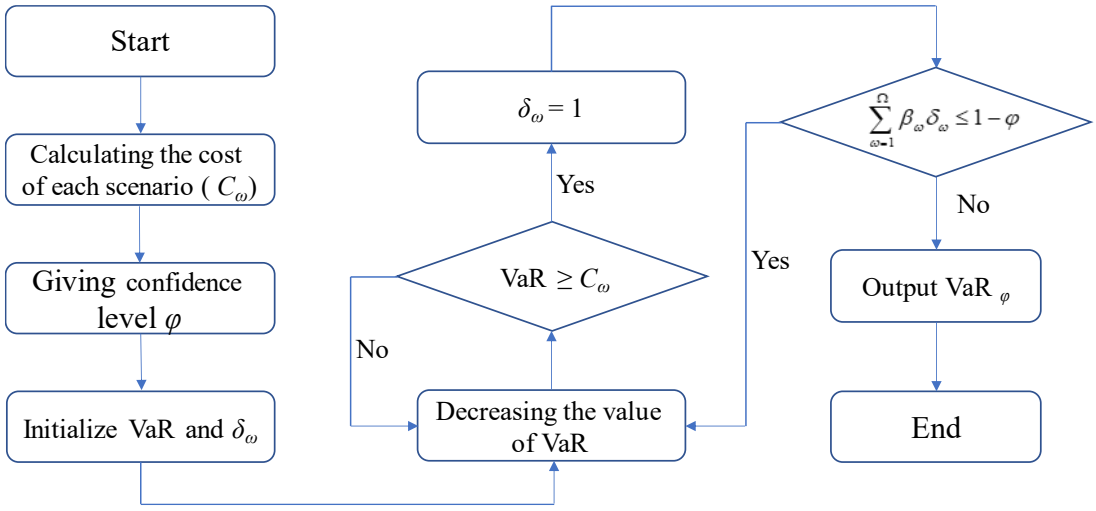


Figure 5.2 Flowchart of VaR Algorithm

As shown in Figure 5.2, before using the VaR criteria, we first calculate the cost of each scenario separately and then determine the confidence level φ. The next step is to initialize VaR and δ_ω, where VaR needs to be initialized and assigned an arbitrarily large value and δ_ω needs to be initialized to 0. Then the value of VaR should be continuously

reduced and each value is compared with the cost of each scenario. When the value of VaR is greater than or equal to the cost of a certain scenario, the value of δ associated with that particular scenario is taken as 1. The probability summation of all scenarios with δ=1 is then ensured to be no more than 1- φ. If the condition is met, the value of VaR is further reduced and the above steps are repeated. Otherwise, the current VaR will be output as the optimal solution at the confidence level (1-φ) × 100%.

5.4 Conditional Value at Risk (CVaR)

5.4.1 Mathematical Formulation

CVaR is a risk measurement technique proposed by Rockafellar and Uryasev in 1997 that is superior to VaR and is defined as the average value of losses in a portfolio under the condition that the portfolio's losses exceed a given VaR value. In other words, given $\varphi \in [0, 1)$, $CVaR_{\varphi}$ is to find the expected value of that part beyond VaR_{φ}, which is expressed as：

$$CVaR = \mathrm{E}_{\omega \in \Omega}\left[C_{\omega} \mid C_{\omega} \geq VaR_{\phi} \right] \tag{5.44}$$

Where C_{ω} denotes the cost per scenario, and VaR_{φ} denotes the value of VaR for a confidence level of φ. In other words, CVaR refers to the expectation beyond the VaR at a certain confidence level. When the confidence level is φ =0, the expectation of beyond this confidence level is not actually exceeded. Hence it is also meaningless for φ=1. Figure 5.2 shows the comparison of CVaR and VaR.

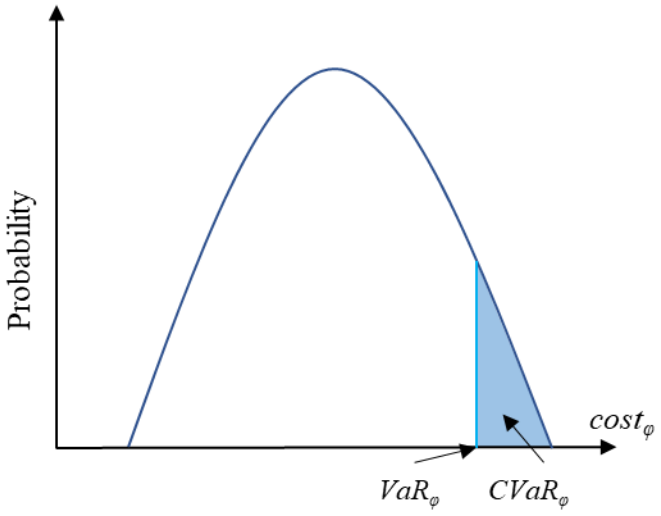


Figure 5.3 Graphical Illustration of CVaR

By minimizing CVaR, the decision maker can minimize the expected cost of (1-φ) × 100% of the worst scenarios in all scenario distributions. As with VaR, by increasing the value of φ, the value of CVaR will also become larger, thus giving more confidence in the results. In order to apply the CVaR criteria to our stochastic optimization model in a linear formulation, we refer to the method shown in the model as follows：

Model 5.3

Min：

$$CVaR_\varphi = \zeta + \frac{1}{1-\varphi}\sum_{\omega}^{\Omega}\beta_\omega \eta_\omega \tag{5.45}$$

Subject to:

$$C(\mathbf{u},\hat{\mathbf{u}},\mathbf{v},\hat{\mathbf{v}},\mathbf{x},\mathbf{y},\mathbf{z},\mathbf{P}^c,\mathbf{B}^c,\mathbf{E}|\omega) - \zeta \le \eta_\omega, \quad \forall \omega \tag{5.46}$$

$$\eta_\omega \ge 0 \tag{5.47}$$

where ζ and η_ω are the two auxiliary variables.

5.4.2 Algorithm Description

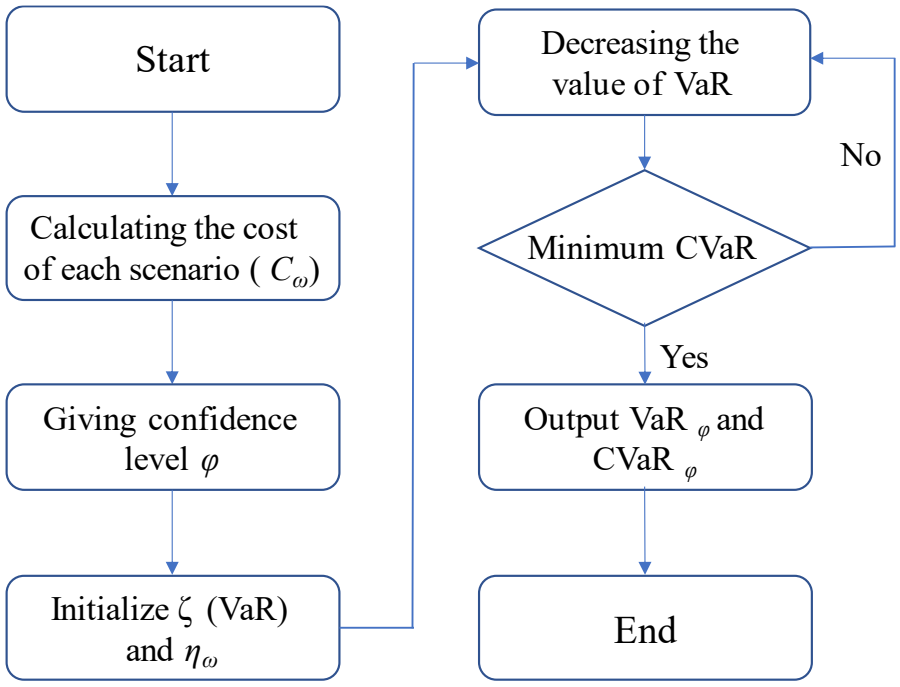


Figure 5.4 Flowchart of CVaR Algorithm

Similar to VaR, we need to calculate the cost of each scenario at given confidence level, and initialize the two variables ζ and η. The optimization process is carried out in the solver to obtain an optimal ζ and η. By analyzing the results, we can find that ζ at each confidence level is actually the VaR at that confidence level, and η is the difference between the cost of each scenario and VaR at this confidence level. The expected cost of all scenarios larger or equal VaR is the final CVaR at this confidence level. It is also because the expectations beyond VaR are taken into account. Hence CVaR is more conservative compared to VaR, and thus more risk averse. Taking tail risk into account, CVaR has a better ability to control risk, and in practice, CVaR is more widely used than VaR.

5.5 Minimax

5.5.1 Mathematical Formulation

The Minimax algorithm, as the name implies, is to minimize the maximum case, where maximum generally means the worst case, such as the most unfavorable case of all the scenarios. And the application in this research is to minimize the cost of the worst scenario. Minimax is a pessimistic algorithm, the algorithm is not to find the theoretical optimal solution, but to optimize the worst solution. The advantage of this algorithm is that it allows the decision maker to choose whether to accept the results from the perspective of the worst case. This criterion assumes that no condition will exceed the result comes from the model, so the evaluation criterion is also the most conservative and risk-averse of the three criteria.

Model 5.4

Min：

$$M \tag{5.48}$$

Subject to:

$$M \geq C(\mathbf{u}, \hat{\mathbf{u}}, \mathbf{v}, \hat{\mathbf{v}}, \mathbf{x}, \mathbf{y}, \mathbf{z}, \mathbf{P}^c, \mathbf{B}^c, \mathbf{E}|\omega) \quad , \forall \omega \tag{5.49}$$

5.5.2 Algorithm Description

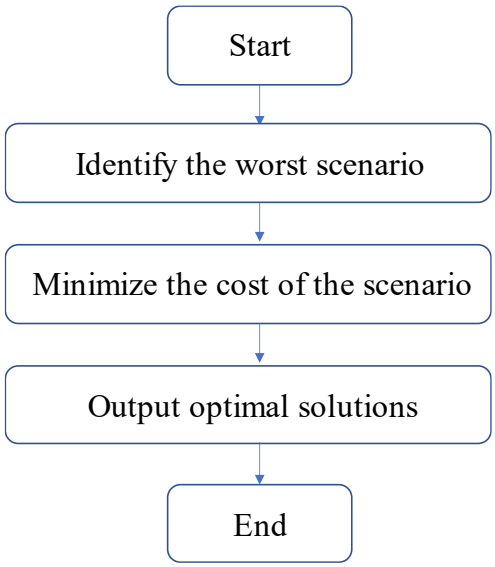


Figure 5.5 Flowchart of Minimax algorithm

As the most conservative criterion, Minimax deals with the problem from the worst point of view, so the worst scenario needs to be selected from all scenarios first, and then searching for the optimal result. However, in the actual application process, each scenario cannot be directly judged, so usually all scenarios are solved separately to get their own optimal solutions first and then the worst result is selected as the output, and the output result is the Minimax result mamong all results. In contrast to the expectation of the cost of all scenarios, the Miniax method does not take into account the probability of each scenario occurring. Compared with VaR and CVaR, Minimax also does not consider the confidence level, so the result given is only the worst case of all possible outcomes.

5.6 Numerical Experiment

5.6.1 Comparison of the Deterministic Model and the Stochastic Model

In this study, we assume that only the CF of wind and solar are random parameters and all other parameters are deterministic parameters. Three scenarios are given in this stochastic model. We take the CF used in Chapter 4 as our medium scenario, which we call Medium, with a 50% probability of occurrence, the other two scenarios are the lower scenario and the higher scenario where the average of the CF in a year is 25% below and above the average of the medium scenario. The probability of occurrence of the lower scenario is 20% and the probability of occurrence of the higher scenario is 30%. It is worth noting that in generating the simulation data, we only increase or decrease the average value of the year by 25%, and the specific value of the CF at a certain moment may be higher in the Lower scenario than in the medium scenario, or even higher than the value in the Higher scenario at that moment. The simulation data obtained by this way can better simulate the data in real situations. The probabilities of the three scenarios and the system costs when each of the three scenarios occurs separately are shown in Table 5.3. The deterministic model proposed in the Chapter 4 is used to solve these three scenarios.

Table 5.3 Summary of the Three Scenarios

	Lower	Medium	Higher
Probability	0.2	0.5	0.3
Cost ($)	179,063,693	178,931,509	177,735,742

AMPL is used to code Model SFMLA. The Gurobi solver is used to search for the optimal solution of the stochastic optimization model. The AMPL codes are running in a PC with Intel(R) Core (TM) i5-7200U CPU @ 2.5GHz, 4 Core(s), 24 GB memory, and 4

Logical Processor. The stochastic model has 162,184 decision variables and 214,812 constraints. It takes about 278 seconds to get the optimal solution. The optimal cost of the stochastic model is $178,854,715. We get the same site selection results as obtained by the deterministic model Factory 3 in Yuma, Factory 4 Tucson and Warehouse 1 in Los Vegas are chosen to open. All four stores are supplied by Warehouse 1. The location decision is summarized in Table 5.4.

Table 5.4 Decisions on Location of Factories and Warehouse

Candidate Location	Facility	Solution	Open
Phoenix	Factory 1	0	no
Reno	Factory 2	0	no
Yuma	Factory 3	1	yes
Tucson	Factory 4	1	yes
Las Vegas	Warehouse 1	1	yes
Los Angeles	Warehouse 2	0	no

Table 5.5 Microgrid Sizing for the 4F-2W-4S Network Design

Model	Microgrid	Factory 3	Factory 4	Warehouse 1	Unit
SFMLA	WT	0	0	3.56	MW
	PV	0	10.88	8.09	MW
	ESS	0	0	0	MWh
FMLA	WT	0	0	3.20	MW
	PV	0	10.36	7.12	MW
	ESS	0	0	0	MWh

Table 5.6 Optimal Costs

Models	System Cost ($)
Deterministic model	178,931,575
Stochastic model (Expectation)	178,854,715
Stochastic model (Even capacity factor)	178,933,345

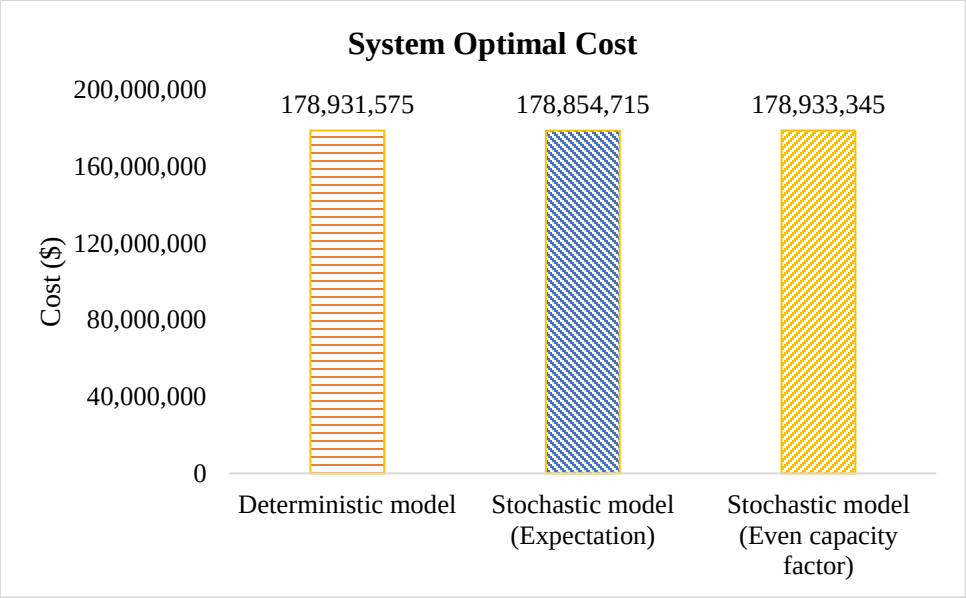


Figure 5.6 System Optimal Cost

Table 5.5 lists the optimal sizing of WT, PV and ESS installed in the factories and warehouse given by both SFMLA model and FMLA model. It is worth noting that, among the three scenarios involved in the SFMLA model, the percentage of Higher scenarios is 30%, while the percentage of Lower scenarios is only 20%, so the value of the CF input in SFMLA is higher than the input in the deterministic model, in order to take advantage of this aspect, the model chooses to increase the sizing of the renewables. Table 5.6 gives the optimal costs for each of the three models. The first one is the optimal cost given by the deterministic model proposed in Chapter 4, and the second one is the stochastic model proposed in this chapter, where the probabilities of the three scenarios are 20%, 50%, and 30%, respectively. The optimal cost is the expectation of the three scenarios. The probabilities of the three scenarios used in the third model are 25%, 50%, and 25% respectively. In this case, the average value of the capacity factor is same with

the average value of the capacity factor input in the deterministic model. The optimal cost is also the expectation of the three scenarios.

We can make two observations from the results of three models. First, when the average value of the capacity factor increases, the system chooses to install more renewables to obtain more power to meet the system demand instead of purchasing from the main grid. Though the installation cost increases due to the increased capacity of the renewables, the total cost of the system decreases. This indicates that in the case of abundant wind and solar energy, the revenue generated by the renewables will be greater than its installation cost. This indicates that the application of renewables can reduce the overall cost of the system when wind and solar energy are abundant. Second, when the capacity factor is the same, the optimal cost given by the stochastic model is greater than that given by the deterministic model. Although the average value of the CF inputted in both models is the same, the stochastic model considers more possibilities and faces a more volatile capacity factor, so it gets a higher overall cost.

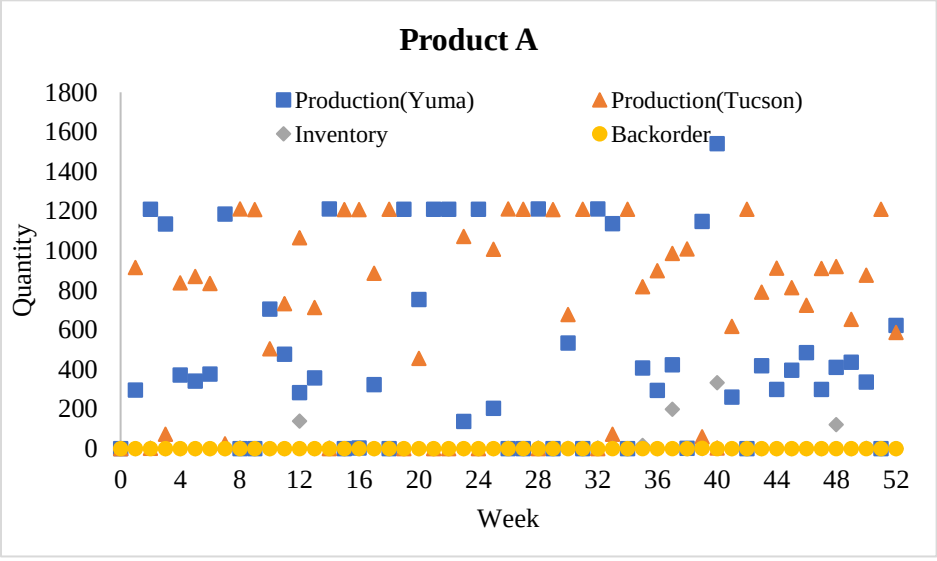


Figure 5.7 Product A Production and Inventory Decision of Model SFMLA

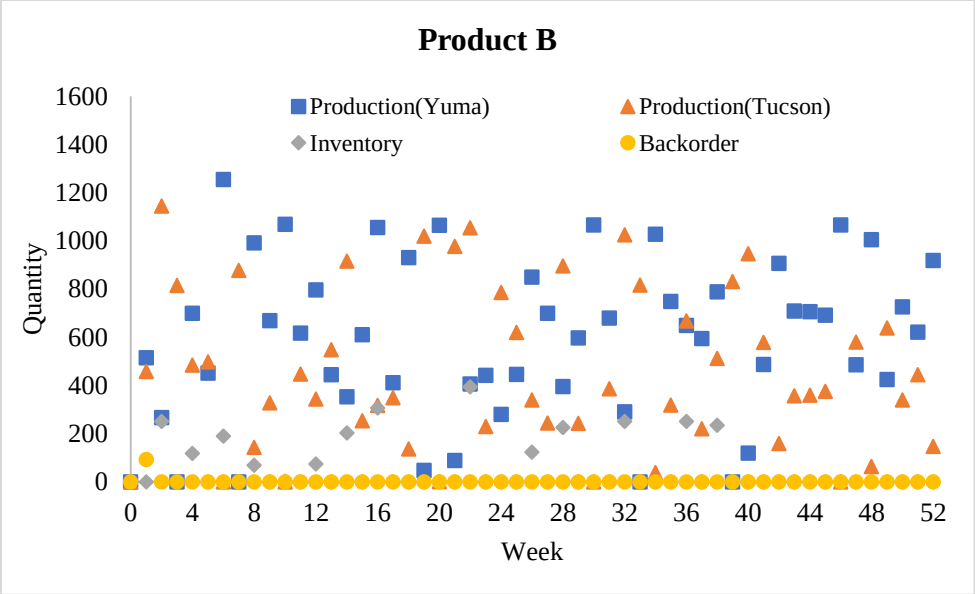


Figure 5.8 Product B Production and Inventory Decision of Model SFMLA

Figure 5.7 and Figure 5.8 depict the production schedule in both Yuma and Tucson, inventory and backorder schedule in Los Vegas given by stochastic model. The overall results are not very different from those given by the deterministic model. The stochastic model gives exactly the same results as the deterministic model for the quantity of products produced per year, but there is a slight difference in the production schedule, with the stochastic model giving higher amount than the deterministic model for inventory and backorder, and we will compare the subtle differences between them below:

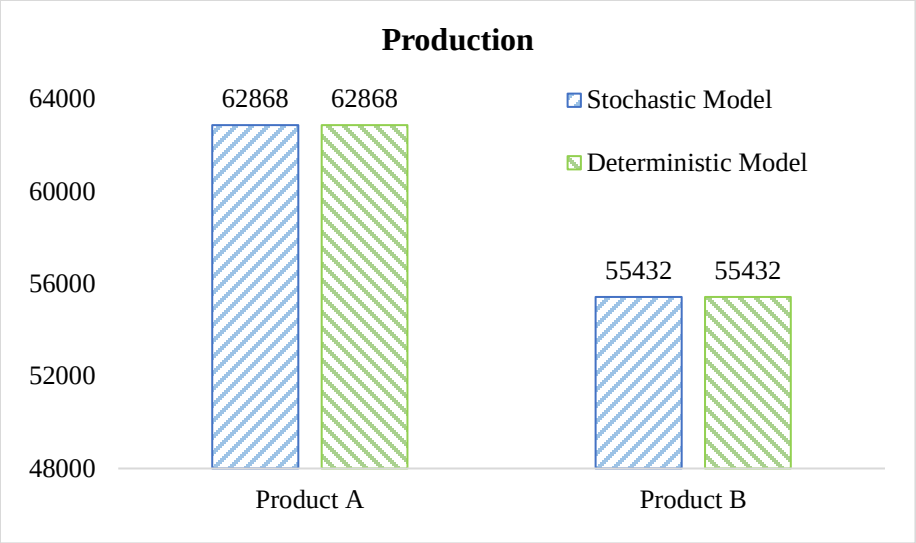


Figure 5.9 Difference in Production Quantity of Two Models

From Figure 5.9 we can see that the two models give the total annual production of the two products without any difference, the demand for the product is determined by the stores, and this constraint is firm, and is not affected by the external environment, the primary prerequisite for the system to function properly is to meet the demand for the product, so regardless of the stochastic model or the deterministic model, both give the minimum amount of production to meet the demand for the product.

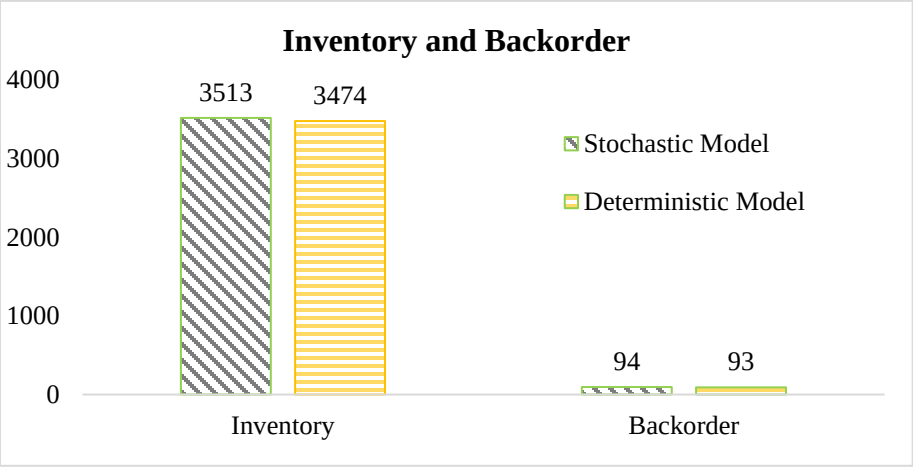


Figure 5.10 Difference in Inventory and Backorder of the Network

The difference in annual inventory and backorder given by these two models is illustrated in figure 5.10. The difference between the results given by the two models is observed for the inventory and the backorder. The total number of results given by the stochastic model is higher than that given by the deterministic model in both inventory and backorder. The reason is that the stochastic model needs to face three more complex and volatile scenarios than the deterministic model, which faces a stable external environment, and therefore needs a larger inventory and backorder as a buffer to maintain the stability of product supply and demand.

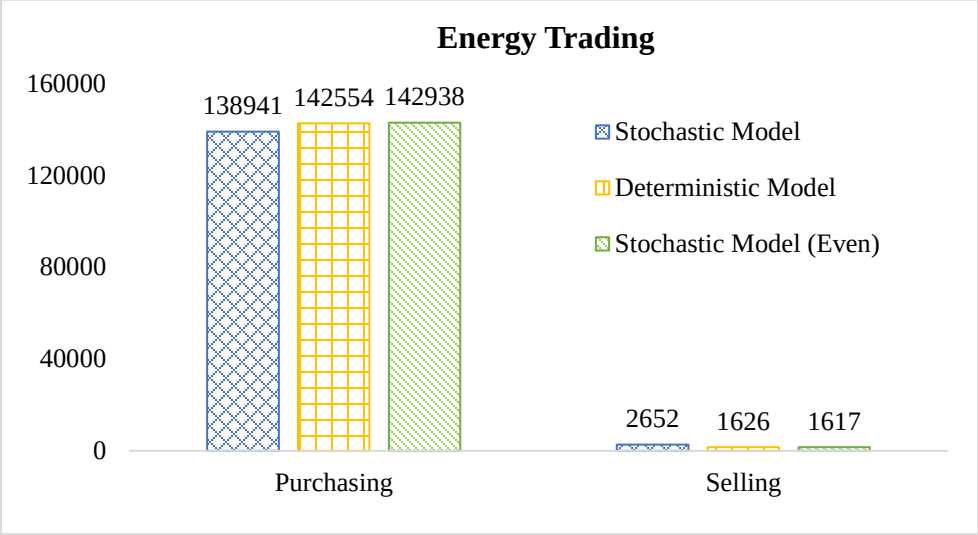


Figure 5.11 Difference in Energy Trading

Figure 5.11. depicts the difference in annual energy trading of the network given by three models. There is also a notable difference in the total amount of annual energy trading of the system given by the three models. The probabilities of the three scenarios input to the Stochastic model are 20%, 50%, and 30%, while the probabilities of the three scenarios input to the stochastic model (Even) are 25%, 50%, and 25%, respectively, and the average of the capacity factor of the three scenarios in this case is consistent with the

average of the capacity factor of one scenario in the deterministic model. Comparing the results of the stochastic model (Even) and the deterministic model, the annual electricity purchase given by the stochastic model (Even) is larger than that given by the deterministic model, while the electricity sold is smaller than that given by the deterministic model. Such results indicate that the stochastic model (Even) requires more energy to cope with fluctuations in the external environment and to allow the system to operate stably. In contrast, the stochastic model compared with the deterministic model shows the opposite result. In terms of purchasing electricity, the stochastic model gives a significantly lower amount of purchased electricity in one year for all facilities than that given by the deterministic model. In terms of electricity sales, the stochastic model gives a much higher annual total for all facilities than the deterministic model. This finding shows that the advantage of the capacity factor in the stochastic model completely compensates for the impact of external fluctuations on energy demand.

5.6.2 Comparison of the Three Criteria

In the case study we assumed four cases with φ equal to 0, 0.3, 0.8, 0.9. Applying the VaR and CVaR decision making criteria to the stochastic model respectively. For the application of Minimax criteria, there is no need to set the confidence level, the criteria just give the worst case for all scenarios. All the results are obtained for the four cases as described in Table 5.7.

Table 5.7 Results of Four Cases

	Case 1 (φ=0)	Case 2 (φ=0.3)	Case 3 (φ=0.8)	Case 4 (φ=0.9)
VaR	177,735,742	177,735,742	178,931,509	179,063,693
CVaR	178,599,216	178,969,276	179,063,693	179,063,693
Minimax	179,063,693			

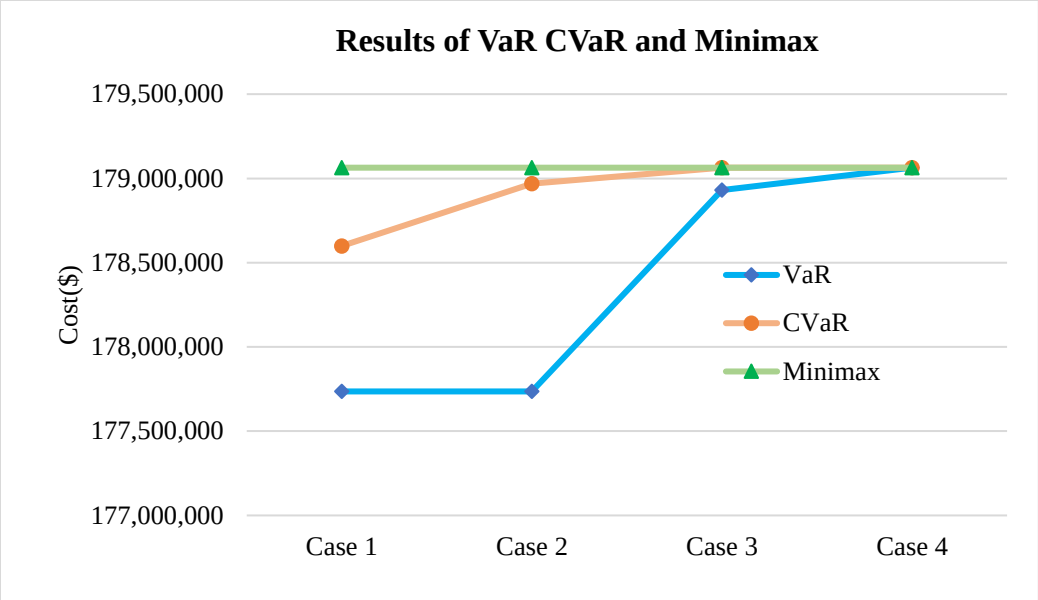


Figure 5.12 The Results of VaR, CVaR and Minimax

From Figure 5.12 we can see that the results given by the criterion CVaR are always greater than the results given by VaR. When φ is taken as 0, (1-φ) equals 100%, which in the criteria of VaR means that there is a 100% probability that there will be one result will be greater than or equal to this result, so VaR gives the minimum result among the three scenarios. However, for CVaR, At the current confidence level, VaR is the smallest value among all scenarios, so the expectation of exceeding the VaR is the expectation of the difference between all scenarios and this VaR. When φ is taken as 0.9, (1-φ) equals 10%, which when applying VaR means that there is only a 10% chance that the result will be exceeded, and the probability of the worst scenario is 20%, so the result of the worst scenario is taken, the same reason can be applied to the result of CVaR, The VaR in this case is the worst result among the three scenarios, so the expectation beyond this result is 0, then the CVaR is taken to the maximum of the three results like VaR. For Minimax, the four cases do not apply to it, and this criterion only takes the worst case of all three scenarios.

By comparing the three criteria, we can see that because CVaR takes into account tail risk, in addition to considering risks within the confidence level, the criteria also take into account the Expectation of risks beyond the confidence level, which allows for a more comprehensive assessment of risk. for the minimized model, it gives higher results and thus is more responsive to the actual results by combating risk. And for Minimax criteria, since only the worst case of all results is considered, it can provide the decision maker with a recommendation for the most conservative decision.

6 CONCLUSION

6.1 Research Summary

Industry 4.0 is the main driver of smart and sustainable manufacturing in terms of horizontal and vertical integration. It provides a set of solutions with which firms can effectively forecast load, manage power and thermal cogeneration, participate in transactive energy trading, and realize cost savings. The application of VPP not only solves the energy crisis and pollution problems, but also overcomes the issues of renewables intermittency. The focus of this thesis is on the design and operations of VPP for smart factory systems within the scope of Industry 4.0. In particular, the thesis work proposes to integrate prosumer energy into multiple facilities of a manufacturing supply chain, including factories, warehouses, retail stores and electric truck fleets. To that end, we need to overcome multi-dimensional barriers in the process of integrating wind- and solar-based distributed generation, such as energy balancing, storage, trading, and pricing.

Onsite renewables are preferred to achieve zero carbon emissions, gain energy independence, and participate in transactive energy market. In this regard, we explore the impact of factory location and microgrid sizing on the overall supply chain cost. First, a deterministic programming model is formulated to address the facility-microgrid, location-allocation problem, which is further transformed into a stochastic decision model to accommodate the uncertainty in capacity factors of wind and solar generation. The results of the stochastic model are analyzed using three criteria, namely value at risk, conditional value at risk, and Minimax. Below the research activities of each chapter are highlighted.

Chapter 2 concentrates on the application of recurrent neural networks on power load forecasting. In order to achieve a reliable and cost-effective energy supply, we first estimate the load of electricity from the demand side. Traditional mathematical and statistical methods make predictions from a single dimension data. Hence the prediction accuracy can be easily compromised if the data is non-stationary or seasonal. We leverage LSTM neural networks to process time series data of electric load. It provides us with new ideas in power load prediction. The proposed model is also applicable to other time series data including wind speed and solar PV irradiance forecasting. In addition, the prediction result becomes no less sensitive to the limited data size. In this thesis, we obtain a new prediction model based on the existing LSTM model by adjusting the network structure and hyperparameters. By using real data from ERCOT for experiments, the model is proved to have very good prediction accuracy.

Chapter 3 tests the feasibility of operating a VPP under a microgrid setting. The VPP is comprised of a CHP, an electrical ESS, a thermal energy storage system, and renewables of wind and solar generation. The VPP is installed in a single factory or industrial facility with the participation of day-ahead energy trading market. The surplus power of the microgrid can be sold to the main grid or stored in the local ESS. In this chapter, we propose a two-stage optimization model, namely, day-ahead market model and intra-day model. The two-stage model aims to minimize the system cost while maintaining the stable operation of the VPP. In the first stage, we use historical data to predict the renewable generation and the factory power load of the next day, and then determine the bidding price and the amount of electricity trading. In the second stage, the output of the CHP unit is adjusted to maintain the power stability of the VPP based on the

real-time renewable generation and power load. The two-stage decision problem is solved using rolling horizon method over the 24 hours period. Through the regulation of the CHP unit, the VPP can maintain the balance of electric and thermal generation and maximize the utilization of renewable resources.

Chapter 4 introduces a facility-microgrid, location-allocation model in a context of multi-echelon manufacturing supply chain. The network contains a set of candidate factories and warehouses with fixed retail stores as demand nodes. The supply chain network attempts to meet the energy demand by harvesting onsite wind and solar generation in conjunction with grid power. A VPP is formed by aggregating geographically dispersed microgrid systems with the goal of minimizing the supply chain cost over one-year planning horizon. This type of new supply chain design problem is referred to as FMLA model. The model aims to determine the locations of factories and warehouses, and the sizing of renewable microgrid system at the strategic level. The FMLA model further schedules energy generation, trading, and storage at the operational level. The model also determines production, inventory, and transportation of the products at the same time. Hence, FMLA is a unified optimization framework by integrating energy into the design and operation of manufacturing supply chain domain. The proposed model is tested in two network instances consisting of up to twelve candidate locations under a variety of climate conditions. Numerical experiments show that the model is robust and scalable under various uncertainties, such as product demand, holding cost, unit energy use, wind speed, weather condition, and electricity price, and network size. Many key parameters used in the numerical experiments are from real-world data. For instance, the capacity factors of WT and PV are estimated

based on the hourly wind speed and weather conditions of twelve US cities between 2004 and 2015.

In Chapter 5, the FMLA model is transformed into a stochastic version considering the uncertainty of real-world weather conditions. The capacity factor values are taken as a random variable consisting of three scenarios, namely low, medium and high. Each scenario contains three sets of hourly capacity factor data with different mean, standard deviation, and the probability of occurrence. The stochastic model is solved, respectively, under value at risk, conditional value at risk, and Minimax optimization. Compared with the deterministic programming, the stochastic model yields a more robust solution in terms of production, transportation, inventory, onsite renewables size, and energy trading.

6.2 Future Research

As a future work, this research can be extended to following directions.

- It can be considered to add charging stations for electric trucks, which can realize vehicle-to-grid and grid-to-vehicle operations. This means electric trucks can serve as a dual role with the involvement of materials transportation and power trading as mobile energy modules. The vehicle-to-grid operation will not only reduce carbon emissions, but also allow for more flexible energy distribution.
- The blockchain concept can also be introduced to decentralize the operation of VPP. Blockchain is a mutually shared, immutable ledger that is capable of recording transactions and tracking assets in a business network. The decentralized concept of blockchain technology is very close

to the characteristics of distributed energy resource. The blockchain technology can make the peer-to-peer energy transactions more effective and secure. At the same time, the anonymity feature can better protect the information of each microgrid or grid edge and make the whole system more secure and reliable.

- More sensor devices can be added to each terminal of the microgrid to achieve edge computing capability through Internet of Things technology. The system can integrate core capabilities such as network, computing, storage, and application into a unified open platform to provide nearest-end services for the power system, generate faster network service response, and meet the basic needs of real-time business, security and privacy protection for power distribution.

APPENDIX SECTION

APPENDIX A

LSTM model code for Chapter 2

```
from __future__ import absolute_import, division, print_function, unicode_literals
import tensorflow as tf
import matplotlib as mpl
import matplotlib.pyplot as plt
import numpy as np
import os
import pandas as pd

mpl.rcParams['figure.figsize'] = (10, 6)
mpl.rcParams['figure.dpi'] = 500
mpl.rcParams['axes.grid'] = False
font1 = {'family': 'Times New Roman',
        'weight': 'normal',
        'size': 20,
        }
font2 = {'family': 'Times New Roman',
        'weight': 'normal',
        'size': 20,
        }

df = pd.read_csv('load_data.csv')


def univariate_data(dataset, start_index, end_index, history_size, target_size):
   data = []
   labels = []

   start_index = start_index + history_size
   if end_index is None:
      end_index = len(dataset) - target_size

   for i in range(start_index, end_index):
      indices = range(i-history_size, i)
      # Reshape data from (history_size,) to (history_size, 1)
      data.append(np.reshape(dataset[indices], (history_size, 1)))
      labels.append(dataset[i+target_size])
   return np.array(data), np.array(labels)


TRAIN_SPLIT = 95000
```

```
tf.random.set_seed(13)

uni_data = df['ERCOT']
uni_data.index = df['Hour_End']

uni_data = uni_data.values

uni_train_mean = uni_data[:TRAIN_SPLIT].mean()
uni_train_std = uni_data[:TRAIN_SPLIT].std()
uni_data = (uni_data-uni_train_mean)/uni_train_std
univariate_past_history = 24
univariate_future_target = 1

x_train_uni, y_train_uni = univariate_data(uni_data, 0, TRAIN_SPLIT,
                                           univariate_past_history,
                                           univariate_future_target)

x_val_uni, y_val_uni = univariate_data(uni_data, TRAIN_SPLIT, None,
                                       univariate_past_history,
                                       univariate_future_target)

def create_time_steps(length):
  return list(range(-length, 0))


def show_plot(plot_data, delta, title):
  labels = ['Historical', 'True Value', 'Prediction']
  marker = ['.-', 'rx', 'go']
  time_steps = create_time_steps(plot_data[0].shape[0])
  if delta:
    future = delta
  else:
    future = 0

  plt.title(title, font2)
  for i, x in enumerate(plot_data):
    if i:
      plt.plot(future, plot_data[i], marker[i], markersize=10, label=labels[i])
    else:
      plt.plot(time_steps, plot_data[i].flatten(), marker[i], label=labels[i])
  plt.legend(prop=font2, loc=1)
  plt.xlim([time_steps[0], (future+5)*2])
  plt.xticks(fontproperties='Times New Roman', size=20)
  plt.yticks(fontproperties='Times New Roman', size=20)
  plt.xlabel('Time-Step', font1)
  return plt
```

```
BATCH_SIZE = 256
BUFFER_SIZE = 500

train_univariate = tf.data.Dataset.from_tensor_slices((x_train_uni, y_train_uni))
train_univariate =
train_univariate.cache().shuffle(BUFFER_SIZE).batch(BATCH_SIZE).repeat()

val_univariate = tf.data.Dataset.from_tensor_slices((x_val_uni, y_val_uni))
val_univariate = val_univariate.batch(BATCH_SIZE).repeat()

simple_lstm_model = tf.keras.models.Sequential([
   tf.keras.layers.LSTM(20, input_shape=x_train_uni.shape[-2:]),
   tf.keras.layers.Dense(1)])

simple_lstm_model.compile(optimizer='adam', loss='msle')

EVALUATION_INTERVAL = 200
EPOCHS = 60

history = simple_lstm_model.fit(train_univariate, epochs=EPOCHS,
                  steps_per_epoch=EVALUATION_INTERVAL,
                  validation_data=val_univariate, validation_steps=50)

plt.plot(history.history['loss'], '-',linewidth=2.0,label='Training loss')
plt.plot(history.history['val_loss'], '-.',linewidth=2.0,label='Validation loss')

plt.ylabel('Loss', font1)
plt.xlabel('Epoch', font1)
plt.legend(prop=font2, loc=(6.5/14, 0.3/0.5))
plt.xticks(fontproperties='Times New Roman', size=20)
plt.yticks(fontproperties='Times New Roman', size=20)

plt.show()

for x, y in val_univariate.take(3):
   plot = show_plot([x[0].numpy(), y[0].numpy(),
   simple_lstm_model.predict(x)[0]], 0, 'One hour ahead prediction')
   plot.show()
```

APPENDIX B

Sample AMPL code for DA Model for Chapter 3

```
set periods:= 0..T;

param T;
param cf;
param cm{1..T};
param co;
param cp{1..T};
param pres{1..T};
param pel{1..T};
param pthl{1..T};
param pechpmax;
param pechpmin;
param pesmax;
param pesmin;
param pthchpsmax;
param pthchpsmin;
param pmda{1..T};


var pechp{1..T} <= pechpmax, >= pechpmin;
var pimb{1..T}>=0;
var pes_ch{1..T} >= 0;
var pes_dis{1..T}  >= 0;
var se{0..T} <= pesmax, >= pesmin;
var sth{0..T} <= pthchpsmax, >= pthchpsmin;
var ths_ch{1..T} >= 0;
var ths_dis{1..T} >= 0;



minimize total_cost: sum{j in 1..T} (pechp[j]*cf + pes_ch[j]*co + pes_dis[j]*co + pimb[j]*cp[j]-
pmda[j]*cm[j]);

subject to e{j in 1..T}:pechp[j]+pes_dis[j]+pres[j]-pes_ch[j]-pmda[j]+pimb[j]>=pel[j];
subject to th{j in 1..T}:0.8*pechp[j]+ths_dis[j]-ths_ch[j]>=pthl[j];


subject to e_s{j in 1..T}:
   se[j]=se[j-1]+pes_ch[j]-pes_dis[j];

subject to se_0: se[0]=0;

subject to th_s{j in 1..T}:
          sth[j]=sth[j-1]+ths_ch[j]-ths_dis[j];

subject to ths_0: sth[0]=0;
```

APPENDIX C

Sample AMPL code for FMLA 3 Model for Chapter 4

```
set production;
set factory;
set warehouse;
set store;
set res;
set renewables;

param T;
param J;
param dis{factory, warehouse};
param dis1{warehouse, store};
param p{production};
param pi{production};
param h{production};
param b{production};
param mu{production, store};
param sigam{production, store};
param vr{production, res};
param w{1..J, factory, res};
param sita{renewables};
param a{renewables};
param B{renewables};
param C{renewables};
param taog{renewables};
param E{production};
param qv;
param m{production};
param N{factory, warehouse};
param wv;
param tw{warehouse};
param Ln{warehouse};
param N1{warehouse, store};
param T1{store};
param λk{1..J, 1..T, factory, renewables};
param λn{1..J, 1..T, warehouse, renewables};
param φes;
param des;
param ρb;
param ρs;
param cs;
param γ{warehouse, production};
param F{factory};
param Fn{warehouse};
param bes;
param M;

var x{production, 1..J, factory, warehouse}>=0 integer;
var y{production, 0..J, warehouse}>=0 integer;
var z{production, 0..J, warehouse}>=0 integer;
var x1{production, 1..J, warehouse, store}>=0 integer;
var u{factory} binary;
```

```
var u1{warehouse} binary;
var v{factory, warehouse, production, 1..J} binary;
var v1{warehouse, store, production} binary;
var Pcgk{factory, renewables}>=0 <=20;
var Pcgn{warehouse, renewables}>=0 <=20;
var Bk{factory, 1..J, 0..T}>=0;
var Bn{warehouse, 1..J, 0..T}>=0;
var Bck{factory}>=0;
var Bcn{warehouse}>=0;
var xt{production, factory, warehouse, 1..J}>=0;
var xt1{production, warehouse, store, 1..J}>=0;
var Ebk{factory, 1..J, 1..T}>=0;
var Esk{factory, 1..J, 1..T}>=0;
var Ebn{warehouse, 1..J, 1..T}>=0;
var Esn{warehouse, 1..J, 1..T}>=0;

minimize total_cost: sum{k in factory}F[k]*u[k]+sum{i in production, j in 1..J, k in factory, n in
warehouse}p[i]*x[i, j, k, n]

      +sum{i in production, j in 1..J, k in factory, n in warehouse}pi[i]*dis[k, n]*x[i, j, k, n]
      +sum{n in warehouse}Fn[n]*u1[n]
      +sum{i in production, j in 0..J, n in warehouse}h[i]*y[i, j, n]
      +sum{i in production, j in 0..J, n in warehouse}b[i]*z[i, j, n]
      +sum{i in production, j in 1..J, n in warehouse, s in store}pi[i]*dis1[n, s]*x1[i, j, n, s]
      +sum{g in renewables, k in factory}sita[g]*a[g]*Pcgk[k, g]
      +sum{j in 1..J, t in 1..T, g in renewables, k in factory}taog[g]*(B[g]-C[g])*Pcgk[k, g]*λk[j, t, k, g]
      +sum{k in factory}Bck[k]*(φes*des+bes)
      +sum{t in 1..T, j in 1..J, k in factory}(ρb*Ebk[k, j, t] - ρs*Esk[k, j, t])
      +sum{g in renewables, n in warehouse}sita[g]*a[g]*Pcgn[n, g]
      +sum{j in 1..J, t in 1..T, g in renewables, n in warehouse}taog[g]*(B[g]-C[g])*Pcgn[n, g]*λn[j, t, n,
g]

      +sum{n in warehouse}Bcn[n]*(φes*des+bes)
      +sum{t in 1..T, j in 1..J, n in warehouse}(ρb*Ebn[n, j, t] - ρs*Esn[n, j, t]);

subj to c_1{s in store, i in production}: sum{n in warehouse}v1[n, s, i] = 1;
subj to c_2{n in warehouse, i in production, j in 1..J}: sum{s in store}x1[i, j, n, s] <= u1[n]*γ[n, i];
subj to c_3{n in warehouse, i in production, j in 1..J}: sum{k in factory}x[i, j, k, n] <= u1[n]*γ[n, i];
subj to c_4{s in store, n in warehouse, i in production}:v1[n, s, i]<=u1[n];
subj to c_5{i in production, n in warehouse}: sum{k in factory}x[i, 1, k, n]+y[i, 0, n]-y[i, 1, n]+z[i, 1, n]
=sum{s in store}x1[i, 1, n, s];

subj to c_6{i in production, j in 2..J-1, n in warehouse}: sum{k in factory}x[i, j, k, n]+y[i, j-1, n]-y[i, j, n]-
z[i, j-1, n]+z[i, j, n] =sum{s in store}x1[i, j, n, s];

subj to c_7{i in production, n in warehouse}: sum{k in factory}x[i, J, k, n]+y[i, J-1, n]-y[i, J, n]-z[i, J-1,
n] =sum{s in store}x1[i, J, n, s];

subj to c_8{i in production, s in store,j in 1..J}: sum{n in warehouse} x1[i, j, n, s]>= mu[i,
s]+1.28*sigam[i, s];

subj to c_9{k in factory, r in res, j in 1..J}:sum{i in production, n in warehouse}vr[i, r]*x[i, j, k, n]<=w[j,
k, r];

subj to c_10{k in factory,  i in production, n in warehouse, j in 1..J}:x[i, j, k, n]-M*v[k, n, i, j]<=0;
```

subj to c_11{s **in** store, i **in** production, n **in** warehouse, j **in** 1..J}:x1[i, j, n, s]-M*v1[n, s, i]<=0;

subj to c_12{i **in** production, n **in** warehouse}: y[i, 0, n]=0;

subj to c_13{k **in** factory, j **in** 1..J, t **in** 1..T}:**sum**{i **in** production, n **in** warehouse}(E[i]+qv*N[k, n]*dis[k, n]*m[i])*xt[i, k, n, j]
+qv*(**sum**{n **in** warehouse, i **in** production}N[k, n]*dis[k, n]*wv*v[k, n, i, j])+Bk[k, j, t]-Bk[k, j, t-1]+Esk[k, j, t]-Ebk[k, j, t]
=**sum**{g **in** renewables}taog[g]*Pcgk[k, g]*λk[j, t, k, g];

subj to c_14{n **in** warehouse, j **in** 1..J, t **in** 1..T}:tw[n]*Ln[n]*u1[n]+qv*(**sum**{k **in** factory, i **in** production}N[k, n]*dis[k, n]*v[k, n, i, j]*wv)
+qv*(**sum**{i **in** production, s **in** store}dis1[n, s]*m[i]*xt1[i, n, s, j])
+qv*2*(**sum**{s **in** store, i **in** production}N1[n, s]*dis1[n,s]*wv*v1[n, s, i])+Bn[n, j, t]-Bn[n, j, t-1]+Esn[n, j, t]-Ebn[n, j, t]
=**sum**{g **in** renewables}taog[g]*Pcgn[n, g]*λn[j, t, n, g];

subj to c_15{k **in** factory, j **in** 1..J, t **in** 1..T}: Esk[k, j, t]-M*u[k]<=0;

subj to c_16 {k **in** factory, j **in** 1..J, t **in** 1..T}: Ebk[k, j, t]-M*u[k]<=0;

subj to c_17{n **in** warehouse, j **in** 1..J, t **in** 1..T}: Esn[n, j, t]-M*u1[n]<=0;

subj to c_18{n **in** warehouse, j **in** 1..J, t **in** 1..T}: Ebn[n, j, t]-M*u1[n]<=0;

subj to c_19{g **in** renewables, k **in** factory}: Pcgk[k, g]-M*u[k]<=0;

subj to c_20{g **in** renewables, n **in** warehouse}: Pcgn[n, g]-M*u1[n]<=0;

subj to c_21{n **in** warehouse}: Bcn[n]-M*u1[n]<=0;

subj to c_22{k **in** factory}: Bck[k]-M*u[k]<=0;

subj to c_23{i **in** production, n **in** warehouse, k **in** factory, j **in** 1..J}:T*(xt[i, k, n, j])=x[i, j, k, n];

subj to c_24{i **in** production, n **in** warehouse, s **in** store, j **in** 1..J}:T*(xt1[i, n, s, j])=x1[i, j, n, s];

subj to c_25{k **in** factory}: Bk[k, 1, 0] = Bck[k];

subj to c_26{n **in** warehouse}: Bn[n, 1, 0] = Bcn[n];

subj to c_27{k **in** factory}: Bk[k, 52, 168] = Bck[k];

subj to c_28{n **in** warehouse}: Bn[n, 52, 168] = Bcn[n];

subj to c_29{t **in** 1..T,j **in** 1..J, k **in** factory}: Bk[k, j, t] <= Bck[k];

subj to c_30{t **in** 1..T,j **in** 1..J, n **in** warehouse}: Bn[n, j, t] <= Bcn[n];

subj to c_31{k **in** factory, j **in** 2..J}: Bk[k, j, 0] = Bk[k, j-1, T];

subj to c_32{n **in** warehouse, j **in** 2..J}: Bn[n, j, 0] = Bn[n, j-1, T];

APPENDIX D

Sample AMPL code for SFMLA Model for Chapter 5

```
set production;
set factory;
set warehouse;
set store;
set res;
set renewables;
set scenarios;


param T;
param J;
param dis{factory, warehouse};
param dis1{warehouse, store};
param p{production};
param pi{production};
param h{production};
param b{production};
param mu{production, store};
param sigam{production, store};
param vr{production, res};
param w{1..J, factory, res};
param sita{renewables};
param a{renewables};
param B{renewables};
param C{renewables};
param taog{renewables};
param E{production};
param qv;
param m{production};
param N{factory, warehouse};
param wv;
param tw{warehouse};
param Ln{warehouse};
param N1{warehouse, store};
param T1{store};
param λk{scenarios, 1..J, 1..T, factory, renewables};
param λn{scenarios, 1..J, 1..T, warehouse, renewables};
param φes;
param des;
param ρb;
param ρs;
param cs;
param γ{warehouse, production};
param F{factory};
param Fn{warehouse};
param bes;
param M;
param β{scenarios};
param φ;
```

```
var x{production, 1..J, factory, warehouse}>=0 integer;
var y{production, 0..J, warehouse}>=0 integer;
var z{production, 0..J, warehouse}>=0 integer;
var x1{production, 1..J, warehouse, store}>=0 integer;
var u{factory} binary;
var u1{warehouse} binary;
var v{factory, warehouse, production, 1..J} binary;
var v1{warehouse, store, production} binary;
var Pcgk{factory, renewables}>=0 <=20;
var Pcgn{warehouse, renewables}>=0 <=20;
var Bk{factory, 1..J, 0..T}>=0;
var Bn{warehouse, 1..J, 0..T}>=0;
var Bck{factory}>=0;
var Bcn{warehouse}>=0;
var xt{production, factory, warehouse, 1..J}>=0;
var xt1{production, warehouse, store, 1..J}>=0;
var Ebk{factory, 1..J, 1..T}>=0;
var Esk{factory, 1..J, 1..T}>=0;
var Ebn{warehouse, 1..J, 1..T}>=0;
var Esn{warehouse, 1..J, 1..T}>=0;


minimize total_cost: sum{k in factory}F[k]*u[k]+sum{i in production, j in 1..J, k in factory, n in
warehouse}p[i]*x[i, j, k, n]

      +sum{i in production, j in 1..J, k in factory, n in warehouse}pi[i]*dis[k, n]*x[i, j, k, n]
      +sum{n in warehouse}Fn[n]*u1[n]
      +sum{i in production, j in 0..J, n in warehouse}h[i]*y[i, j, n]
      +sum{i in production, j in 0..J, n in warehouse}b[i]*z[i, j, n]
      +sum{i in production, j in 1..J, n in warehouse, s in store}pi[i]*dis1[n, s]*x1[i, j, n, s]
      +sum{g in renewables, k in factory}sita[g]*a[g]*Pcgk[k, g]
      +sum{j in 1..J, t in 1..T, g in renewables, k in factory, δ in scenarios}β[δ]*taog[g]*(B[g]-
C[g])*Pcgk[k, g]*λk[δ, j, t, k, g]
      +sum{k in factory}Bck[k]*(φes*des+bes)
      +sum{t in 1..T, j in 1..J, k in factory}(ρb*Ebk[k, j, t] - ρs*Esk[k, j, t])
      +sum{g in renewables, n in warehouse}sita[g]*a[g]*Pcgn[n, g]
      +sum{j in 1..J, t in 1..T, g in renewables, n in warehouse, δ in scenarios}β[δ]*taog[g]*(B[g]-
C[g])*Pcgn[n, g]*λn[δ, j, t, n, g]
      +sum{n in warehouse}Bcn[n]*(φes*des+bes)
      +sum{t in 1..T, j in 1..J, n in warehouse}(ρb*Ebn[n, j, t] - ρs*Esn[n, j, t]);

subj to c_1{s in store, i in production}: sum{n in warehouse}v1[n, s, i] = 1;

subj to c_2{n in warehouse, i in production, j in 1..J}: sum{s in store}x1[i, j, n, s] <= u1[n]*γ[n, i];

subj to c_3{n in warehouse, i in production, j in 1..J}: sum{k in factory}x[i, j, k, n] <= u1[n]*γ[n, i];

subj to c_4{s in store, n in warehouse, i in production}:v1[n, s, i]<=u1[n];
subj to c_5{i in production, n in warehouse}: sum{k in factory}x[i, 1, k, n]+y[i, 0, n]-y[i, 1, n]+z[i, 1, n]
=sum{s in store}x1[i, 1, n, s];
subj to c_6{i in production, j in 2..J-1, n in warehouse}: sum{k in factory}x[i, j, k, n]+y[i, j-1, n]-y[i, j, n]-
z[i, j-1, n]+z[i, j, n] =sum{s in store}x1[i, j, n, s];
subj to c_7{i in production, n in warehouse}: sum{k in factory}x[i, J, k, n]+y[i, J-1, n]-y[i, J, n]-z[i, J-1,
n] =sum{s in store}x1[i, J, n, s];
```

subj to c_8{i **in** production, s **in** store,j **in** 1..J}: **sum**{n **in** warehouse} x1[i, j, n, s]>= mu[i, s]+1.28*sigam[i, s];
subj to c_9{k **in** factory, r **in** res, j **in** 1..J}:**sum**{i **in** production, n **in** warehouse}vr[i, r]*x[i, j, k, n]<=w[j, k, r];
subj to c_10{k **in** factory, i **in** production, n **in** warehouse, j **in** 1..J}:x[i, j, k, n]-M*v[k, n, i, j]<=0;
subj to c_11{s **in** store, i **in** production, n **in** warehouse, j **in** 1..J}:x1[i, j, n, s]-M*v1[n, s, i]<=0;
subj to c_12{i **in** production, n **in** warehouse}: y[i, 0, n]=0;

subj to c_13{k **in** factory, j **in** 1..J, t **in** 1..T}:**sum**{i **in** production, n **in** warehouse}(E[i]+qv*N[k, n]*dis[k, n]*m[i])*xt[i, k, n, j]
+qv*(**sum**{n **in** warehouse, i **in** production}N[k, n]*dis[k, n]*wv*v[k, n, i, j])+Bk[k, j, t]-Bk[k, j, t-1]+Esk[k, j, t]-Ebk[k, j, t]
=**sum**{g **in** renewables, δ **in** scenarios}β[δ]*taog[g]*Pcgk[k, g]*λk[δ, j, t, k, g];

subj to c_14{n **in** warehouse, j **in** 1..J, t **in** 1..T}:tw[n]*Ln[n]*u1[n]+qv*(**sum**{k **in** factory, i **in** production}N[k, n]*dis[k, n]*v[k, n, i, j]*wv)
+qv*(**sum**{i **in** production, s **in** store}dis1[n, s]*m[i]*xt1[i, n, s, j])
+qv*2*(**sum**{s **in** store, i **in** production}N1[n, s]*dis1[n,s]*wv*v1[n, s, i])+Bn[n, j, t]-Bn[n, j, t-1]+Esn[n, j, t]-Ebn[n, j, t]
=**sum**{g **in** renewables, δ **in** scenarios}β[δ]*taog[g]*Pcgn[n, g]*λn[δ, j, t, n, g];

subj to c_15{k **in** factory, j **in** 1..J, t **in** 1..T}: Esk[k, j, t]-M*u[k]<=0;

subj to c_16 {k **in** factory, j **in** 1..J, t **in** 1..T}: Ebk[k, j, t]-M*u[k]<=0;

subj to c_17{n **in** warehouse, j **in** 1..J, t **in** 1..T}: Esn[n, j, t]-M*u1[n]<=0;

subj to c_18{n **in** warehouse, j **in** 1..J, t **in** 1..T}: Ebn[n, j, t]-M*u1[n]<=0;

subj to c_19{g **in** renewables, k **in** factory}: Pcgk[k, g]-M*u[k]<=0;

subj to c_20{g **in** renewables, n **in** warehouse}: Pcgn[n, g]-M*u1[n]<=0;

subj to c_21{n **in** warehouse}: Bcn[n]-M*u1[n]<=0;

subj to c_22{k **in** factory}: Bck[k]-M*u[k]<=0;

subj to c_23{i **in** production, n **in** warehouse, k **in** factory, j **in** 1..J}:T*(xt[i, k, n, j])=x[i, j, k, n];

subj to c_24{i **in** production, n **in** warehouse, s **in** store, j **in** 1..J}:T*(xt1[i, n, s, j])=x1[i, j, n, s];

subj to c_25{k **in** factory}: Bk[k, 1, 0] = Bck[k];

subj to c_26{n **in** warehouse}: Bn[n, 1, 0] = Bcn[n];

subj to c_27{k **in** factory}: Bk[k, 52, 168] = Bck[k];

subj to c_28{n **in** warehouse}: Bn[n, 52, 168] = Bcn[n];

subj to c_29{t **in** 1..T,j **in** 1..J, k **in** factory}: Bk[k, j, t] <= Bck[k];

subj to c_30{t **in** 1..T,j **in** 1..J, n **in** warehouse}: Bn[n, j, t] <= Bcn[n];

subj to c_31{k **in** factory, j **in** 2..J}: Bk[k, j, 0] = Bk[k, j-1, T];

subj to c_32{n **in** warehouse, j **in** 2..J}: Bn[n, j, 0] = Bn[n, j-1, T];

APPENDIX E

Table E1: Weekly Available Machine Hours in Candidate Factories (F=Factory)

Week	F1	F2	F3	F4	F5	F6	F7	F8
1	17692	21624	17082	25624	23024	22184	24098	24080
2	23724	43491	34356	34356	30589	24149	29738	26029
3	15376	18792	22269	22268	17872	15721	22194	20185
4	35358	43215	22758	34138	40170	41077	30716	27221
5	25275	20594	16268	36606	25260	16507	34811	22297
6	25260	30874	36582	36584	35019	30910	32024	33215
7	15648	19124	22662	22660	17008	21249	18987	18018
8	24658	45207	23808	35712	40709	44113	38563	42854
9	16648	20348	16074	36168	26387	17001	34012	17682
10	25486	46725	36912	36912	35563	28121	30229	30336
11	15498	28413	22446	22446	20725	27607	22289	22086
12	36753	29948	23658	35486	26668	27037	31205	35100
13	16960	20728	16374	24562	16797	23529	21855	16547
14	38961	31746	37617	56424	51771	51514	42605	45900
15	15182	27834	14658	32982	23977	25039	25427	24263
16	39393	48147	25356	57054	33361	44152	50169	45417
17	23367	28560	15042	22562	28485	26858	15880	23678
18	23130	28270	22332	33500	32223	28469	28526	24130
19	17460	21340	21072	31608	17930	26510	26698	22892
20	25968	47610	37611	56415	30472	38779	42704	38692
21	28149	22936	27177	27178	28057	26469	25085	27376
22	40254	32800	38865	58296	41756	52028	35306	34056
23	19890	24312	12802	28806	19627	20978	26012	22700
24	24042	44076	34818	52227	24795	40414	42782	44685
25	14454	26499	13956	31401	29674	15598	17305	19225
26	21120	25814	20392	30588	30433	20576	24223	30010
27	26088	21256	16792	25188	23968	25516	22430	21468
28	40467	32974	39072	39070	40286	35033	40040	36605
29	14858	27240	14346	32277	17252	28571	29528	27726
30	35721	43659	34491	34490	37789	39507	35544	42058
31	16910	31002	16328	36738	34543	34237	30588	32132
32	36177	44217	34929	34930	40893	36006	36953	41923
33	22158	27084	21396	21396	26507	22165	24445	26408
34	25590	46914	24708	37060	44592	26986	44976	40516
35	25347	30978	24471	24472	28629	25565	28345	30924
36	31509	38511	20282	30422	28048	29294	22169	38439
37	21801	26646	21048	21048	23495	22278	23614	24118
38	19636	23998	18958	28438	21650	27010	20153	22314
39	15434	18864	22353	22354	20657	18127	18293	21494
40	34860	42606	33657	50484	37536	37068	49416	49716
41	24621	20062	15850	23774	17061	18832	17844	18517

42	22566	27580	21788	49023	37014	42678	39615	23847
43	24570	20020	23721	35583	21691	31885	28363	34102
44	22486	41226	21712	32568	35989	40196	40102	34207
45	23739	29013	22920	34380	28076	26117	30452	29106
46	34812	42549	33612	33614	37419	39904	40037	39074
47	17040	31239	16452	37017	20846	30061	30260	18378
48	31785	38847	30687	30686	35950	32082	30943	31713
49	17796	21750	17182	25772	21591	20133	22656	17724
50	23600	43269	22788	34182	41114	27191	36026	29116
51	27810	22660	14918	33567	25011	28704	20912	18304
52	33153	27014	32013	32012	32110	28690	29503	29200

Table E2: Weekly Available Labor Hours in Candidate Factories (F=Factory)

Week	F1	F2	F3	F4	F5	F6	F7	F8
1	17692	21624	17082	25624	23024	22184	24098	24080
2	23724	43491	34356	34356	30589	24149	29738	26029
3	15376	18792	22269	22268	17872	15721	22194	20185
4	35358	43215	22758	34138	40170	41077	30716	27221
5	25275	20594	16268	36606	25260	16507	34811	22297
6	25260	30874	36582	36584	35019	30910	32024	33215
7	15648	19124	22662	22660	17008	21249	18987	18018
8	24658	45207	23808	35712	40709	44113	38563	42854
9	16648	20348	16074	36168	26387	17001	34012	17682
10	25486	46725	36912	36912	35563	28121	30229	30336
11	15498	28413	22446	22446	20725	27607	22289	22086
12	36753	29948	23658	35486	26668	27037	31205	35100
13	16960	20728	16374	24562	16797	23529	21855	16547
14	38961	31746	37617	56424	51771	51514	42605	45900
15	15182	27834	14658	32982	23977	25039	25427	24263
16	39393	48147	25356	57054	33361	44152	50169	45417
17	23367	28560	15042	22562	28485	26858	15880	23678
18	23130	28270	22332	33500	32223	28469	28526	24130
19	17460	21340	21072	31608	17930	26510	26698	22892
20	25968	47610	37611	56415	30472	38779	42704	38692
21	28149	22936	27177	27178	28057	26469	25085	27376
22	40254	32800	38865	58296	41756	52028	35306	34056
23	19890	24312	12802	28806	19627	20978	26012	22700
24	24042	44076	34818	52227	24795	40414	42782	44685
25	14454	26499	13956	31401	29674	15598	17305	19225
26	21120	25814	20392	30588	30433	20576	24223	30010
27	26088	21256	16792	25188	23968	25516	22430	21468
28	40467	32974	39072	39070	40286	35033	40040	36605
29	14858	27240	14346	32277	17252	28571	29528	27726
30	35721	43659	34491	34490	37789	39507	35544	42058

31	16910	31002	16328	36738	34543	34237	30588	32132
32	36177	44217	34929	34930	40893	36006	36953	41923
33	22158	27084	21396	21396	26507	22165	24445	26408
34	25590	46914	24708	37060	44592	26986	44976	40516
35	25347	30978	24471	24472	28629	25565	28345	30924
36	31509	38511	20282	30422	28048	29294	22169	38439
37	21801	26646	21048	21048	23495	22278	23614	24118
38	19636	23998	18958	28438	21650	27010	20153	22314
39	15434	18864	22353	22354	20657	18127	18293	21494
40	34860	42606	33657	50484	37536	37068	49416	49716
41	24621	20062	15850	23774	17061	18832	17844	18517
42	22566	27580	21788	49023	37014	42678	39615	23847
43	24570	20020	23721	35583	21691	31885	28363	34102
44	22486	41226	21712	32568	35989	40196	40102	34207
45	23739	29013	22920	34380	28076	26117	30452	29106
46	34812	42549	33612	33614	37419	39904	40037	39074
47	17040	31239	16452	37017	20846	30061	30260	18378
48	31785	38847	30687	30686	35950	32082	30943	31713
49	17796	21750	17182	25772	21591	20133	22656	17724
50	23600	43269	22788	34182	41114	27191	36026	29116
51	27810	22660	14918	33567	25011	28704	20912	18304
52	33153	27014	32013	32012	32110	28690	29503	29200

Table E3: Mean and Standard Deviation (StDev) of Capacity Factor

Facility	F1		F2		F3		F4	
Microgrid	WT	PV	WT	PV	WT	PV	WT	PV
Mean	0.116	0.344	0.168	0.374	0.225	0.416	0.178	0.497
StDev	0.051	0.192	0.214	0.208	0.258	0.231	0.198	0.273
Facility	F5		F6		F7		F7	
Microgrid	WT	PV	WT	PV	WT	PV	WT	PV
Mean	0.259	0.240	0.141	0.340	0.227	0.226	0.464	0.128
StDev	0.277	0.140	0.148	0.188	0.266	0.253	0.221	0.149
Facility	W1		W2		W3		W4	
Microgrid	WT	PV	WT	PV	WT	PV	WT	PV
Mean	0.244	0.469	0.244	0.308	0.354	0.181	0.243	0.173
StDev	0.298	0.257	0.298	0.173	0.202	0.200	0.214	0.194

REFERENCES

1. Alizadeh, M., Ma, J., Mahdavi-Amiri, N., Marufuzzaman, M., & Jaradat, R. (2019). A stochastic programming model for a capacitated location-allocation problem with heterogeneous demands. *Computers & Industrial Engineering*, *137*, 106055.
2. Aybar-Ruiz, A., Jiménez-Fernandez, S., Cornejo-Bueno, L., Casanova-Mateo, C., Sanz-Justo, J., Salvador-Gonzalez, P., & Salcedo-Sanz, S. (2016). A novel grouping genetic algorithm–extreme learning machine approach for global solar radiation prediction from numerical weather models inputs. *Solar Energy*, *132*, 129-142.
3. Bhardwaj, A., Kamboj, V. K., Shukla, V. K., Singh, B., & Khurana, P. (2012). Unit commitment in electrical power system-a literature review. In *2012 IEEE international power engineering and optimization conference, Melaka, Malaysia*, pp. 275-280.
4. Bilgili, M., & Ozgoren, M. (2011). Daily total global solar radiation modeling from several meteorological data. *Meteorology and Atmospheric Physics*, *112*(3), 125-138.
5. Blackhall, L., Kuiper, G., Nicholls, L., & Scott, P. (2020). Optimising the value of distributed energy resources. *The Electricity Journal*, *33*(9), 106838.
6. Carrion, M., & Arroyo, J. M. (2006). A computationally efficient mixed-integer linear formulation for the thermal unit commitment problem. *IEEE Transactions on Power Systems*, *21*(3), 1371-1378.
7. Chen, Y. H., Lu, S. Y., Chang, Y. R., Lee, T. T., & Hu, M. C. (2013). Economic analysis and optimal energy management models for microgrid systems: A case study in Taiwan. *Applied Energy*, *103*, 145-154.

8. Chittum, A., & Relf, G. (2019). Valuing distributed energy resources: Combined heat and power and the modern grid. *The Electricity Journal*, *32*(1), 52-57.
9. Cooper, L. (1963). Location-allocation problems. *Operations research*, *11*(3), 331-343.
10. Daskin, M. S., Snyder, L. V., & Berger, R. T. (2005). Facility location in supply chain design. In *Logistics systems: Design and Optimization*, Springer, Boston, MA, pp. 39-65.
11. Della Vedova, M. L., & Facchinetti, T. (2012, September). Real-time scheduling for industrial load management. In *2012 IEEE International Energy Conference and Exhibition (ENERGYCON)*, pp. 707-713.
12. Di Somma, M., Yan, B., Bianco, N., Graditi, G., Luh, P. B., Mongibello, L., & Naso, V. (2015). Operation optimization of a distributed energy system considering energy costs and exergy efficiency. *Energy Conversion and Management*, *103*, 739-751.
13. EIA. (2019). Annual Energy Outlook 2019 with Projections to 2050. The U.S. Energy Information Administration (EIA) Report, U.S. Department of Energy, Washington, DC 20585, https://www.eia.gov/aeo, (accessed on March 19, 2020).
14. Ekonomou, L., Christodoulou, C. A., & Mladenov, V. (2016). A short-term load forecasting method using artificial neural networks and wavelet analysis. *International Journal of Power Systems*, *1*, 64-68.
15. Evins, R. (2016). A bi-level design and operation optimization process applied to an energy centre. *Journal of Building Performance Simulation*, *9*(3), 255-271.
16. Fabian, C. I. (2008). Handling CVaR objectives and constraints in two-stage stochastic models. *European Journal of Operational Research*, *191*(3), 888-911.

17. Giaouris, D., Papadopoulos, A. I., Seferlis, P., Papadopoulou, S., Voutetakis, S., Stergiopoulos, F., & Elmasides, C. (2014). Optimum energy management in smart grids based on power pinch analysis. *Chemical Engineering*, 39.
18. Giaouris, D. et al. (2013). Performance investigation of a hybrid renewable power generation and storage system using systemic power management models. *Energy*, *61*, 621-635.
19. Girard, R., Laquaine, K., & Kariniotakis, G. (2013). Assessment of wind power predictability as a decision factor in the investment phase of wind farms. *Applied Energy*, *101*, 609-617.
20. Guo, Z., Zhao, W., Lu, H., & Wang, J. (2012). Multi-step forecasting for wind speed using a modified EMD-based artificial neural network model. *Renewable Energy*, *37*(1), 241-249.
21. Hadera, H., Harjunkoski, I., Grossmann, I. E., Sand, G., & Engell, S. (2014). Steel production scheduling optimization under time-sensitive electricity costs. *Computer Aided Chemical Engineering*, vol. 33, pp. 373-378.
22. Halpern, J. Y., & Leung, S. (2015). Weighted sets of probabilities and minimax weighted expected regret: a new approach for representing uncertainty and making decisions. *Theory and Decision*, *79*(3), 415-450.
23. Hochreiter, S., & Schmidhuber, J. (1997). Long short-term memory. *Neural Computation*, *9*(8), 1735-1780.
24. Huang, C. J., & Kuo, P. H. (2018). A short-term wind speed forecasting model by using artificial neural networks with stochastic optimization for renewable energy systems. *Energies*, *11*(10), 2777.

25. Huang, G. B., Zhu, Q. Y., & Siew, C. K. (2006). Extreme learning machine: theory and applications. *Neurocomputing*, *70*(1-3), 489-501.
26. Hurwicz, L. (1952). *A Criterion for Decision-making under Uncertainty*. Technical Report 355, Cowles Commission.
27. Inman, R. H., Pedro, H. T., & Coimbra, C. F. (2013). Solar forecasting methods for renewable energy integration. *Progress in Energy and Combustion Science*, *39*(6), 535-576.
28. Javed, F., Arshad, N., Wallin, F., Vassileva, I., & Dahlquist, E. (2012). Forecasting for demand response in smart grids: An analysis on use of anthropologic and structural data and short term multiple loads forecasting. *Applied Energy*, *96*, 150-160.
29. Ji, W., & Chee, K. C. (2011). Prediction of hourly solar radiation using a novel hybrid model of ARMA and TDNN. *Solar Energy*, *85*(5), 808-817.
30. Kalogirou, S. A. (2013). *Solar Energy Engineering: Processes and Systems.* Academic Press.
31. Karmellos, M., Georgiou, P. N., & Mavrotas, G. (2019). A comparison of methods for the optimal design of Distributed Energy Systems under uncertainty. *Energy*, *178*, 318-333.
32. Khatib, T., Mohamed, A., & Sopian, K. (2012). A review of solar energy modeling techniques. *Renewable and Sustainable Energy Reviews*, *16*(5), 2864-2869.
33. Kopanos, G. M., Georgiadis, M. C., & Pistikopoulos, E. N. (2013). Energy production planning of a network of micro combined heat and power generators. *Applied Energy*, *102*, 1522-1534.

34. Kopanos, G. M., & Pistikopoulos, E. N. (2014). Reactive scheduling by a multiparametric programming rolling horizon framework: a case of a network of combined heat and power units. *Industrial & Engineering Chemistry Research*, *53*(11), 4366-4386.
35. Kuo, P. H., & Huang, C. J. (2018). A high precision artificial neural networks model for short-term energy load forecasting. *Energies*, *11*(1), 213.
36. Li, Z., Ding, R., & Floudas, C. A. (2011). A comparative theoretical and computational study on robust counterpart optimization: I. Robust linear optimization and robust mixed integer linear optimization. *Industrial & Engineering Chemistry Research*, *50*(18), 10567-10603.
37. Lopez, G., Batlles, F. J., & Tovar-Pescador, J. (2005). Selection of input parameters to model direct solar irradiance by using artificial neural networks. *Energy*, *30*(9), 1675-1684.
38. Manfren, M., Caputo, P., & Costa, G. (2011). Paradigm shift in urban energy systems through distributed generation: Methods and models. *Applied Energy*, *88*(4), 1032-1048.
39. Marietta, M. P., Graells, M., & Guerrero, J. M. (2014, May). A rolling horizon rescheduling strategy for flexible energy in a microgrid. In *2014 IEEE International Energy Conference (ENERGYCON)*, pp. 1297-1303.
40. Mavromatidis, G., Orehounig, K., & Carmeliet, J. (2018). Uncertainty and global sensitivity analysis for the optimal design of distributed energy systems. *Applied Energy*, *214*, 219-238.

41. Rezaei, F., Najafi, A. A., & Ramezanian, R. (2020). Mean-conditional value at risk model for the stochastic project scheduling problem. *Computers & Industrial Engineering*, *142*, 106356.
42. Koraki, D., & Strunz, K. (2017). Wind and solar power integration in electricity markets and distribution networks through service-centric virtual power plants. *IEEE Transactions on Power Systems*, *33*(1), 473-485.
43. Mavromatidis, G., Orehounig, K., & Carmeliet, J. (2018). Comparison of alternative decision-making criteria in a two-stage stochastic program for the design of distributed energy systems under uncertainty. *Energy*, *156*, 709-724.
44. Mehleri, E. D., Sarimveis, H., Markatos, N. C., & Papageorgiou, L. G. (2012). A mathematical programming approach for optimal design of distributed energy systems at the neighbourhood level. *Energy*, *44*(1), 96-104.
45. Mitra, S., Grossmann, I. E., Pinto, J. M., & Arora, N. (2012). Optimal production planning under time-sensitive electricity prices for continuous power-intensive processes. *Computers & Chemical Engineering*, *38*, 171-184.
46. Mohsenian-Rad, A. H., & Leon-Garcia, A. (2010). Optimal residential load control with price prediction in real-time electricity pricing environments. *IEEE Transactions on Smart Grid*, *1*(2), 120-133.
47. More, A., & Deo, M. C. (2003). Forecasting wind with neural networks. *Marine Structures*, *16*(1), 35-49.
48. Nolde, K., & Morari, M. (2010). Electrical load tracking scheduling of a steel plant. *Computers & Chemical Engineering*, *34*(11), 1899-1903.

49. Nwauka, O., Telukdarie, A., & Enslin, J. (2018). Virtual power plant basic requirements for integration of distributed energy resources driven by industry 4.0. *In Proceedings of the International Conference on Industrial Engineering and Operations Management*, Paris, France, pp. 511-523.

50. Ortiz-Astorquiza, C., Contreras, I., & Laporte, G. (2018). Multi-level facility location problems. *European Journal of Operational Research*, *267*(3), 791-805.

51. Pappas, S. S., Ekonomou, L., Moussas, V. C., Karampelas, P., & Katsikas, S. K. (2008). Adaptive load forecasting of the Hellenic electric grid. *Journal of Zhejiang University-Science A*, *9*(12), 1724-1730.

52. Pham, A., Jin, T., Novoa, C., & Qin, J. (2019). A multi-site production and microgrid planning model for net-zero energy operations. *International Journal of Production Economics*, *218*, 260-274.

53. Pruitt, K. A., Braun, R. J., & Newman, A. M. (2013). Evaluating shortfalls in mixed-integer programming approaches for the optimal design and dispatch of distributed generation systems. *Applied Energy*, *102*, 386-398.

54. Qi, B., Zhao, W., Wang, X., Li, S., & Runge, T. (2019, July). A low-cost driver and passenger activity detection system based on deep learning and multiple sensor fusion. In *2019 5th International Conference on Transportation Information and Safety (ICTIS)*, pp. 170-176.

55. Qi, B., Zhao, W., Zhang, H., Jin, Z., Wang, X., & Runge, T. (2019, July). Automated traffic volume analytics at road intersections using computer vision techniques. In *2019 5th International Conference on Transportation Information and Safety (ICTIS)*, pp. 161-169.

56. Rockafellar, R. T., & Uryasev, S. (2000). Optimization of conditional value-at-risk. *Journal of Risk, 2*, 21-42.

57. Salcedo-Sanz, S., Casanova-Mateo, C., Pastor-Sanchez, A., & Sanchez-Giron, M. (2014). Daily global solar radiation prediction based on a hybrid coral reefs optimization–Extreme learning machine approach. *Solar Energy, 105*, 91-98.

58. Shapiro, A., Tekaya, W., da Costa, J. P., & Soares, M. P. (2013). Risk neutral and risk averse stochastic dual dynamic programming method. *European Journal of Operational Research*, *224*(2), 375-391.

59. Sharafi, M., & ElMekkawy, T. Y. (2015). Stochastic optimization of hybrid renewable energy systems using sampling average method. *Renewable and Sustainable Energy Reviews*, *52*, 1668-1679.

60. Silvente, J., Aguirre, A., Crexells, G., Zamarripa, M., Méndez, C., Graells, M., & Espuna, A. (2013). Hybrid time representation for the scheduling of energy supply and demand in smart grids. *Computer Aided Chemical Engineering*, vol. 32, pp. 553-558.

61. Silvente, J., Aguirre, A. M., Zamarripa, M. A., Mendez, C. A., Graells, M., & Espuña, A. (2015). Improved time representation model for the simultaneous energy supply and demand management in microgrids. *Energy*, *87*, 615-627.

62. Silvente, J., Graells, M., Espuna, A., & Salas, P. (2012). An optimization model for the management of energy supply and demand in smart grids. In *2012 IEEE International Energy Conference and Exhibition (ENERGYCON)*, pp. 368-373.

63. Silvente, J., Kopanos, G. M., Pistikopoulos, E. N., & Espuna, A. (2014). Reactive Scheduling for the Coordination of Energy Supply and Demand Management in Microgrids. *Computer Aided Chemical Engineering*, vol. 33, pp. 493-498. Elsevier.
64. Silvente, J., Kopanos, G. M., Pistikopoulos, E. N., & Espuna, A. (2015). A rolling horizon optimization framework for the simultaneous energy supply and demand planning in microgrids. *Applied Energy*, *155*, 485-501.
65. Soroudi, A., & Amraee, T. (2013). Decision making under uncertainty in energy systems: State of the art. *Renewable and Sustainable Energy Reviews*, *28*, 376-384.
66. Soubdhan, T., Ndong, J., Ould-Baba, H., & Do, M. T. (2016). A robust forecasting framework based on the Kalman filtering approach with a twofold parameter tuning procedure: Application to solar and photovoltaic prediction. *Solar Energy*, *131*, 246-259.
67. Sozen, A., Arcaklioglu, E., & Ozalp, M. (2004). Estimation of solar potential in Turkey by artificial neural networks using meteorological and geographical data. *Energy Conversion and Management*, *45*(18-19), 3033-3052.
68. Velik, R., & Nicolay, P. (2014). Grid-price-dependent energy management in microgrids using a modified simulated annealing triple-optimizer. *Applied Energy*, *130*, 384-395.
69. Voyant, C., Muselli, M., Paoli, C., & Nivet, M. L. (2011). Optimization of an artificial neural network dedicated to the multivariate forecasting of daily global radiation. *Energy*, *36*(1), 348-359.

70. Wang, L., & Singh, C. (2009). Multicriteria design of hybrid power generation systems based on a modified particle swarm optimization algorithm. *IEEE Transactions on Energy Conversion*, *24*(1), 163-172.
71. www.keras.io, "Keras", Accessed online between October 2019 and March 2020.
72. Xiong, J., Ng, T. S. A., & Wang, S. (2016). An optimization model for economic feasibility analysis and design of decentralized waste-to-energy systems. *Energy*, *101*, 239-251.
73. Yang, Y., Zhang, S., & Xiao, Y. (2017). Optimal design of distributed energy resource systems based on two-stage stochastic programming. *Applied Thermal Engineering*, *110*, 1358-1370.
74. Zamarripa, M., Vasquez, J. C., Guerrero, J. M., & Graells, M. (2011). Detailed operation scheduling and control for renewable energy powered microgrids. *Computer Aided Chemical Engineering*, *29*, 1819-1823.
75. Zhang, J., Wei, Y., Tan, Z. F., Ke, W., & Tian, W. (2017). A hybrid method for short-term wind speed forecasting. *Sustainability*, *9*(4), 596.
76. Zhao, B., Zhang, X., Li, P., Wang, K., Xue, M., & Wang, C. (2014). Optimal sizing, operating strategy and operational experience of a stand-alone microgrid on Dongfushan Island. *Applied Energy*, *113*, 1656-1666.
77. Zhao, W., Li, T., Qi, B., Nie, Q., & Runge, T. (2021). Terrain Analytics for Precision Agriculture with Automated Vehicle Sensors and Data Fusion. *Sustainability*, *13*(5), 2905.

78. Zhao, W., Xu, L., Qi, B., Hu, J., Wang, T., & Runge, T. (2020). Vivid: Augmenting vision-based indoor navigation system with edge computing. *IEEE Access*, *8*, 42909-42923.

79. Zhao, W., Yamada, W., Li, T., Digman, M., & Runge, T. (2021). Augmenting crop detection for precision agriculture with deep visual transfer learning—A case study of bale detection. *Remote Sensing*, *13*(1), 23.

80. Zhou, Z., Zhang, J., Liu, P., Li, Z., Georgiadis, M. C., & Pistikopoulos, E. N. (2013). A two-stage stochastic programming model for the optimal design of distributed energy systems. *Applied Energy*, *103*, 135-144.

81. Zondervan, E., Grossmann, I. E., & de Haan, A. B. (2010). Energy optimization in the process industries: Unit Commitment at systems level. *Computer Aided Chemical Engineering*, *28*, 931-936.